Aus dem Institut für Molekularbiologie und Tumorforschung
Geschäftsführender Direktor: Prof. Dr. Rolf Müller

des Fachbereichs Medizin der Philipps-Universität Marburg

Identifizierung und Charakterisierung des inversen PPARβ/δ-Agonisten DG172

Kumulative Dissertation zur Erlangung des Doktorgrades der Naturwissenschaften

dem Fachbereich Medizin

der Philipps-Universität Marburg

vorgelegt von

Sonja Lieber, geb. Daum

aus Marburg

Marburg, 2014

Angenommen vom Fachbereich Medizin der Philipps-Universität Marburg am: 12.12.2014

Gedruckt mit Genehmigung des Fachbereichs.

Dekan: Prof. Dr. Helmut Schäfer
Referent: Prof. Dr. Rolf Müller
1. Korreferent: Prof. Dr. Stefan Bauer

Inhaltsverzeichnis

Abkürzungsverzeichnis

AF	Aktivierungsfunktion
ANGPTL4	*Angiopoietin-like 4*
atRA	*all-trans*-Retinsäure
Bcl6	*B-Cell Lymphoma 6 Protein*
BMC	*Bone Marrow Cell*
CARM1	*Coactivator-Associated Arginine Methyltransferase 1*
CBP/p300	*CREB-Binding Protein*
CD	*Cluster of Differentiation*
C/EBP	*CCAAT/Enhancer Binding Protein*
ChIP	Chromatin-Immun-Präzipitation
DBD	DNA-Bindungsdomäne
DC	*Dendritic Cell*
DC-Sign	*Dendritic Cell-Specific Intercellular Adhesion Molecule-3-Grabbing Non-Integrin*
DR	*Direct Repeat*
FACS	*Fluorescence-Activated Cell Sorting*
GFI1	*Growth Factor Independent 1 Transcription Repressor*
GM-CSF	*Granulocyte Macrophage Colony-Stimulating Factor*
GMP	*Granulocyte-Macrophage-Progenitor*
Gr1	*Granulocyte Receptor 1*
HDAC3	Histondeacetylase 3
HETE	Hydroxyeicosatetraensäure
IL-4	Interleukin-4
IRF8	*Interferon Regulatory Factor 8*
LBD	Ligandenbindungsdomäne
LPS	Lipopolysaccharid
LT-HSC	*Long-Term Hematopoietic Stem Cell*
Ly6	*Lymphocyte Antigen 6*
M-CSF	*Macrophage Colony-Stimulating Factor*
Mcp-1	*Monocyte Chemotactic Protein 1*
MHC II	*Major Histocompatibility Complex II*
Mmp9	Matrix-Metalloprotease 9
NCoR	*Nuclear Receptor Co-Repressor*
NIH	*National Institute of Health*
NSAIDS	*Non Steroidal Anti Inflammatory Drugs*

PGC1	PPAR Coaktivator 1
PGI_2	Prostazyklin
PGJ_2	Prostaglandin J2
PPAR	*Peroxisome Proliferator-Activated Receptor*
PPRE	*PPAR Response Element*
PU.1	*Purine Rich Box 1*
RXR	*Retinoid X Receptor*
S100a8	*S100 Calcium Binding Protein 8*
SAR	*Structure Activity Relationship*
SHARP	*SMRT and Histone Deacetylase-Associated Repressor Protein*
SMRT	*Silencing Mediator of Retinoid and Thyroid Receptors*
SMRT-ID2	*SMRT-Interaction Domain 2*
SRC	*Steroid Receptor Co-Activator*
TGF	*Transforming Growth Factor*
TR-FRET	*Time-Resolved Fluorescence Resonance Energy Transfer*
TZD	Thiazolidindion

1 Zusammenfassung

In den vergangenen Jahren konnten Nachweise erbracht werden, dass PPARβ/δ an einer Vielzahl schwerer Erkrankungen wie Krebs, Atherosklerose und Diabetes mellitus beteiligt ist. Eine mögliche therapeutische Option könnte daher eine Modulation dieses Rezeptors mittels spezifischer inhibitorischer Liganden sein. Zu Beginn der vorliegenden Arbeit waren zwar hochaffine PPARβ/δ-Agonisten verfügbar, jedoch waren alle beschriebenen inhibitorischen Liganden entweder nicht selektiv, nicht bioverfügbar oder zeigten eine pharmakologisch ungünstige, irreversible Interaktion mit PPARβ/δ. Zur Untersuchung des therapeutischen Potenzials von PPARβ/δ-Liganden war die Entwicklung neuer bioverfügbarer, selektiver inhibitorischer Liganden daher dringend geboten. Diese beinhalten sowohl Antagonisten, die durch eine Bindung an PPARβ/δ kompetitiv dessen Aktivität hemmen, als auch inverse Agonisten, die durch eine zusätzliche Rekrutierung von Corepressoren aktiv zu dessen Repressorfunktion beitragen.

In Vorarbeiten zum ersten Teil dieser Arbeit wurden mittels TR-FRET-basierter Assays 2693 Substanzen einer Substanzbibliothek des National Institute of Health (NIH) auf ihre Bindung an PPARβ/δ sowie auf ihre Fähigkeit Corepressoren zu rekrutieren untersucht. Die vielversprechendste Substanz des Screens wurde als Leitstruktur für weitere Modifikationen zur Optimierung der Affinität und inhibitorischen Wirksamkeit verwendet. Durch die sich anschließende Analyse der Struktur-Wirkungsbeziehung (SAR-Studie, „Structure Activity Relationship“) konnte DG172 ([(Z)-2-(2-Bromophenyl)-3-{4-(1-Methyl-Piperazin)Amino]Phenyl}Acrylonitril) als optimales Derivat identifiziert werden. DG172 wies eine hohe Bindungsaffinität für PPARβ/δ mit stark invers agonistischer Aktivität auf. Zudem konnte eine Bindung an die PPAR-Subtypen α und γ ausgeschlossen und seine Bioverfügbarkeit nach oraler Gabe in Mäusen nachgewiesen werden. Damit ist DG172 der erste beschriebene bioverfügbare, inverse PPARβ/δ-Agonist mit sehr hoher Selektivität und somit ein vielversprechendes Instrument zur Untersuchung der biologischen und pathophysiologischen Funktionen von PPARβ/δ.

Aufgrund einer Vielzahl von Belegen, dass PPARβ/δ auch in immunassoziierten Prozessen eine Rolle spielt, sollte im zweiten Teil der Arbeit mit Hilfe *Ppard*-defizienter Mäuse und DG172 eine mögliche Funktion des Rezeptors während der Myelopoese untersucht werden. Bereits in einem frühen Stadium dieser Untersuchungen wurde ein neuer, PPARβ/δ-unabhängiger Effekt durch DG172 auf die Differenzierung von Knochenmarkzellen festgestellt. Weitere Analysen ergaben, dass DG172 deutlich die GM-CSF-induzierte Differenzierung primärer Knochenmarkzellen zu dendritischen

Zellen förderte und dabei synergistisch mit IL-4 wirkte. Diese positive Wirkung auf die Differenzierung und Reifung dendritischer Zellen ging einher mit einer Reduktion der Differenzierung zu neutrophilen Granulozyten. Microarray-Analysen zeigten spezifische Transkriptom-Veränderungen, die diese Interpretation bestätigten. Dieser PPARβ/δ-unabhängige Effekt von DG172 war zudem hoch spezifisch in Bezug auf den Zelltyp und das Differenzierungsstadium myeloider Zellen. Schließlich konnten wir durch eine Struktur-Funktions-Analyse ausgehend von DG172 zeigen, dass die PPARβ/δ-unabhängige Beeinflussung der Myelopoese von der PPARβ/δ-Bindung separierbar ist. So war durch Halogenierung in der *para*-Position des oberen Aromaten ein Wirkstoff darstellbar, der die Differenzierung zu dendritischen Zellen ohne nennenswerten Effekt auf PPARβ/δ stimulierte.

Summary

Research of the past years has provided clear evidence that PPARβ/δ is associated with major diseases including cancer, atherosclerosis and diabetes mellitus. Modulation of this receptor by specific inhibitory ligands represents a potential therapeutic option. At the beginning of this work highly affine agonists for PPARβ/δ were available, but all described inhibitory ligands were either not selective, not bioavailable or showed a pharmacologically undesirable, irreversible interaction with PPARβ/δ. To investigate the therapeutic potential of PPARβ/δ ligands the development of new was highly desirable. These include antagonists, which inhibit PPARβ/δ activity by competition with endogenous ligands, and inverse agonists, which actively trigger corepressor recruitment and establishment of an active transcriptional repressor complex.

Screening of a 2693 substances of a NIH compound library by TR-FRET based assays for PPARβ/δ binding and corepressors recruitment had already been performed as part of preliminary studies. The most promising compound of the screen was used as lead structure for further modifications to optimize the affinity and the inhibitory efficacy. Further structure-activity relationship (SAR) studies led to the identification of DG172 ([(Z)-2-(2-Bromophenyl)-3-{[4-(1-methyl-piperazine)amino]phenyl}acrylonitrile) as the optimal derivative. DG172 showed a high binding affinity with strong inverse agonistic properties. Furthermore, binding of this compound to the PPAR subtypes α and γ could be excluded and its bioavailability after oral administration into mice could be demonstrated. Therefore DG172 is the first bioavailable inverse PPARβ/δ agonist with high selectivity and thus a promising tool to analyze the biological and pathophysiological functions of PPARβ/δ.

Since PPARβ/δ has also been described to play a role in immunological processes, the second aim of this work was to analyze possible functions of this receptor in myelopoiesis using *Ppard*-deficient mice and DG172. At an early stage of this study a novel PPARβ/δ-independent effect of DG172 on the differentiation of bone marrow cells (BMCs) became evident. Further analyses showed that DG172 strongly augmented GM-CSF-induced differentiation of BMCs towards dendritic cells, which was synergistic with IL-4. This positive effect on differentiation and maturation of dendritic cells was accompanied with a reduction of differentiation towards neutrophilic granulocytes. Microarray analyzes showed specific DG172-induced alterations of the transcriptome which confirmed this interpretation. This PPARβ/δ independent effect of DG172 was highly specific with regard to the celltype and the differentiation stage of myeloid cells. Finally, structure-function analyses showed that the PPARβ/δ-independent effect of DG172 on myelopoiesis is separable from PPARβ/δ binding. Thus, halogenation at the the *para* position of the upper phenyl ring in DG172 yielded a compound that enhanced dendritic cell differentiation in the absence of appreciable binding to PPARβ/δ.

2 Einleitung

2.1 Peroxisome Proliferator-Activated Receptors (PPARs)

Bei den „Peroxisome Proliferator-Activated Receptors“, kurz PPARs, handelt es sich um Fettsäure-regulierte Transkriptionsfaktoren, die der Superfamilie der Kernrezeptoren angehören. Zur Familie der PPARs gehören drei Subtypen, PPARα, PPARβ/δ und PPARγ, welche eine hohe Sequenz- und Struktur-Homologie aufweisen. Als Transkriptionsfaktoren regulieren sie Zielgene, die Schlüsselfunktionen im Glukose- und Fett-Metabolismus und damit bei der Energiehomöostase einnehmen (Wahli and Michalik 2012). Darüber hinaus konnte in den letzten Jahren auch eine Rolle der PPARs in der Regulation von Immunprozessen nachgewiesen werden (Kostadinova 2005; Yang et al., 2010). Übereinstimmend mit ihren physiologischen Funktionen wurden PPARs auch mit zahlreichen pathophysiologischen Prozessen wie Atherosklerosis, Diabetes mellitus, Krebs und inflammatorischen Funktionsstörungen assoziiert (Desvergne et al., 2006; Peters et al., 2012; Wahli and Michalik 2012). Aufgrund ihrer Liganden-abhängigen Regulation stellen PPARs ein geeignetes Ziel für die Behandlung mit ihnen assoziierter Erkrankungen dar. In den nachfolgenden Abschnitten wird daher näher auf ihre Struktur sowie auf die von ihnen gesteuerte transkriptionelle Regulation eingegangen und abschließend ihr Einfluss auf biologische und pathophysiologische Prozesse erläutert.

2.1.1 Struktur

PPARs sind, wie auch alle anderen Kernrezeptoren, aus unterschiedlichen funktionalen Domänen aufgebaut (Laudet et al., 1990). An die innerhalb der drei Subtypen nur wenig konservierte N-terminale, Liganden-unabhängige Transaktivierungsfunktion (AF-1) schließt sich die hochkonservierte DNA-Bindedomäne (DBD) an, die innerhalb regulatorischer Regionen PPAR-responsiver Gene spezifische „PPAR response elements“, kurz PPREs, erkennt (Hsu et al., 1998). Auch die am C-Terminus gelegene Ligandenbindungsdomäne (LBD) ist eine zwischen den Subtypen konservierte Region, die jedoch eine relativ hohe Divergenz zwischen PPARβ/δ und den anderen beiden Subtypen aufweist und im Falle von PPARβ/δ durch eine zusätzliche Helix ein größeres Spektrum strukturell unterschiedlicher endogener und synthetischer Liganden erlaubt (Nolte et al., 1998; Xu et al., 2001). Die innerhalb der LBD liegende Liganden-abhängige Aktivierungsdomäne AF-2 ist an der Bildung der Coaktivator-Bindetasche beteiligt (Aranda and Pascual 2001; Nolte et al., 1998).

Zwischen DBD und LBD ist zudem eine sehr variable „Hinge“-Region lokalisiert, die eine Rotation der DBD durch Ligandenbindung ermöglicht.

2.1.2 Regulation der Transkription

2.1.2.1 DNA-Bindung

Zur transkriptionellen Regulation der Zielgene ist eine Heterodimerisierung der PPARs mit ihren obligatorischen Bindungspartnern RXR („Retinoid X receptor“) α, β und γ notwendig. Eine Heterodimerisierung der PPARs mit RXR-Monomeren kann sowohl in Anwesenheit als auch in Abwesenheit von Liganden stattfinden (Feige et al., 2005; Nolte et al., 1998). Da es sich hier um sogenannte permissive Heterodimere handelt, muss zur Aktivierung der PPAR:RXR-Heterodimere eine Bindung entweder durch einen RXR- oder durch einen PPAR-Liganden erfolgen (Mangelsdorf and Evans 1995). Die Bindung der Heterodimere findet immer in gleicher Orientierung (5´-PPAR:RXR-3´) an spezifischen „Response Elements“ des direkten Wiederholungstyps (DR-1), den PPREs, mit der Konsensus-Sequenz AGGTCA statt, welche durch ein beliebiges Nukleotid unterbrochen ist (Mangelsdorf & Evans, 1995; Palmer et al., 1995). Für PPARβ/δ-reprimierte Gene konnte darüber hinaus eine weitere Konsensus-Sequenz (GGGTCA-N-AGGTCA) identifiziert werden (Adhikary et al., 2011), sowie auch für Gene, die synergistisch durch TGFβ („Transforming Growth Factor“) und PPARβ/δ induziert werden (AGGGGA-N-AGGGGA) (Kaddatz et al., 2010). Zusätzlich wird die Bindung der Heterodimere an die DNA durch die 5´-flankierte Region des PPREs vermittelt, mit welcher die „Hinge“-Region der PPARs interagiert (Chandra et al., 2008; Hsu et al., 1998).

2.1.2.2 Cofaktoren

Für die transkriptionelle Aktivität der PPARs sind Cofaktoren notwendig, die eine Modifikation der Chromatinstruktur hervorrufen. In Abwesenheit eines Liganden liegen PPAR:RXR-Heterodimere in einem Komplex mit Corepressoren vor, die entweder selbst Histondeacetylase-Aktivität besitzen oder alternativ Histondeacetylasen rekrutieren (Guan et al., 2005). Als Corepressoren, die in Abwesenheit eines Liganden mit dem PPAR:RXR-Heterodimer komplexieren, wurden bisher NCoR („Nuclear Receptor Co-Repressor“), SMRT („Silencing Mediator of Retinoid and Thyroid Receptors“) und SHARP („SMRT and Histone Deacetylase-Associated Repressor Protein“) identifiziert (Krogsdam et al., 2002; Shi et al., 2002; Yu et al., 2005).

Durch die Interaktion spezifischer Agonisten kommt es zu einer Konformationsänderung der Ligandenbindungsdomäne (Wurtz et al., 1996), die eine Dissoziation der Corepressoren (Escher und Wahli 2000) sowie eine Rekrutierung von Coaktivatoren nach sich zieht (Heery et al., 1997; Torchia et al., 1997). Coaktivatoren wie CBP/p300 („CREB-Binding Protein“) und SRC-1/2/3 („Steroid Receptor Co-Activator“) besitzen eine intrinsische Histonacetylase-Aktivität und erzeugen eine Auflockerung des Chromatins (Dowell et al., 1997a; Krey et al., 1997), wohingegen das Coaktivator-assoziierte Protein CARM1 („Coactivator-Associated Arginine Methyltranferase 1“) über eine Methyltransferase-Aktivität verfügt (Dowell et al., 1997; Gelman et al., 1999; Lim et al., 2004). Der Cofaktor PGC1α („PPARγ Co-Activator 1α“) besitzt dagegen selbst keine enzymatische Aktivität, sondern verstärkt eine Rekrutierung der oben genannten Coaktivatoren (Lin et al., 2005).

2.1.2.3 Liganden

PPARs dienen innerhalb der Zelle als Lipidsensoren und setzen als solche nahrungsbedingte Veränderungen im Lipid- und Fettsäurehaushalt in metabolische Aktivität um (Evans et al., 2004). Natürliche endogene Liganden setzen sich daher aus einem breiten Spektrum gesättigter und ungesättigter Fettsäuren und deren Derivate zusammen (Berger and Moller 2002). Aufgrund der mäßigen Konservierung der LBD werden die unterschiedlichen PPAR-Subtypen durch verschiedenste Liganden reguliert (Michalik et al., 2006).

Eine spezifische Aktivierung des Subtypen PPARα wird vor allem für langkettige, ungesättigte Fettsäuren wie z. B. das Arachidonsäure-Derivat 8(S)-Hydroxy-eicosatetraensäure (HETE) beschrieben (Hihi et al., 2002; Zomer et al. 2000). Eine schwache Aktivierung von PPARα konnte zudem für Prostaglandine wie 15d-PGJ_2 nachgewiesen werden (Forman et al., 1997; Hihi et al., 2002). Im Gegensatz zu der nur schwachen Aktivierung von PPARα stellt 15d-PGJ_2 einen potenten, endogenen Liganden für PPARγ dar (Forman et al., 1995). Auch PPARβ/δ wird durch ungesättigte Fettsäuren wie Arachidonsäure, Linolsäure und Eicosapentaensäure, sowie durch Prostanoide des Cyclooxygenase-Metabolismus aktiviert (Forman et al., 1995; Yu et al., 1995). Untersuchungen unserer Arbeitsgruppe konnten den Arachidonsäure-Metaboliten 15-HETE als potenten, endogenen Liganden von PPARβ/δ identifizieren (Naruhn et al., 2010). Aufgrund der beschriebenen Affinität eines synthetischen Prostazyklin-Analogons wurde auch Prostazyklin (PGI_2) selbst als endogener PPARβ/δ-Ligand diskutiert (Gupta et al., 2000; Lim and Dey 2002; Fauti et al., 2006).

Auch *all-trans*-Retinsäure (atRA) wird als potenzieller Ligand für PPARβ/δ kontrovers diskutiert (Borland et al., 2008; Rieck et al., 2008).

Exogene, synthetische Agonisten, die in den vergangenen Jahren entwickelt wurden, weisen eine wesentlich höhere Affinität und Subtypspezifität auf. Zu ihnen zählen Fibrate, NSAIDS („Non Steroidal Anti Inflammatory Drugs“) und Thiazolidindione (TZDs) (Escher und Wahli 2000). Die Substanzklassen der Fibrate und der NSAIDS aktivieren PPARα. Allerdings wurde für beide Substanzgruppen bei hohen Konzentrationen auch ein aktivierender Effekt auf PPARγ beschrieben (Escher und Wahli 2000; Kliewer et al., 1997). TZDs wie Rosiglitazon wurden zur spezifischen Aktivierung von PPARγ bei Diabetes mellitus eingesetzt (Lehmann et al., 1995). Beträchtliche Nebenwirkungen Rosiglitazon-enthaltender Pharmaka haben in der Europäischen Union jedoch zur Marktrücknahme geführt. Auch für PPARβ/δ wurden eine Reihe hochaffiner Agonisten entwickelt, zu denen GW501516, L165,041 und GW0742 zählen (Hihi et al., 2002; Marin et al., 2006). Für den PPARβ/δ-spezifischen Liganden GW501516 sind zum jetzigen Zeitpunkt klinische Studien der Phase II zur Behandlung von Dyslipidämien abgeschlossen (Pelton, 2006).

Neben aktivierenden synthetischen Liganden stehen auch verschiedene inhibitorische Liganden für PPARs zur Verfügung. Die Aktivität von PPARα kann durch GW6471 gehemmt werden (Ding et al., 2007). Mit GW9662 steht zudem ein spezifischer PPARγ-Antagonist zur Verfügung (Leesnitzer et a., 2002). Neben dem inversen Agonisten GSK0660 konnten in unserer Arbeitsgruppe weitere PPARβ/δ-spezifische inverse Agonisten wie ST247, einem GSK0660-Derivat, sowie der Antagonist PT-S58 entwickelt werden (Naruhn et al., 2011).

2.1.3 Funktion von PPARβ/δ in biologischen und pathophysiologischen Prozessen

Die Funktionen von PPARβ/δ in biologischen und pathophysiologischen Prozessen sind aufgrund seiner ubiquitären Expression sehr vielfältig. PPARβ/δ reguliert Zielgene, die in den Fettsäure- und Cholesterol-Katabolismus involviert sind und übt entsprechend einen Einfluss auf die Energiehomöostase aus (Desvergne et al., 2006; Peters et al., 2000). Darüber hinaus kontrolliert PPARβ/δ in verschiedenen Zelltypen die Proliferation, Differenzierung und das Überleben der Zellen (Müller et al., 2008). Auch bei der Myelinisierung von Axonen im zentralen Nervensystem (Peters et al., 2000) und der Wundheilung konnte ein Einfluss von PPARβ/δ nachgewiesen werden (Di-Poï et al., 2002).

Die Rolle von PPARβ/δ in pathophysiologischen Prozessen wird zum Teil kontrovers diskutiert. So ist beispielsweise eine Beteiligung dieses Kernrezeptors bei Entstehungsprozessen der Atherosklerose zwar nachgewiesen (Evans et al., 2004), jedoch konnte bisher noch nicht geklärt werden, ob PPARβ/δ eine Entstehung dieser Erkrankung fördert oder ihr entgegenwirkt (Lee et al., 2003, Vosper et al., 2001). Ebenso widersprüchlich sind bisherige Studien, die sich mit der Rolle von PPARβ/δ in der Tumorgenese beschäftigen. So führt die Ligandenaktivierung des Rezeptors in verschiedenen Tumorzelllinien zu einem anti-proliferativen Effekt (Hollingshead et al., 2008; Hollingshead und Killins 2007), für eine pro-tumorigene Eigenschaft von PPARβ/δ sprechen jedoch Erkenntnisse, dass eine *Ppard*-Deletion in einer Wachstumshemmung syngener Tumoren resultiert (Müller-Brüsselbach et al., 2007).

2.1.4 Rolle von PPARβ/δ in inflammatorischen Prozessen

In verschiedenen Studien wurde eine Assoziation von PPARβ/δ mit inflammatorischen und immunregulatorischen Prozessen nachgewiesen.

So wurde beispielsweise beschrieben, dass PPARβ/δ-Agonisten bei der experimentellen autoimmunen Encephalomyelitis, einem Modell der Multiplen Sklerose, eine Entmyelinisierung der Markscheiden und damit einen Verlust der Axone verhindern (Kanakasabai et al., 2010). Auch bei der Polarisierung von Makrophagen zum anti-inflammatorischen M2-Typ in der Leber und im Fettgewebe wird PPARβ/δ eine zentrale Rolle zugeschrieben (Kang et al., 2008; Odegaard et al., 2008). In murinen Makrophagen interagiert PPARβ/δ in Abwesenheit von Liganden nachweislich mit Bcl6, was dazu führt, dass eine Repression pro-inflammatorischer Gene wie *Mcp-1* und *Mmp9* durch Bcl6 verhindert wird (Lee et al., 2003). Darüber hinaus ist PPARβ/δ in immunrelevanten Zellen auch ein direkter Einfluss auf die Expression von Zytokinen, Adhäsionsmolekülen und extrazellulären Matrixproteinen zugeschrieben worden (Kilgore & Billin, 2008).

2.2 Hämatopoese & Myelopoese

Als Hämatopoese wird der schrittweise Prozess der zellulären Blutbildung aus hämatopoetischen Stammzellen bezeichnet. Am Anfang dieses Prozesses steht eine kleine Subpopulation von Knochenmarkzellen, sogenannte LT-HSCs („Long-Term Hematopoietic Stem Cells“). LT-HSCs sind zur asymmetrischen Teilung fähig, so dass aus ihnen sowohl identische Tochterzellen als auch Zellen mit dem Potenzial zu sämtlichen Blutzellen zu differenzieren hervorgehen können. Über einen mehrstufigen

Differenzierungsprozess verlieren die in der Hämatopoese entstehenden Zellen ihr Selbsterneuerungspotenzial und nehmen gleichzeitig einen höheren Differenzierungsgrad an (Kondo et al., 2003; Weissman et al., 2001; Ogawa et al., 1993; Adolfsson et al., 2001; Osawa et al., 1996; Morrison et al., 1995; Christensen et al., 2001).

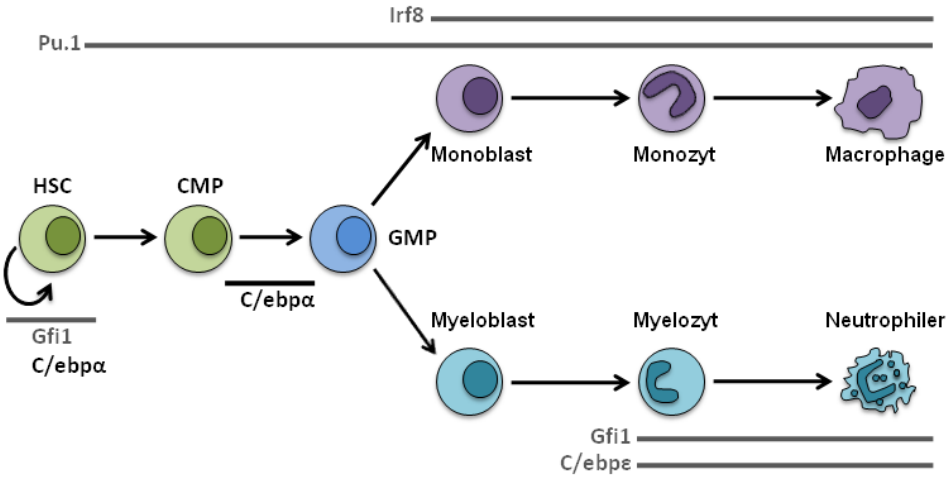

Schema 1: Hämatopoese (modifiziert nach Rosenbauer & Tenen)

Die Bildung myeloider Zellen wird durch wenige Transkriptionsfaktoren gesteuert, zu denen PU.1 („Purine Rich Box 1“), IRF8 („Interferon Regulatory Factor 8“) sowie GFI1 („Growth Factor Independent 1 Transcription Repressor“) und C/EBPε („CCAAT/Enhancer Binding Protein ε“) gehören (Zhang et al., 1997; Tanaka et al., 1995; Yamanaka et al., 1997; Hock et al., 2003). Die Expression von PU.1 unterscheidet sich zwischen den verschiedenen hämatopoetischen Zelllinien (Nutt et al., 2005; Back et al., 2005), wobei die Höhe seiner Expression scheinbar ausschlaggebend für die Differenzierungsrichtung ist, da eine geringe Expression mit der Bildung von Granulozyten assoziiert ist, wohingegen hohe Expressionraten der Differenzierung in Richtung Makrophagen zugeschrieben werden (Dahl et al., 2003; Rosenbauer et al., 2004). Im Falle der Differenzierung zu Antigen-präsentierenden Zellen ist ab dem GMP-Stadium („Granulocyte-Makrophage-Progenitors“) ein weiterer Transkriptionsfaktor, IRF8, von zentraler Bedeutung, welcher von GMPs, Makrophagen und dendritischen Zellen, jedoch nicht von Granulozyten exprimiert wird (Tamura et al., 2000). Für die Differenzierung zu Granulozyten spielen ebenfalls zwei Transkriptionsfaktoren eine herausragende Rolle, GFI1 und C/EBPε. In Knock-out-Modellen konnte gezeigt werden, dass sowohl das Fehlen von *Gfi1* als auch das Fehlen von *C/ebpε* zu einem Ausfall der Granulopoese führt, der mit dem Verlust von

Neutrophilen einhergeht (Yamanaka et al., 1997; Hock et al., 2003; Karsunky et al., 2002; Hock et al., 2006; Karsunky et al., 2002).

2.3 Ziel der vorliegenden Arbeit

Um die Funktion von PPARβ/δ bei biologischen und pathophysiologischen Prozessen zu untersuchen, sind spezifische Agonisten und *Ppard*-defiziente Mäuse gängige Instrumente. Da dieser Rezeptor jedoch vermutlich hauptsächlich repressorische Aktivität besitzt, sollte die Entwicklung spezifischer inverser Agonisten im Vordergrund stehen. Aus pharmakologischer Sicht ist es außerdem wünschenswert, bioverfügbare Liganden für eine mögliche Behandlung PPARβ/δ-assoziierter Erkrankungen zur Verfügung zu haben. Daher war das Ziel dieser Arbeit, neue PPARβ/δ-selektive inverse Agonisten zu identifizieren, durch die nicht nur die Funktionen von PPARβ/δ weiter aufgeklärt werden können, sondern die durch ihre Bioverfügbarkeit in der Zukunft auch therapeutisch einsetzbar sind.

Aufgrund vielzähliger Hinweise, dass PPARβ/δ immunregulatorische Prozesse beeinflusst, sollte im zweiten Teil der Arbeit untersucht werden, ob der Kernrezeptor auch in die Myelopoese eingreift. Da bereits in einem frühen Stadium der Untersuchungen ein starker PPARβ/δ-unabhängiger Effekt von DG172 erkennbar war, sollte im weiteren Verlauf dieser Effekt näher charakterisiert werden.

3 Ergebnisse

3.1 DG172: Ein bioverfügbarer PPARβ/δ-selektiver Ligand mit invers agonistischen Eigenschaften

Sonja Lieber, Frithjof Scheer, Wolfgang Meissner, Simone Naruhn, Till Adhikary, Sabine Müller-Brüsselbach, Wibke E. Diederich and Rolf Müller (2012) [(Z)-2-(2-bromophenyl)-3-{1-methyl-piperazin) amino] phenyl} acrylonitrile (DG172): An orally bioavailable PPARβ/δ-selective ligand with inverse agonistic properties. J. Med. Chem. 55: 2858-2868

Um die biologischen Funktionen von PPARβ/δ und die damit verbundenen komplexen transkriptionellen Signalwege besser verstehen zu können, ist es notwendig, die Entwicklung spezifischer Liganden voranzutreiben. So konnten in den vergangenen Jahren synthetische, bioverfügbare Agonisten entwickelt werden, die hochspezifisch für PPARβ/δ sind und reversibel binden. Da PPARβ/δ jedoch auch als Repressor bestimmter Zielgene fungiert, besteht ebenso Bedarf an der Entwicklung inhibitorischer Liganden, welche die gleichen Kriterien (Bioverfügbarkeit, Spezifität etc.) erfüllen. Substanzen wie GSK3787, GSK0660 und ST247, die bisher aus diesen Bemühungen hervorgegangen sind, sind entweder nicht spezifisch für PPARβ/δ und binden irreversibel (GSK3787) oder sie sind nicht bioverfügbar (GSK0660 und ST247) (Naruhn et al., 2011; Palkar et al., 2010; Shearer et al., 2010; Shearer et al. 2007).
Angesichts fehlender inhibitorischer PPARβ/δ-spezifischer Liganden, die für eine *in vivo*-Behandlung in Frage kommen, wurden über 2500 Substanzen einer Substanz-Bibliothek des NIH (National Institute of Health; Bethesda, Maryland (USA)) mit Hilfe eines „Time Resolved-Förster Resonanz Energie Transfer“ (TR-FRET)-basierten kompetitiven Ligandenbindungsassays auf mögliche Interaktionen mit PPARβ/δ untersucht. Die Funktionsweise des Assays beruht auf der Bindung eines fluoreszenten PAN-PPAR-Liganden (Fluorescein-Emission bei 520 nm) an die indirekt Terbium-markierte PPARβ/δ-LBD (Tb-Emission bei 495 nm). Durch die Interaktion des Liganden mit der LBD gelangen die beiden Fluorophore in unmittelbare Nähe zueinander, so dass bei Anregung des Terbiums ein Fluoreszenz-Resonanz-Energie-Transfer auf Fluorescein stattfindet. Die Verdrängung des markierten Liganden durch eine nicht markierte Testsubstanz äußert sich in einer konzentrationsabhängigen Abnahme der FRET-Ratio (520 nm/495 nm). Aus dieser Untersuchung gingen fast 200 Substanzen hervor, die in der Lage waren, an die PPARβ/δ-LBD zu binden und entsprechend den PAN-PPAR-Liganden zu verdrängen. Die Durchführung TR-FRET-basierter Coaktivator- und Corepressor-Rekrutierungs-Assays führte zur Identifizierung mehrerer Verbindungen, die sowohl eine Hemmung der Coaktivator-Interaktion mit der

LBD als auch eine verstärkte Corepressor-Rekrutierung zur LBD zeigten (Tabelle S1). Luziferase-Reportergen-Assays und Expressionsanalysen endogener PPARβ/δ-Zielgene wie *ANGPTL4* zeigten, dass (Z)-3-[4-(Dimethylamino)phenyl]-2-Phenylacrylnitril (Verbindung **1;** Schema 2) die transkriptionelle Aktivität von PPARβ/δ am effizientesten beeinflusste (Tabelle S1), so dass diese als Leitstruktur für die weitere Entwicklung optimierter Verbindungen in der sich anschließenden SAR-Studie hergenommen wurde.

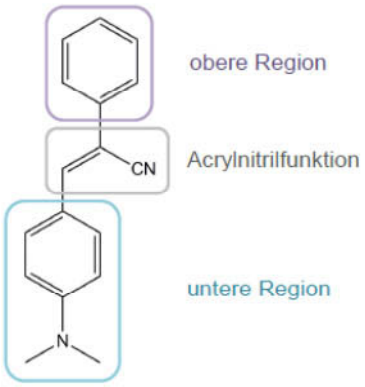

Schema 2: Strategie der Optimierung von Verbindung 1

In einer ersten Serie wurden Modifikationen des zentralen Acrylnitril-Restes vorgenommen, welche ausnahmslos zu einem Verlust der Affinität dieser Substanzen zur LBD führten (Abbildung S1). Auch der Austausch der *para*-Dimethylaminogruppe gegen andere funktionelle Gruppen an der unteren Region der Leitstruktur führte fast ausschließlich zu einem Aktivitätsverlust. Der systematische Austausch der Dimethylaminogruppe durch andere substituierte Amine in dieser zweiten Serie führte zu einer Aktivitätszunahme, umso sterisch anspruchsvoller der angebrachte Rest war. Vor allem durch sechsgliedrige Heterozyklen wie Piperidin in Verbindung mit einer Methylgruppe (Verbindungen **16** & **20**) war eine Aktivitätsverbesserung möglich. Diese konnte sogar durch die Anwesenheit eines zweiten Stickstoffs im Piperazin (Verbindung **22**) noch gesteigert werden. Endgültig bestätigt wurde diese Beobachtung durch eine additive Affinitätssteigerung unter Verwendung eines Methylpiperazinderivates (Verbindung **23**), in dem beide Strukturmerkmale enthalten sind (Abbildung 2). Die dritte Serie beinhaltete Modifikationen des Aromaten an der oberen Region der Leitstruktur. Wurden Substituenten in der *para*-Position des Phenylrings angebracht, führten diese Veränderungen grundsätzlich zum Verlust der Affinität. Als effizienteste Modifikationen in dieser Serie konnten letztlich die Halogen-Substituenten Chlor und Brom in der *ortho*-Position identifiziert werden (Verbindungen **29** & **31**) (Abbildung 3). Die Kombination der affinsten Substitutionen aus Serie zwei

(Einsatz des 4-Methylpiperazins) und drei (Halogenierung des Phenylrings) ergaben die Verbindung **37** (im Folgenden DG172 genannt).

Verbindung **29** und DG172 wurden weiteren Analysen bezüglich ihrer Affinität und Spezifität zu PPARβ/δ sowie ihrer inhibitorischen Effizienz unterzogen. Wie zu erwarten war, ergab eine Untersuchung mittels TR-FRET-basiertem Ligandenverdrängungsassay eine deutlich höhere Affinität von DG172 zu PPARβ/δ (IC_{50} = 26,9 nM) verglichen mit der Affinität der Verbindung **29** (IC_{50} ~ 180 nM). Durch den direkten Vergleich von DG172 mit den Verbindungen **1** (Leitstruktur) und **29** (*ortho*-Halogenierung) in diesem Assay wurde zudem bestätigt, dass die Kombination des 4-Methylpiperazins in der unteren Region mit der *ortho*-Bromierung des Phenylrings in der oberen Region einen additiven Effekt auf die Affinität hat (Abbildung 4a). In einem Corepressor-Rekrutierungs-Assay konnte durch beide Verbindungen eine deutliche Rekrutierung des Corepressor-Peptids SMRT-ID2 an die LBD beobachtet werden (Abbildung 4b). Um eine mögliche Affinität der Verbindungen zu PPARα und PPARγ ausschließen zu können, wurde ebenfalls die TR-FRET-Methode herangezogen. Abbildung 5 zeigt, dass Verbindung **29** und DG172 zu keiner nennenswerten Verdrängung des PAN-PPAR-Liganden von den Ligandenbindungsdomänen der Subtypen PPARα und PPARγ führen. Zudem wurden Luziferase-Reportergen-Assays mit dem LexA-Reporterkonstrukt und LexA-DBD-PPAR-LBD-Fusionsproteinen aller PPAR-Subtypen durchgeführt. In diesem zellbasierten Assay konnten Verbindung **29** und DG172 ausschließlich die Agonisten-induzierte transkriptionelle Aktivität von PPARβ/δ reprimieren (Abbildung 6a-c). Expressionsanalysen des etablierten PPARβ/δ-Zielgens *Angptl4* nach der Behandlung muriner Myoblasten (Abbildung 7a) und primärer Makrophagen (Abbildung 7b) mit DG172 zeigten eine ausgeprägte Repression der *Angptl4*-Expression (IC_{50} = 9,5 nM). Eine Chromatin-Immun-Präzipitation (ChIP-Analyse) der *ANGPTL4*-Promotor-Region in WPMY-1 Myofibroblasten gab darüber Aufschluss, dass durch die Behandlung dieser Zellen mit DG172 eine signifikant verstärkte Rekrutierung der Histondeacetylase 3 stattfindet (Abbildung 8). Nachdem sowohl in TR-FRET-basierten Assays als auch im zellulären System eine hocheffiziente Inhibition der PPARβ/δ-Aktivität durch DG172 gezeigt wurde, folgten pharmakokinetische Analysen zum Nachweis der Bioverfügbarkeit dieser Verbindung für mögliche *in vivo*-Applikationen. Die orale Verabreichung von 5 mg/kg ergab einen maximalen Plasmaspiegel (C_{max}) von 94 ng/ml, was einer Konzentration von 207 nM entspricht (Abbildung 9). Damit lag die maximale Plasmakonzentration nach oraler Verabreichung weit über den IC_{50}-Werten der *in vitro*- und der zellbasierten Assays. Darüber hinaus wurde in der pharmakokinetischen

Analyse nach oraler Verabreichung eine Halbwertszeit von DG172 im Blut von über sechs Stunden und eine Bioverfügbarkeit von 72 % nachgewiesen.

Der Eigenanteil zur Erstellung dieser Publikation umfasst den Versuchsaufbau, die Versuchsdurchführung und die Datenanalyse zu Figure 2, Figure 3, Figure 4A und B, Figure 5, Figure 6, Figure 7 und Table S2.

3.2 Eine PPARβ/δ-unabhängige Verschiebung der Differenzierung myeloider Knochenmarkszellen ausgelöst durch den inversen Agonisten DG172

Sonja Lieber, Frithjof Scheer, Florian Finkernagel, Wolfgang Meissner, Gavin Giel, Cornelia Brendel, Wibke E. Diederich, Sabine Müller-Brüsselbach and Rolf Müller (submitted, 2014)

In den vergangenen Jahren mehrten sich die Hinweise, dass PPARβ/δ auch eine immunregulatorische Rolle einnimmt (Kostadinova et al., 2005; Wahli and Michalik 2012; Yang et al., 2010).

In der vorliegenden Studie wurde entsprechend mit Hilfe von PPARβ/δ-selektiven Liganden und *Ppard*-defizienten Mäusen eine mögliche Beeinflussung der Myelopoese durch PPARβ/δ untersucht.

Die Differenzierung muriner Knochenmarkzellen (BMCs, „Bone marrow cells“) unter dem Wachstumsfaktor GM-CSF führt zu einer gemischten Population adhärenter und nicht-adhärenter Zellen, die sich aus neutrophilen Granulozyten, Makrophagen und dendritischen Zellen zusammensetzt (Inaba et al., 1992). Eine kombinierte Behandlung mit GM-CSF und dem Zytokin IL-4 fördert verstärkt die Differenzierung unreifer dendritischer Zellen (Schuler et al., 1999). Die Aktivität bzw. das Vorhandensein bestimmter Transkriptionsfaktoren ist für die Differenzierungsrichtung während der Myelopoese verantwortlich. Die Analyse dieser Transkriptionsfaktoren wie auch der Nachweis selektiv exprimierter Oberflächenmarker helfen bei der Unterscheidung der verschiedenen myeloiden Zelltypen (Inaba et al., 1992; Lee & Wang, 2013; León et al., 2014; Weischenfeldt & Porse, 2008; Schuler et al., 1999) und wurden in der vorliegenden Studie als experimentelles System genutzt.

Die Behandlung der BMCs während der Differenzierung unter GM-CSF mit IL-4 und/oder DG172 führte zu deutlichen morphologischen Veränderungen. Besonders auffällig wurden diese Veränderungen unter dem Einfluss von LPS. Mit IL-4 und LPS behandelte Zellen nahmen die Morphologie von reifen dendritischen Zellen (DC) mit den charakteristischen zytoplasmatischen Fortsätzen an (Abbildung 1C).

Interessanterweise wurde durch die Gabe von DG172 zusätzlich zu IL-4 der gleiche morphologische Effekt erzielt wie unter LPS-Behandlung (Abbildung 1D). FACS-Analysen der DC-Oberflächenmarker CD11c und MHCII zur weiteren Charakterisierung dieser Zellen ließen drei klar voneinander trennbare Populationen erkennen, P1 ($CD11c^{lo}/MHCII^{-}$), P2 ($CD11c^{hi}/MHCII^{lo}$) und P3 ($CD11c^{hi}/MHCII^{hi}$). Unter dem Einfluss von DG172 wurde eine Verschiebung der Zellen in Richtung P2 und P3 beobachtet. Die kombinierte Behandlung der BMCs mit IL-4 und DG172 während der Differenzierung schlug sich in einer extremen Zunahme der Population 3 mit dem Einhergehen einer Abnahme der Population 1 nieder, so dass von einem synergistischen Effekt ausgegangen werden kann (Abbildung 2A und B). Hervorzuheben ist hier, dass die beschriebenen Effekte auch in *Pparb*-defizienten Zellen beobachtet wurden (Abbildung 2C und D). Die parallel durchgeführte FACS-Phänotypisierung mittels der Oberflächenmarker CD14 und F4/80 zeigte, dass vor allem die CD14-Expression der Population 2 durch DG172 negativ beeinflusst wurde (Abbildung 3 A und B). Zudem nahm unter dem Einfluss von DG172 die F4/80-Expression sowohl in Population 2 als auch in Population 3 ab (Abbildung 3C und D). Die Analyse der klassischen Oberflächenmarker Ly6B und Gr1 neutrophiler Granulozyten im FACS ließ ebenfalls drei Populationen erkennen: PA ($Ly6B^{-}/Gr1^{-}$), PB ($Ly6B^{+}/Gr1^{-}$) und PC ($Ly6B^{+}/Gr1^{+}$), wobei die Population C ausdifferenzierte neutrophile Granulozyten repräsentiert. Eine Untersuchung dieser Populationen auf die DC-Oberflächenmarker CD11c und MHCII ergab, dass ausschließlich Zellen der Population A, die für granulozytäre Marker negativ sind, Oberflächenmarker dendritischer Zellen stark exprimieren und entsprechend der Population 3 der vorangegangenen Analyse zuzuordnen sind (Abbildung 4A). Eine Abnahme der neutrophilen Granulozyten im Laufe der Differenzierung kann als normaler Prozess eingestuft werden, allerdings wurde diese Abnahme durch DG172 erheblich beschleunigt, wenn eine minimale Dauer der Ligandenexposition von drei Tagen gegeben war (Abbildung 4B).

Eine funktionelle Annotation DG172-regulierter Gene anhand von Microarray-Daten ergab als führende Kategorien unter anderem „Immunantwort“, „Zellfortbewegung“ „Entwicklung und Funktion des hämatologischen Systems“ sowie „gezielte Fortbewegung von Immunzellen“ (Abbildung 5D und E). Die Aufteilung der DG172-regulierten Gene in einer funktionellen Analyse nach den zwei Hauptdifferenzierungsrichtungen der Myelopoese machte deutlich, dass charakteristische Gene neutrophiler Granulozyten wie *S100a8* und *Mmp9* stark reprimiert wurden, wohingegen charakteristische Gene Antigen-präsentierender Zellen wie *CD209* (*DC-Sign*) deutlich induziert wurden (Abbildung 6A und B). Der Einfluss von

DG172 auf die Differenzierung myeloider Zellen konnte neben diesen Transkriptom-Analysen exemplarisch an S100a8 auch durch Western-Blot-Analysen validiert werden (Abbildung 6C). Da die myeloide Differenzierung durch bestimmte Transkriptionsfaktoren gesteuert wird und diese Faktoren meist sowohl auf die Linie als auch auf ein begrenztes Stadium der Differenzierung begrenzt sind (Rosenbauer and Tenen 2007), wurde zur weiteren Charakterisierung des DG172-Effektes anhand der Array-Daten die Expression der korrespondierenden Gene analysiert. Ähnlich wie bei der vorangegangenen Analyse resultierte die Behandlung der Zellen mit DG172 auch bezüglich Linien- bzw. Zeitpunkt-spezifischer Transkriptionsfaktoren in einer Repression der Gene, die mit Neutrophilen assoziiert sind, wohingegen die Gene der APC-assoziierten Transkriptionsfaktoren induziert wurden (Abbildung 7A und C; APC: antigen presenting cells).

Zur Aufklärung des Zeitpunktes, an dem DG172 einen Einfluss auf die myeloide Differenzierung nimmt, wurden BMCs zu verschiedenen Zeitpunkten der Differenzierung mit DG172 behandelt. Anschließende Microarray-Analysen zeigten, dass über 50% der DG172-regulierten Gene in Zellen, die an Tag 2 der Differenzierung behandelt wurden, auch in Zellen reguliert wurden, die sechs Tage unter DG172-Einfluss standen. Wurden die Zellen zu einem späten Zeitpunkt (Tag 5) mit DG172 behandelt, konnte eine Überlappung nur noch bei ca. 5% der Gene beobachtet werden (Abbildung 5C). Diese Resultate decken sich mit FACS-Analysen der Oberflächenmarker CD11c und MHCII von BMCs, die zu verschiedenen Zeitpunkten behandelt wurden. Auch hier waren die Effekte auf die Marker-Expression am stärksten ausgeprägt, wenn DG172 ab Tag 1 bzw. Tag 2 der Differenzierung zugegeben wurde (Abbildung 8C und D). Anhand einer Expressionsanalyse charakteristischer Gene neutrophiler Granulozyten wurde der Einfluss von DG172 ebenfalls auf eine frühe Phase der Differenzierung um Tag 2 nachgewiesen (Abbildung 9A). Wurden BMCs unter dem Einfluss von M-CSF gleichzeitig mit DG172 behandelt, ließen sich keine Effekte von DG172 auf die Expression dieser Gene beobachten. Jedoch war sowohl in Zellen M-CSF-gesteuerter als auch in Zellen GM-CSF-gesteuerter Differenzierung ein PPARβ/δ-abhängiger Effekt von DG172 nachweisbar (Abbildung 9B). Gleiches traf für Thioglykollat-angelockte Makrophagen aus *Ppard*-Wildtyp- und Null-Mäusen sowie murine NIH/3T3 Fibroblasten zu. Auch hier blieb die Repression des charakterischen Neutrophilen-Gens *S100a8* nach DG172-Behandlung aus und klassische PPARβ/δ-Zielgene wie *Angptl4* wurden in Wildtyp-Makrophagen und murinen Fibroblasten reprimiert (Abbildung 9C).

Strukturanalysen mittels verschiedener DG172-Derivate geben Anlass zu der Vermutung, dass PPARβ/δ-abhängige und unabhängige DG172-Effekte strukturell

voneinander trennbar sind. FACS-Analysen der CD11c- und MHCII-Expression zeigten, dass nur Derivate mit einem *N*-Methylpiperazin am unteren Aromaten DG172-ähnliche Effekte auf die BMC-Differenzierung hatten, wohingegen diese Gruppe für die Bindung an PPARβ/δ im TR-FRET-basierten Assay nicht zwingend notwendig zu sein scheint. Eine Halogenierung in der *para*-Position des oberen Aromaten führt zu einem völligen Verlust der Affinität solcher Derivate gegenüber PPARβ/δ (Lieber et al., 2012). DG139, eine Verbindung, die eine Halogenierung in der *para*-Position besitzt, sowie ein tertiäres Amin statt des *N*-Methylpiperazins, konnte weder die BMC-Differenzierung beeinflussen noch den PAN-PPAR-Liganden im TR-FRET-basierten Assay verdrängen. Durch einen Austausch des tertiären Amins durch *N*-Methylpiperazin (DG228) wurden die Struktureigenschaften vereint, die eine BMC-Differenzierung mutmaßlich beeinflussen und eine Bindung an PPARβ/δ verhindern. Durch FACS- und TR-FRET-Analysen konnte bestätigt werden, dass DG228 die BMC-Differenzierung stark beeinflusst, ohne eine nennenswerte Bindung an PPARβ/δ zu zeigen (Abbildung 10).

Der Eigenanteil zur Erstellung dieser Publikation umfasst die Beteiligung am Schreiben des Manuskripts sowie Versuchsaufbau, Durchführung und Datenanalyse zu Figure 1, Figure 2, Figure 3, Figure 4, Figure 6B und C, Figure 7C, Figure 8, Figure 9 und Figure 10 und Versuchsaufbau und Durchführung zu Figure 5, Figure 6A und Figure 7A.

4 Diskussion

4.1 DG172: Ein bioverfügbarer PPARβ/δ-selektiver Ligand mit invers agonistischen Eigenschaften

In Lieber et al., 2012 wurde in einer SAR-Studie mittels TR-FRET-basierter Assays nach neuen chemischen Strukturen gesucht, die als Leitstruktur für verbesserte inverse PPARβ/δ-Agonisten dienen sollten.

Aufgrund ihrer in verschiedenen Assays nachgewiesenen inhibitorischen Eigenschaften wurde NSC636948 (Verbindung **1**) als Leitstruktur für die weitere Strukturoptimierung hergenommen.

Modifikationen der ersten Serie, die an der Acrylnitrilfunktion vorgenommen wurden, führten zu einem Verlust der Aktivität, was darauf schließen lässt, dass dieser Rest entscheidend für die inhibitorische Aktivität ist (Abbildung S1).

Die Beobachtung, dass substituierte Amine in direkter Nachbarschaft des unteren Phenylrings zu einer Aktivitätssteigerung führten, deutet darauf hin, dass die Verstärkung der Mesomerie durch das entstandene *push-pull*-System essentiell für die Bindung an PPARβ/δ ist. Diese Annahme konnte durch das Einbringen eines Dimethylaminomethylenrests in der *para*-Position bestätigt werden. Hier führte die Unterbrechung des *push-pull*-Systems durch die Methylgruppe zum Verlust der Affinität. Zudem führte der Austausch der *para*-Dimethylaminogruppe zu der Erkenntnis, dass sowohl durch eine Methylgruppe an, als auch durch einen zweiten Stickstoff in einem Sechsring eine Affinitätssteigerung erreicht wurde und diese vereinten Strukturmerkmale im *N*-Methylpiperazin additive Auswirkungen hatten (Abbildung 2). Diese Ergebnisse legen die Vermutung nahe, dass für eine optimale Bindung an PPARβ/δ sowohl ein *push-pull*-System als auch ein bestimmter sterischer Anspruch gegeben sein müssen.

Substitutionen am Aromaten der oberen Region führten zu einem Aktivitätsverlust der Derivate, wenn diese an der *para*-Position vorgenommen wurden. Möglicherweise kommt es bei Substitutionen in dieser Position zu sterischen Hinderungen, die eine Bindung in der PPARβ/δ-LBD verhindern. Unterstützt wird diese Vermutung durch die Beobachtung, dass die Verschiebung des Substituenten an die *ortho*-Position zu einem starken Affinitätsgewinn führte. Als effizienteste Substituenten in der *ortho*-Position erwiesen sich hierbei die Halogene Chlor, Iod und Brom. Obwohl ebenfalls ein Halogen, führte die Substitution durch Fluor zu keinem Aktivitätsgewinn (Abbildung 3). Ein Grund hierfür könnte eine ungünstige Elektronenverteilung durch den stärkeren negativen induktiven Effekt des Fluors sein. Eine Kombination des *N*-Methylpiperazins

mit der Halogenierung der *ortho*-Position ergab Verbindung **37** (DG172). Durch einen Vergleich von DG172 mit Verbindung **29** (*ortho*-Halogenierung) und Verbindung **1** wurde ein additiver Effekt der besten Modifikationen nachgewiesen (Abbildung 4a). Neben einer deutlich verbesserten Affinität zu PPARβ/δ wurde sowohl durch Verbindung **29** als auch durch DG172 eine verstärkte Rekrutierung des synthetischen Corepressor-Peptids SMRT-ID2 erreicht, welche eine Charakterisierung dieser Liganden als inverse Agonisten zulässt (Abbildung 4b). Da beide Verbindungen keine nachweisbaren Effekte auf die Subtypen α und γ hatten (Abbildung 5a und b), ist es sehr wahrscheinlich, dass die Repression des etablierten PPARβ/δ-Zielgens *Angptl4* in murinen C2C12 Myoblasten auf die Bindung der beiden inversen Agonisten an PPARβ/δ zurückzuführen ist (Abbildung 7). Die sich anschließende Chromatin-Immun-Präzipitation zeigte eine deutlich verstärkte Rekrutierung der HDAC3 an den *ANGPTL4* Promotor durch DG172, was mit einer Repression der Transaktivierung assoziiert ist (Abbildung 8). Die vergleichbare Rekrutierung der Histondeacetylase durch GSK0660 lässt sich nicht mit der höheren Effizienz von DG172 in vorangegangenen Analysen der *Angptl4*-Expression in Einklang bringen. Es ist möglich, dass durch eine Behandlung mit DG172 weitere, bisher nicht identifizierte Corepressoren rekrutiert werden, die für die deutlich stärkere Repression des Zielgens verantwortlich sind. In pharmakokinetischen Analysen konnte zudem gezeigt werden, dass DG172 im Gegensatz zu Verbindung **29** nach oraler Verabreichung in ausreichender Konzentration (ca. 200 nM) im Blutplasma nachweisbar und somit bioverfügbar ist, was den Schluss zulässt, dass das *N*-Methylpiperazin neben der erhöhten Affinität zu PPARβ/δ auch für die Bioverfügbarkeit verantwortlich ist (Abbildung 9).

In ersten *in vivo*-Analysen mittels Thioglykollat-angelockter Makrophagen aus *Ppard*-Wildtyp- und Null-Mäusen wurden sowohl die sehr guten inhibitorischen Eigenschaften als auch die hohe Selektivität des inversen Agonisten DG172 bestätigt (Abbildung 7b).

DG172 stellt damit als erster Subtyp-spezifischer, bioverfügbarer und inverser PPARβ/δ-Agonist ein hervorragendes Werkzeug zur Untersuchung biologischer und pathophysiologischer Funktionen von PPARβ/δ dar, der auch für *in vivo*-Applikationen geeignet ist.

4.2 Eine PPARβ/δ-unabhängige Verschiebung der Differenzierung myeloider Knochenmarkszellen ausgelöst durch den inversen Agonisten DG172

In der vorliegenden Studie wurde mit Hilfe von BMCs aus *Ppard*-Wildtyp- und Null-Mäusen sowie PPARβ/δ-spezifischer Liganden eine mögliche Beeinflussung der Myelopoese durch PPARβ/δ analysiert.

Die morphologischen Veränderungen von BMCs durch DG172 unter dem Differenzierungs-Stimulus GM-CSF legte die Vermutung nahe, dass PPARβ/δ bzw. der inverse Agonist DG172 entweder einen Einfluss auf die Differenzierung zu Makrophagen oder auf die Differenzierung zu dendritischen Zellen hat (Abbildung 1B), da eine Differenzierung unter GM-CSF zu einer gemischten Population aus Makrophagen, dendritischen Zellen und Neutrophilen führt (Inaba et al., 1992). Die kombinierte Behandlung mit IL-4 und LPS während der Differenzierung unter GM-CSF fördert bekanntermaßen die Generierung und Reifung dendritischer Zellen (Dearman und Cumberbatch, 2009; Schuler et al., 1999). Die Beobachtung, dass durch DG172 ein morphologisch identischer Effekt wie unter LPS-Behandlung erreicht wurde, deutet darauf hin, dass der inverse Agonist einen Einfluss auf die Differenzierung bzw. Reifung dendritischer Zellen hat (Abbildung 1D und E). Zu beachten ist hier allerdings, dass sich der morphologische Effekt durch LPS bereits nach 24 – 36 Stunden einstellte, wohingegen eine DG172-Exposition ab einem frühen Stadium der Differenzierung notwendig war, um diese Morphologie zu erhalten. Eine Aktivierung der unreifen dendritischen Zellen durch LPS oder andere Stimuli beinhaltet auch immer deren endgültige Reifung. Möglicherweise wird unter DG172-Einfluss eine Reifung der dendritischen Zellen gefördert, ohne direkt eine Aktivierung zur Folge zu haben. Anschließende FACS-Analysen untermauerten die Hypothese, dass DG172 seinen Einfluss vor allem auf die Differenzierung dendritischer Zellen ausübt. Durch die Behandlung der BMCs mit DG172 konnte eine starke Zunahme der Population 3 ($CD11c^{hi}MHCII^{hi}$) verzeichnet werden. Die Tatsache, dass durch kombinierte Behandlung von IL-4 und DG172 noch ein Anwachsen der Population 3 erreicht wurde, lässt einen synergistischen Effekt von DG172 und IL-4 vermuten. Zusätzlich wurde durch DG172 die Differenzierung einer zweiten Population (P2; $CD11c^{hi}MHCII^{lo}$) induziert (Abbildung 2A und B). Möglicherweise handelt es sich bei dieser Population um unreife dendritische Zellen, die unter GM-CSF-Einfluss in Kultur schon beschrieben wurden (León et al., 2014; Masurier et al., 1999). Da unter dem zusätzlichen IL-4-Stimulus die Population 3 der reifen dendritischen Zellen auf Kosten der Population 2 zunimmt, würde dies auch eine Erklärung für den beobachteten synergistischen Effekt

liefern: DG172 fördert die Differenzierung der P1 zu P2 und der P2 zu P3, wobei IL-4 letztere zusätzlich induziert. Sämtliche oben beschriebenen Effekte wurden sowohl in den BMCs aus *Ppard*-Wildtyp- als auch in BMCs aus *Ppard*-Null-Mäusen beobachtet, was eine Beteiligung von PPARβ/δ ausschließt (Abbildung 2C und D). Die Untersuchung verschiedener DG172-Derivate zeigte, dass eine strukturelle Trennung zwischen PPARβ/δ-abhängigem Effekt auf klassische Zielgene und PPARβ/δ-unabhängigem Effekt auf die BMC-Differenzierung möglich ist und ein *N*-Methylpiperazin in der para-Position des unteren Phenyls für die Beeinflussung der Differenzierung notwendig ist (Abbildung 10).

Die Analyse der Granulozyten-spezifischen Oberflächenmarker Ly6B und Gr1 ließ zudem einen Effekt von DG172 auf die Neutrophilen-Population erkennen (Abbildung 4A). Isolierte BMCs enthalten schon reife neutrophile Granulozyten, deren Population im Laufe der Differenzierung zwar abnimmt, die jedoch durch differenzierende BMCs teilweise ersetzt werden (Inaba et al., 1992). Die Abnahme dieser Zellen wurde durch die Behandlung mit DG172 deutlich beschleunigt (Abbildung 4B). Hier könnten verschiedene Mechanismen als Erklärung dienen. Zum einen ist es möglich, dass DG172 zu einem frühen Zeitpunkt die Myelopoese beeinflusst und im Stadium der Granulozyten-Makrophagen-Progenitoren (GMPs) die Differenzierung in Richtung der monozytären Linie drängt. Oder der Effekt von DG172 greift zu einem späteren Zeitpunkt nach dem GMP-Stadium und blockt die Granulopoese zum Vorteil der Monozyten- und DC-Differenzierung.

Untersuchungen zur Eingrenzung des Zeitpunktes, in dem DG172 in die Myelopoese eingreift, lieferten eindeutig den Hinweis, dass DG172 schon zu einem frühen Zeitpunkt die BMC-Differenzierung beeinflusst. Nach drei Tagen kontinuierlicher Behandlung wurde eine Abnahme der doppelt positiven Zellen für die Marker Ly6b und Gr1 (Population C) sichtbar. Dabei scheint die Verringerung der Population C mit einer Zunahme der Population A ($Ly6B^{-}/Gr1^{-}$) zu korrelieren (Abbildung 4B). Ausschließlich Zellen der Population A waren zudem $CD11c^{hi}/MHCII^{hi}$, ein eindeutiger Hinweis darauf, dass es sich bei dieser Population um die Population 3 der vorangegangenen FACS-Analysen handelte und die verstärkte Differenzierung dendritischer Zellen auf Kosten neutrophiler Granulozyten ging (Abbildung 4A). Eine frühe Beeinflussung der Myelopoese nach Behandlung der BMCs mit DG172 konnte auch durch RT-qPCR-Analysen bestätigt werden. Klassische Neutrophilen-Gene wie *S100a8* und *Mmp9* wurden umso stärker reprimiert, je früher mit einer Behandlung begonnen wurde (Abbildung 9).

In Microarray-Analysen behandelter BMCs aus *Ppard*-Null-Mäusen wurde zudem eine Beeinflussung des Transkriptoms durch DG172 festgestellt, die sich mit den

vorangegangenen Resultaten deckt. Gene, deren Expression mit neutrophilen Granulozyten assoziiert sind wurden stark reprimiert, wohingegen charakteristische Gene Antigen-präsentierender Zellen wie Makrophagen und dendritische Zellen induziert wurden (Abbildung 6A und B). Zudem wurden auch für Transkriptionsfaktoren codierende Gene, die für die Differenzierung neutrophiler Granulozyten verantwortlich gemacht werden, deutlich reprimiert. Die Expression der für die Differenzierung von APCs notwendigen Transkriptionsfaktoren wurde entsprechend induziert (Abbildung 7A und B). Die nachweisliche Beeinflussung dieser Gene unterstützt die Hypothese, dass DG172 zu einem frühen Zeitpunkt der Myelopoese im Stadium der GMPs seinen Einfluss nimmt. Eine funktionelle Annotation der regulierten Gene belegt zudem, dass eine Vielzahl dieser Gene bei der Entwicklung und Funktion des hämatologischen Systems und einer Immunantwort relevant sind.

Welches Protein das Ziel von DG172 in der Myelopoese ist, konnte bisher nicht geklärt werden.

Aufgrund seiner nachgewiesenen Bioverfügbarkeit stellt DG172 jedoch ein vielversprechendes Mittel für therapeutische Applikationen dar. Hierfür muss in sich anschließenden Untersuchungen festgestellt werden, ob die gleichen Effekte auf die Differenzierung auch in humanen BMCs beobachtet werden können und DG172 somit therapeutisch anwendbar wäre.

5 Literaturverzeichnis

Adhikary T, Kaddatz K, Finkernagel F, Schönbauer A, Meissner W, Scharfe M, Jarek M, Blöcker H, Müller-Brüsselbach S, Müller R (2011) Genomewide analyses define different modes of transcriptional regulation by peroxisome proliferator-activated receptor-β/δ. PLoS One 6: e16344

Adolfsson J, Borge OJ, Bryder D, Theilgaard-Mönch K, Astrand-Grundström I, Sitnicka E, Sasaki Y, Jacobsen SE (2001) Upregulation of Flt3 expression within the bone marrow Lin(-)Sca1(+)c-kit(+) stem cell compartment is accompanied by loss of self-renewal capacity. Immunity 15: 659-669

Aranda A, Pascual A (2001) Nuclear hormone receptors and gene expression. Physiol Rev 81: 1269-12304

Back J, Allman D, Chan S, Kastner P (2005) Visualizing PU.1 activity during hematopoiesis. Exp Hematol 33: 395-402

Berger J, Moller DE (2002) The mechanisms of action of PPARs. Annu Rev Med 53: 409-435

Borland MG, Foreman JE, Girroir EE, Zolfaghari R, Sharma AK, Amin S, Gonzalez FJ, Ross AC, Peters JM (2008) Ligand activation of peroxisome proliferator-activated receptor-beta/delta inhibits cell proliferation in human HaCaT keratinocytes. Mol Pharmacol 74: 1429-1442

Chandra V, Huang P, Hamuro Y, Raghuram S, Wang Y, Burris TP, Rastinejad F (2008) Structure of the intact PPAR-gamma-RXR- nuclear receptor complex on DNA. Nature 465: 350-356

Christensen JL, Weissman IL (2001) Flk-2 is a marker in hematopoietic stem cell differentiation: a simple method to isolate long-term stem cells. Proc Natl Acad Sci U S A 98: 14541-14546

Dahl R, Walsh JC, Lancki D, Laslo P, Iyer SR, Singh H, Simon MC (2003) Regulation of macrophage and neutrophil cell fates by the PU.1:C/EBPalpha ratio and granulocyte colony stimulating factor. Nat Immunol 4: 1029-1036

Dearman RJ, Cumberbatch M, Maxwell G, Basketter DA, Kimber I (2009) Toll-like receptor ligand activation of murine bone marrow-derived dendritic cells. Immunology 126: 475-484

Desvergne B, Michalik L, Wahli W (2006) Transcriptional regulation of metabolism. Physiol Rev 86: 465-514

Di-Poï N, Tan NS, Michalik L, Wahli W, Desvergne B (2002) Antiapoptotic role of PPARbeta in keratinocytes via transcriptional control of the Akt1 signaling pathway. Mol Cell 10: 721-733

Ding L, Liang XG, Lou YJ (2007) Time-dependence of cardiomyocyte differentiation disturbed by peroxisome proliferator-activated receptor alpha inhibitor GW6471 in murine embryonic stem cells in vitro. Acta Pharmacol Sin 28: 634-642

Dowell P, Ishmael JE, Avram D, Peterson VJ, Nevrivy DJ, Leid M (1997) p300 functions as a coactivator for the peroxisome proliferator-activated receptor alpha. J Biol Chem 272: 33435-33443

Escher P, Wahli W (2000) Peroxisome proliferator-activated receptors: insight into multiple cellular functions. Mutat Res 448: 121-138

Evans RM, Barish GD, Wang YX (2004) PPARs and the complex journey to obesity. Nat Med 10: 355-361

Fauti T, Müller-Brüsselbach S, Kreutzer M, Rieck M, Meissner W, Rapp U, Schweer H, Kömhoff M, Müller R (2006) Induction of PPARbeta and prostacyclin (PGI2) synthesis by RAF signaling: failure of PGI2 to activate PPARbeta. FEBS J 273: 170-179

Feige JN, Gelman L, Tudor C, Engelborghs Y, Wahli W, Desvergne B (2005) Fluorescence imaging reveals the nuclear behavior of peroxisome proliferator-activated receptor/retinoid X receptor heterodimers in the absence and presence of ligand. J Biol Chem 280: 17880-17890

Forman BM, Chen J, Evans RM (1997) Hypolipidemic drugs, polyunsaturated fatty acids, and eicosanoids are ligands for peroxisome proliferator-activated receptors alpha and delta. Proc Natl Acad Sci U S A 94: 4312-4317

Forman BM, Tontonoz P, Chen J, Brun RP, Spiegelman BM, Evans RM (1995) 15-Deoxy-delta 12, 14-prostaglandin J2 is a ligand for the adipocyte determination factor PPAR gamma. Cell 83: 803-812

Gelman L, Auwerx J (1999) Peroxisome proliferator-activated receptors: mediators of a fast food impact on gene regulation. Curr Opin Clin Nutr Metab Care 2: 307-312

Guan HP, Ishizuka T, Chui PC, Lehrke M, Lazar MA (2005) Corepressors selectively control the transcriptional activity of PPARgamma in adipocytes. Genes Dev 19: 453-461

Gupta RA, Tan J, Krause WF, Geraci MW, Willson TM, Dey SK, DuBois RN (2000) Prostacyclin-mediated activation of peroxisome proliferator-activated receptor delta in colorectal cancer. Proc Natl Acad Sci U S A 97: 13275-13280

Heery DM, Kalkhoven E, Hoare S, Parker MG (1997) A signature motif in transcriptional co-activators mediates binding to nuclear receptors. Nature 387: 733-736

Hihi AK, Michalik L, Wahli W (2002) PPARs: transcriptional effectors of fatty acids and their derivatives. Cell Mol Life Sci 59: 790-798

Hock H, Hamblen MJ, Rooke HM, Traver D, Bronson RT, Cameron S, Orkin SH (2003) Intrinsic requirement for zinc finger transcription factor Gfi-1 in neutrophil differentiation. Immunity 18: 109-120

Hock H, Orkin SH (2006) Zinc-finger transcription factor Gfi-1: versatile regulator of lymphocytes, neutrophils and hematopoietic stem cells. Curr Opin Hematol 13: 1-6

Hollingshead HE, Borland MG, Billin AN, Willson TM, Gonzalez FJ, Peters JM (2008) Ligand activation of peroxisome proliferator-activated receptor beta/delta (PPARbeta/delta) and inhibition of cyclooxygenase 2 (COX2) attenuate colon

carcinogenesis through independent signaling mechanisms. Carcinogenesis 29: 169-176

Hollingshead HE, Killins RL, Borland MG, Girroir EE, Billin AN, Willson TM, Sharma AK, Amin S, Gonzalez FJ, Peters JM (2007) Peroxisome proliferator-activated receptor-beta/delta (PPARbeta/delta) ligands do not potentiate growth of human cancer cell lines. Carcinogenesis 28: 2641-2649

Hsu MH, Palmer CN, Song W, Griffin KJ, Johnson EF (1998) A carboxyl-terminal extension of the zinc fnger domain contributes to the specificity and polarity of peroxisome proliferator-activated receptor DNA binding. J Biol Chem 273: 27988-27997

Inaba K, Inaba M, Romani N, Aya H, Deguchi M, Ikehara S, Muramatsu S, Steinman RM (1992) Generation of large numbers of dendritic cells from mouse bone marrow cultures supplemented with granulocyte/macrophage colony-stimulating factor. J Exp Med 176: 1693-1702

Kanakasabei S, Chearwae W, Walline CC, Iams W, Adams SM, Bright JJ (2010) Peroxisome proliferator-activated receptor delta agonists inhibit T helper type 1 (Th1) and Th17 responses in experimental allergic encephalomyelitis. Immunology 130: 572-588

Kang K, Reilly SM, Karabacak V, Gangl MR, Fitzgerald K, Hatano B, Lee CH (2008) Adipocyte-derived Th2 cytokines and myeloid PPARdelta regulate macrophage polarization and insulin sensitivity. Cell Metab 7: 485-495

Karsunky H, Zeng H, Schmidt T, Zevnik B, Kluge R, Schmid KW, Dührsen U, Möröy T (2002) Inflammatory reactions and severe neutropenia in mice lacking the transcriptional repressor Gfi1. Nat Genet 30: 295-300

Kilgore KS, Billin AN (2008) PPARbeta/delta ligands as modulators of the inflammatory response. Curr Opin Investig Drugs 9: 463-469

Kliewer SA, Sundseth SS, Jones SA, Brown PJ, Wisely GB, Koble CS, Devchand P, Wahli W, Willson TM, Lenhard JM, Lehmann JM (1997) Fatty acids and eicosanoids regulate gene expression through direct interactions with peroxisome proliferator-activated receptors alpha and gamma. Proc Natl Acad Sci U S A 94: 4318-4323

Kondo M, Wagers AJ, Manz MG, Prohaska SS, Scherer DC, Beilhack GF, Shizuru JA, Weissman IL (2003) Biology of hematopoietic stem cells and progenitors: implications for clinical application. Annu Rev Immunol 21: 759-806

Kostadinova R, Wahli W, Michalik L (2005) PPARs in diseases: control mechanisms of inflammation. Curr Med Chem 25: 2995-3009

Krey G, Braissant O, L'Horset F, Kalkhoven E, Perroud M, Parker MG, Wahli W (1997) Fatty acids, eicosanoids, and hypolipidemic agents identified as ligands of peroxisome proliferator-activated receptors by coactivator-dependent receptor ligand assay. Mol Endocrinol 6: 779-791

Krogsdam AM, Nielsen CA, Neve S, Holst D, Helledie T, Thomsen B, Bendixen C, Mandrup S, Kristiansen K (2002) Nulear receptor corepressor-dependent repression of peroxisome proliferator-activated receptor delta-mediated transactivation. Biochem J 363: 157-165

Laudet V, Hänni C, Coll J, Catzeflis F, Stéhelin D (1992) Evolution of the nuclear receptor gene superfamily. EMBO J 11: 1003-1013

Lee CH, Chawla A, Urbiztondo N, Liao D, Boisvert WA, Evans RM, Curtiss LK: (2003) Transcriptional repression of atherogenic inflammation: modulation by PPARdelta. Science 302: 453-457

Lee PY, Wang JX, Parisini E, Dascher CC, Nigrovic PA (2013) Ly6 family proteins in neutrophil biology. J Leukoc Biol 94: 585-594

Leesnitzer LM, Parks DJ, Bledsoe RK, Cobb JE, Collins JL, Consler TG, Davis RG, Hull-Ryde EA, Lenhard JM, Patel L, Plunket KD, Shenk JL, Stimmel JB, Therapontos C, Willson TM, Blanchard SG (2002) Functional consequences of cysteine modification in the ligand binding sites of peroxisome proliferator activated receptors by GW9662. Biochemistry 41: 6640-6650

Lehmann JM, Moore LB, Smith-Oliver TA, Wilkison WO, Willson TM, Kliewer SA (1995) An antidiabetic thiazolidinedione is a high affinity ligand for peroxisome proliferator-activated receptor gamma (PPAR gamma). J Biol Chem 270: 12953-12956

Léon B, Martinez del Hoyo G, Parrillas V, Vargas HH, Sanchez-Mateos P, Longo N, Lopez-Bravo M, Ardavin C (2004) Dendritic cell differentiation potential of mouse monocytes: monocytes represent immediate precursors of CD8- and CD8+ splenic dendritic cells. Blood 103: 2668-2676

Lim H, Dey SK (2002) A novel pathway of prostacyclin signaling-hanging out with nuclear receptors. Endocrinology 143: 3207-3210

Lim HJ, Moon I, Han K (2004) Transcriptional cofactors exhibit differential preference toward peroxisome proliferator-activated receptors alpha and delta in uterine cells. Endocrinology 145: 2886-2895

Lin J, Handschin C, Spiegelman BM (2005) Metabolic control through the PGC-1 family of transcription coactivators. Cell Metab 6: 361-370

Mangelsdorf DJ, Evans RM (1995) The RXR heterodimers and orphan receptors. Cell 83: 841-850

Marin HE, Peraza MA, Billin AN, Willson TM, Ward JM, Kennett MJ, Gonzalez FJ, Peters JM (2006) Ligand activation of peroxisome proliferator-activated receptor beta inhibits colon carcinogenesis. Cancer Res 66: 4394-4401

Masurier C, Pioche-Durieu C, Colombo BM, Lacave R, Lemoine FM, Klatzmann D and Guigon M (1999) Immunophenotypical and functional heterogeneity of dendritic cells generated from murine bone marrow cultured with different cytokine combinations: implications for anti-tumoral cell therapy. Immunology 96: 569-577

Michalik L, Auwerx J, Berger JP, Chatterjee VK, Glass CK, Gonzalez FJ, Grimaldi PA, Kadowaki T, Lazar MA, O'Rahilly S, Palmer CN, Plutzky J, Reddy JK, Spiegelman BM, Staels B, Wahli W (2006) International Union of Pharmacology. LXI. Peroxisome proliferator-activated receptors. Pharmacol Rev 58: 726-741

Morrison SJ, Uchida N, Weissman IL (1995) the biology of hematopoietic stem cells. Annu Rev Cell Dev Biol 11: 35-71

Müller R, Rieck M, Müller-Brüsselbach S (2008) Regulation of cell proliferation and differentiation by PPARbeta/delta. PPAR Res 2008: 614852

Müller-Brüsselbach S, Kömhoff M, Rieck M, Meissner W, Kaddatz K, Adamkiewicz J, Keil B, Klose KJ, Moll R, Burdick AD, Peters JM, Müller R (2007) Deregulation of tumor angiogenesis and blockade of tumor growth in PPARbeta-deficient mice. EMBO J 26: 3686-3698

Naruhn S, Meissner W, Adhikary T, Kaddatz K, Klein T, Watzer B, Müller-Brüsselbach S, Müller R (2010) 15-hydroxyeicosatetraenoic acid is a preferential peroxisome proliferator-activated receptor beta/delta agonist. Mol Pharmacol 77: 171-184

Naruhn S, Toth PM, Adhikary T, Kaddatz K, Pape V, Dörr S, Klebe G, Müller-Brüsselbach S, Diederich WE, Müller R (2011) High-affinity peroxisome proliferator-activated receptor β/δ-specific ligands with pure antagonistic or inverse agonistic properties. Mol Pharmacol 80: 828-838

Nolte RT, Wisely GB, Westin S, Cobb JE, Lambert MH, Kurokawa R, Rosenfeld MG, Willson TM, Glass CK, Milburn MV (1998) Ligand binding and co-activator assembly of the peroxisome proliferator-activated receptor-gamma. Nature 395: 137-143

Nutt SL, Metcalf D, D'Amico A, Polli M, Wu L (2005) Dynamic regulation of PU.1 expression in multipotent hematopoietic progenitors. J Exp Med 201: 221-231

Odegaard JI, Ricardo-Gonzalez RR, Red Eagle A, Vats D, Morel CR, Goforth MH, Subramanian V, Mukundan L, Ferrante AW, Chawla A (2008) Alternative M2 activation of Kupffer cells by PPARdelta ameliorates obesity-induced insulin resistance. Cell Metab 7: 496-507

Ogawa M (1993) Differentiation and proliferation of hematopoietic stem cells. Blood 81: 2844-2853

Osawa M, Hanada K, Hamada H, Nakauchi H (1996) Long-term lymphohematopoietic reconstitution by a single CD34-low/negative hematopoietic stem cell. Science 273: 242-245

Palkar PS, Borland MG, Naruhn S, Ferry CH, Lee C, Sk UH, Sharma AK, Amin S, Murray IA, Anderson CR, Perdew GH, Gonzalez FJ, Müller R, Peters JM (2010) Cellular and pharmacological selectivity of the peroxisome proliferator-activated receptor-beta/delta antagonist GSK3787. Mol Pharmacol 78: 419-430

Palmer CN, Hsu MH, Griffin HJ, Johnson EF (1995) Novel sequence determinants in peroxisome proliferator signaling. J Biol Chem 270: 16114-16121

Pelton P (2006) GW-501516 GlaxoSmithWellkline/Ligand. Curr Opin Investig Drugs 7: 360-370

Peters JM, Lee SS, Li W, Ward JM, Gavrilova O, Everett C, Reitman ML, Hudson LD, Gonzalez FJ (2000) Growth, adipose, brain, and skin alterations resulting from targeted disruption of the mouse peroxisome proliferator-activated receptor beta(delta). Mol Cell Biol 20: 5119-5128

Peters JM, Shah YM, Gonzalez FJ (2012) The role of peroxisome proliferator-activated receptors in carcinogenesis and chemoprevention. Nat Rev Cancer 12: 181-195

Rieck M, Meissner W, Ries S, Müller-Brüsselbach S, Müller R (2008) Ligand-mediated regulation of peroxisome proliferator-activated receptor (PPAR) beta/delta: a comparative analysis of PPAR-selective agonists and all-trans retinoic acid. Mol Pharmacol 74:1269-1277

Rosenbauer F, Wagner K, Kutok JL, Iwasaki H, Le Beau MM, Okuno Y, Akashi K, Flering S, Tenen DG (2004) Acute myeloid leukemia induced by graded reduction of a lineage-specific transcription factor, PU.1. Nat Genet 36: 624-630

Schuler G, Lutz MB, Bender A, Thurner B, Röder C, Young J, Romani N (1999) A guide to the isolation and propagation of dendritic cells, in Dendritic Cells: Biology and Clinical Applications (Lotze MT and Thomson AW eds) pp 515-533, Academic San Diego, CA, USA

Shearer BG, Wiethe RW, Ashe A, Billin AN, Way JM, Stanley TB, Wagner CD, Xu RX, Leesnitzer LM, Merrihew RV, Shearer TW, Jeune MR, Ulrich JC, Willson TM (2010) Identification and characterization of 4-chloro-N-(2-{[5-trifluoromethyl)-2-pyridyl]sulfonyl}ethyl)benzamide (GSK3787), a selective and irreversible peroxisome proliferator-activated receptor delta (PPARdelta) antagonist. J Med Chem 53: 1857-1861

Shearer BG, Steger DJ, Way JM, Stanley TB, Lobe DC, Grillot DA, Iannone MA, Lazar MA, Willson TM, Billin AN (2007) Identification and characterization of a selective peroxisome proliferator-activated receptor beta/delta (NR1C2) antagonist. Mol Endocrinol 22: 523-529

Shi Y, Hon M, Evans RM (2002) The peroxisome proliferator-activated receptor delta, an integrator of transcriptional repression and nuclear receptor signaling. Proc Natl Acad Sci U S A 99: 2613-2618

Tamura T, Nagamura-Inoue T, Shmeltzer Z, Kuwata T, Ozato K (2000) ICSBP directs bipotential myeloid progenitor cells to differentiate into mature macrophages. Immunity 13: 155-165

Tanaka T, Akira S, Yoshida K, Umemoto M, Yoneda Y, Shirafuji N, Fujiwara H, Suematsu S, Yoshida N, Kishimoto T (1995) Targeted disruption of the NF-IL6 gene discloses its essential role in bacteria killing and tumor cytotoxicity by macrophages. Cell 80: 353-361

Torchia J, Rose DW, Inostroza J, Kamei Y, Westin S, Glass CK, Rosenfeld MG (1997) The transcriptional co-activator p/CIP binds CBP and mediates nuclear-receptor function. Nature 387: 677-684

Vosper H, Patel L, Graham TL, Khoudeli GA, Hill A, Macphee CH, Pinto I, Smith SA, Suckling KE, Wolf CR, Palmer CN (2001) The perxosime proliferator-activated receptor delta promotes lipid accumulation in human macrophages. J Biol Chem 276: 44258-44265

Wahli W, Michalik L (2012) PPARs at the crossroads of lipid signaling and inflammation. Trends Endocrinol Metab 23: 351-363

Weischenfeldt J and Porse B (2008) Bone marrow-derived macrophages (BMM): Isolations and applications. CSH Protoc 2008: pdb prot5080

Weissman IL, Anderson DJ, Gage F (2001) Stem and progenitor cells: origins, phenotypes, lineage commitments, and transdifferentiations. Annu Rev Cell Dev Biol 17: 387-403

Wurtz JM, Bourguet W, Renaud, JP, Vivat V, Chambon P, Moras D, Gronemeyer H (1996) A canonical structure for the ligand-binding domain of nuclear receptors. Nat Struct Biol 3: 206

Xu HE, Lambert MH, Montana VG, Plunket KD, Moore LB, Collins JL, Oplinger JA, Kliewer SA, Gampe RT Jr, McKee DD, Moore JT, Willson TM (2001) Structural determinants of ligand binding selectivity between the peroxisome proliferator-activated receptors. Proc Natl Acad Sci U S A 98: 13919-13924

Yamanaka R, Barlow C, Lekstrom-Himes J, Castilla LH, Liu PP, Eckhaus M, Decker T, Wynshaw-Boris A, Xanthopoulos KG (1997) Impaired granulopoiesis, myelodysplasia, and early lethality in CCAAT/enhancer binding protein epsilon-deficient mice. Proc Natl Acad Sci U S A 94: 13187-13192

Yang Y, Lovett-Racke AE, Racke MK (2010) Regulation of immune responses and autoimmune encephalomyelitis by PPARs. PPAR Res 2010

Yu C, Markan K, Temple KA, Deplewski D, Brady MJ, Cohen RN (2005) The nulear receptor corepressors NCoR and SMRT decrease peroxisome proliferator-activated receptor gamma transcriptional activity and repress 3T3-L1 adipogenesis. J Biol Chem 280: 13600-13605

Yu K, Bayona W, Kallen CB, Harding HP, Ravera CP, McMahon G, Brown M, Lazar MA (1995) Differential activation of peroxisome proliferator-activated receptors by eicosanoids. J Biol Chem 270: 23975-23983

Zhang DE, Zhang P, Wang ND, Hetherington CJ, Darlington GJ, Tenen DG (1997) Absence of granulocyte colony-stimulating factor signaling and neutrophil development in CCAAT enhancer binding protein alpha-deficient mice. Proc Natl Acad Sci U S A 94: 569-574

Zomer AW, van Der Burg B, Jansen GA, Wanders RJ, Poll-The BT, van Der Saag PT (2000) Pristanic acid and phytanic acid: naturally occurring ligands for the nuclear receptor peroxisome proliferator-activated receptor alpha. J Lipid Res 41: 1801-1807

6 Anhang

6.1 Verzeichnis der akademischen Lehrer

Meine akademischen Lehrer waren die Damen und Herren in Marburg:
Adamkiewicz, Aigner, Bastians, Bauer, Bremmer, Burchert, Daut, del Rey, Decher, Eilers, Elsässer, Fritz, Garn, Garten, Grzeschik, Gudermann, Haselik, Hassel, Hilt, Huber, Jacob, Jungclas, Kirchner, Klenk, Koch, Kösters, Koolman, Krebber, Lang, Lill, Löffler, Lohoff, Lüers, Lutz, Meißner, Moll, Müller, Müller-Brüsselbach, Oeffner, Portenier, Röhm, Renz, Schäfer, Schulz, Suske, Voigt, Weihe, und Westermann.

6.2 Danksagung

Mein besonderer Dank geht an Prof. Dr. Rolf Müller für das Überlassen des interessanten Promotionsthemas, die Betreuung und Unterstützung während der gesamten Zeit und den Freiraum zur Entwicklung wissenschaftlicher Fähigkeiten.
Allen Mitgliedern der Arbeitsgruppe danke ich für die überaus schöne Zusammenarbeit, wobei ich besonders meinen Dank an PD Dr. Wolfgang Meißner und PD Dr. Sabine Müller-Brüsselbach richte, die mit wissenschaftlichem Rat immer zur Stelle waren, um mein Projekt voranzutreiben und für neue Motivation gesorgt haben.
Danke auch an Evelyn Schnitzer, Julia Obert, Dr. Simone Naruhn, Dr. Josefine Stockert, Dr. Kerstin Kaddatz und Dr. Verena Rohnalter. Euch ist es zu verdanken, dass man jeden Tag das Gefühl hatte, mit Freunden statt Kollegen zusammenzuarbeiten.
Bedanken möchte ich mich auch ganz besonders bei Katja Kräling. Du hast mir immer zur rechten Zeit den Kopf wieder gerade gerückt und warst in jeder Situation für mich da. Danke für deine bedingungslose Freundschaft!
Meinen Großeltern danke ich für ihre Unterstützung und Hilfe, ohne die das späte Studium nicht möglich gewesen wäre.
Markus, dir kann ich gar nicht genug danken. Ich war bestimmt nicht immer einfach, aber du warst immer für mich da, hast an mich geglaubt und Kritik geübt, wenn es angebracht war. Danke auch dafür, dass du meine Monologe nach stressigen Labortagen über dich hast ergehen lassen und es dabei auch noch geschafft hast, interessiert zu wirken. Deine „wissenschaftlichen“ Gespräche mit Jenny über PCRs haben dafür gesorgt, dass ich mich nicht immer allzu ernst genommen habe. Du hast deine eigenen Wünsche während der letzten Jahre hinten angestellt, jetzt bist du an der Reihe. Danke, ich liebe dich.

Journal of Medicinal Chemistry

Article

pubs.acs.org/jmc

(*Z*)-2-(2-Bromophenyl)-3-{[4-(1-methyl-piperazine)amino]phenyl}-acrylonitrile (DG172): An Orally Bioavailable PPARβ/δ-Selective Ligand with Inverse Agonistic Properties

Sonja Lieber,[†,§] Frithjof Scheer,[‡,§] Wolfgang Meissner,[†] Simone Naruhn,[†] Till Adhikary,[†] Sabine Müller-Brüsselbach,[†] Wibke E. Diederich,*[,‡] and Rolf Müller*[,†]

[†]Institute of Molecular Biology and Tumor Research (IMT), Philipps University, Emil-Mannkopff-Strasse 2, 35033 Marburg, Germany

[‡]Institute of Pharmaceutical Chemistry, Philipps-University, Marbacher Weg 6, 35032 Marburg, Germany

Supporting Information

ABSTRACT: The ligand-regulated nuclear receptor peroxisome proliferator-activated receptor β/δ (PPARβ/δ) is a potential pharmacological target due to its role in disease-related biological processes. We used TR-FRET-based competitive ligand binding and coregulator interaction assays to screen 2693 compounds of the Open Chemical Repository of the NCI/NIH Developmental Therapeutics Program for inhibitory PPARβ/δ ligands. One compound, (*Z*)-3-(4-dimethylamino-phenyl)-2-phenyl-acrylonitrile, was used for a systematic SAR study. This led to the design of derivative **37**, (*Z*)-2-(2-bromophenyl)-3-{[4-(1-methyl-piperazine)amino]phenyl}acrylonitrile (DG172), a novel PPARβ/δ-selective ligand showing high binding affinity (IC_{50} = 27 nM) and potent inverse agonistic properties. **37** selectively inhibited the agonist-induced activity of PPARβ/δ, enhanced transcriptional corepressor recruitment, and down-regulated transcription of the PPARβ/δ target gene *Angptl4* in mouse myoblasts (IC_{50} = 9.5 nM). Importantly, **37** was bioavailable after oral application to mice with peak plasma levels in the concentration range of its maximal inhibitory potency, suggesting that **37** will be an invaluable tool to elucidate the functions and therapeutic potential of PPARβ/δ.

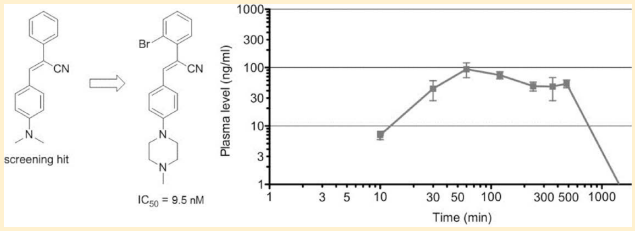

INTRODUCTION

Members of the class II subset of nuclear receptors, including the thyroid hormone receptor, the retinoic acid receptor, and peroxisome proliferator-activated receptors (PPARs), can actively repress target genes in the absence of ligand binding but activate the same genes if bound by an agonistic ligand.[1] These activities are linked to the induction of distinct local chromatin structures depending on the presence or absence of an agonistic ligand. The three PPAR subtypes (PPARα, PPARβ/δ, and PPARγ) regulate their target genes through binding to specific DNA elements (PPREs) as obligatory heterodimers with the retinoid X receptor. Certain lipids, fatty acid metabolites, and subtype-selective synthetic ligands modulate their transcriptional activity,[2−4] suggesting that PPARs act as sensors for both endogenous and exogenous stimuli, which impinge not only on intermediary metabolism but also on inflammatory pathways.[5] In addition to these functions, PPARs figure in development, wound healing, cell differentiation, proliferation, and apoptosis.[6−8]

PPRE-bound PPARβ/δ complexes have functions in both transcriptional repression and transcriptional activation. Agonistic ligands induce a conformational change in PPARs that favors the association with coactivators and the dissociation of corepressors.[9] Many PPAR-interacting coregulators have been described, including histone acetyl transferases (HATs) and HAT-recruiting coregulators, histone deacetylases (HDACs) and HDAC recruiting factors, protein arginine methyl transferases, and factors with chromatin remodeling functions. While the role of histone acetylation in PPAR-mediated transcriptional activation is well established, the exact role of other enzymatic modifications and coregulators remains unclear, in particular for the PPARβ/δ subtype. The mechanisms of PPARβ/δ-mediated repression by PPRE-bound unliganded receptors are even less understood. A number of corepressors have been identified, such as class I HDACs, NCoR/SMRT, and SHARP,[10] but their precise function in the regulation of specific target genes involving the ordered assembly and disassembly of multiprotein complexes is not known. The complexity of PPARβ/δ-mediated transcriptional regulation is further complicated by the fact that distinct regulatory mechanisms govern the expression of different sets of target genes.[11] Thus, repression appears to represent the major mode of PPARβ/δ-mediated transcriptional regulation, and only a subset of target genes is subject to an agonist-mediated switch from active repression to activation. Finally, PPARs can also regulate genes without making direct DNA contacts by directly interacting with specific transcription factors, as exemplified by the repression of BCL-6 by PPARβ/δ.[12]

Received: January 2, 2012
Published: February 27, 2012

Because of these complexities, the correlation of biological functions and transcriptional pathways regulated by PPARβ/δ is difficult. This is exemplified by the genetic disruption of *Ppard* genes, which can have opposite effects of individual PPARβ/δ target genes, depending on their mode of transcriptional regulation, which in turn hampers the assessment of PPARβ/δ as a potential target for pharmacological inhibition. While potent synthetic agonists that are bioavailable, selective for PPARβ/δ, and bind reversibly are available, inhibitory ligands for PPARβ/δ fulfilling these criteria have not been described to date. Both 2-(2-methyl-4-((4-methyl-2-(naphthalen-1-yl)thiazol-5-yl)methylthio)phenoxy)acetic acid (SR13904)[13] and 4-chloro-*N*-(2-((5-trifluoromethyl-2-pyridyl)sulfonyl-)ethyl)benzamide (GSK3787)[14,15] are not specific for PPARβ/δ, and GSK3787 binds PPARβ/δ irreversibly, which is pharmacologically undesirable. 3-(((2-Methoxy-4-(phenylamino)phenyl)amino)sulfonyl)-2-thiophenecarboxylate (GSK0660)[16] is PPARβ/δ subtype-specific but is not bioavailable. This also applies to methyl 3-(*N*-(4-(hexylamino)-2-methoxyphenyl)sulfamoyl)thiophene-2-carboxylate (ST247), a recently developed GSK0660 derivative with greatly improved affinity.[17,18] These ligands are not only competitive antagonists but exert their inhibitory function as inverse agonists, as indicated by their inhibitory effect on the basal expression of PPARβ/δ target genes and an increased recruitment of transcriptional corepressors.[15−17] Finally, a biphenylcarboxylic acid-based antagonist has been described, but its in vivo performance has not been addressed.[19]

In light of the lack of inhibitory PPARβ/δ ligands suitable for in vivo applications, we have searched for novel chemical structures that could serve as leads for the development of improved inverse agonists. Toward this end, we screened a chemical compound library and identified several stilbene-based or -related inhibitory PPARβ/δ ligands. One of these compounds was chosen for further development and the establishment of structure−activity relationships. This finally yielded a compound with the desired properties, including high affinity, specificity, and bioavailability after oral application.

RESULTS AND DISCUSSION

Screening for Inhibitory PPARβ/δ Ligands. A TR-FRET-based competitive ligand-binding assay was used to screen 2693 compounds of the Open Chemical Repository of the NCI/NIH Developmental Therapeutics Program for PPARβ/δ ligands. In this assay, the terbium-labeled PPARβ/δ LBD interacts with the fluorescent PPAR ligand Fluormone Pan-PPAR Green, which produces FRET from terbium (495 nm) to Pan-PPAR Green (520 nm). Displacement of the fluorescent ligand by an unlabeled test compound results in a quantifiable attenuation of FRET. Out of 191 identified compounds, 10 disrupted the interaction of the PPARβ/δ LBD with a coactivator peptide in a TR-FRET-based assay (Supporting Information Table S1). Four of these compounds possess a stilbene-based or -related core structure. In this assay, interaction of the PPARβ/δ LBD (indirectly labeled by terbium) with the fluorescein-labeled coactivator peptide C33 is determined. The data therefore indicates that these 10 compounds act as inhibitory ligands. Eight of these ligands were also able to trigger the association with the SMRT-ID2 peptide, derived from the interaction domain 2 of the corepressor SMRT, which qualifies these compounds as inverse agonists. Two of these ligands, NSC667251 and compound **1** (NSC636948), also showed efficacy in cell-based assays, i.e., repression of agonist-induced transcription in a luciferase reporter assay and repression of the endogenous PPARβ/δ target gene ANGPTL4 (Supporting Information Table S1). Compound **1**, which is (*Z*)-3-[4-(dimethylamino)phenyl]-2-phenylacrylnitrile, was used as a lead structure for further development, as described in detail below.

Among the eight compounds identified as inverse agonists is the clinically important drug (*Z*)-2-[4-(1,2-diphenylbut-1-enyl)-phenoxy]-*N*,*N*-dimethylethanamine (tamoxifen) (Supporting Information Table S1). However, in spite of efficient corepressor recruitment in vitro, no activity was detectable in the cell-based assays. The same observations were made with three metabolites of tamoxifen, i.e., 4-OH-tamoxifen, *N*-desmethyl-tamoxifen, and endoxifen (Supporting Information Table S2). Because these compounds are able to modulate estrogen receptor-driven gene expression in intact cells, their failure to affect PPARβ/δ activity cannot be attributed to a lack of cellular uptake. It is possible that the subcellular compartmentalization of tamoxifen and its metabolites is a limiting step restricting the accessibility of target proteins. We also analyzed other commercially available stilbenes, including the pharmacologically relevant compounds resveratrol and diethylstilbestrol, but did not observe any significant activities (Supporting Information Table S2). These observations show that binding to PPARβ/δ is not a general property of stilbenes.

Optimization of the Screening Hit 1. **1** was chosen as starting point for optimization (Figure 1). We first turned our attention toward the central acrylonitrile moiety. However, modification at this position, e.g., by hydrogenation **2**, removal **3** or alteration of the position of the nitrile functionality **4**, or elongation leading to the 1,3-butadiensystem **5** resulted in a complete loss of activity (Supporting Information Figure S1). Therefore, the acrylonitrile moiety seems to be crucial for activity. We then examined the effect of the *para*-dimethylamino-substituent present in **1**. Removal (**6**) or replacement by a variety of either electron-withdrawing or electron-donating functional groups (**7**−**12**) again led to a significant drop in affinity. The only exception turned out to be **13** bearing a primary amino functionality in *para*-position, indicating that the existence of an electron-related push−pull system is essential for activity (Supporting Information Figure S1). Consequently, introduction of a dimethylaminomethylene substituent in *para*-position **14** (Figure 2) and thus disruption of the conjugated push−pull system also diminished the binding affinity toward the PPARβ/δ-LDB significantly. Because the *para*-dimethylamino derivative **1** possessed a higher binding affinity than the unsubstituted *para*-amino-representative **13**, we focused our attention on the substitution pattern of this essential amino group to achieve a further increase in binding affinity (Figure 2). Besides tertiary amines of varying ring sizes, such as in pyrrolidine- (**15**),

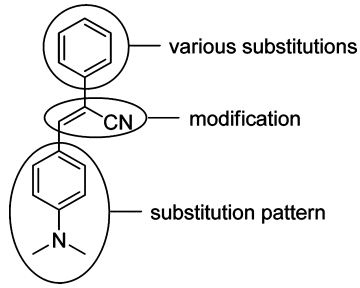

Figure 1. Strategy for optimization of the initial screening hit **1**.

dx.doi.org/10.1021/jm2017122 | J. Med. Chem. 2012, 55, 2858−2868

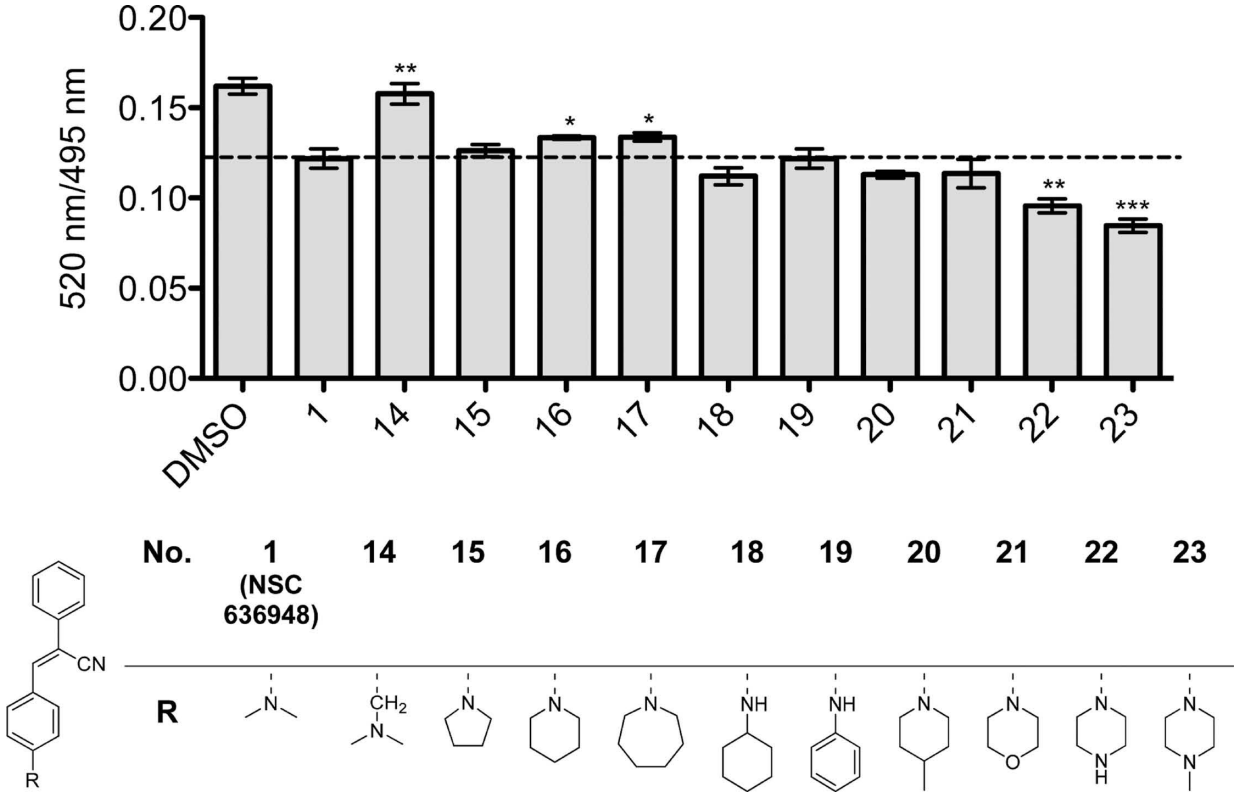

Figure 2. Activity of **1** and the indicated derivatives as PPARβ/δ ligands determined in vitro by competitive ligand binding assay. Displacement of a fluorescent PPAR ligand (Fluormone Pan-PPAR Green) from recombinant GST-PPARβ/δ by the indicated compounds was determined by TR-FRET. Each compound was tested at a concentration of 1 μM. Results are expressed as the ratio of fluorescence intensity at 520 nm (fluorescein emission excited by terbium emission) and 495 nm (terbium emission). All data points represent averages of triplicates (±SD). ***, **, and *: significant difference to compound **1** by *t* test ($P < 0.001$, $P < 0.01$, and $P < 0.05$, respectively).

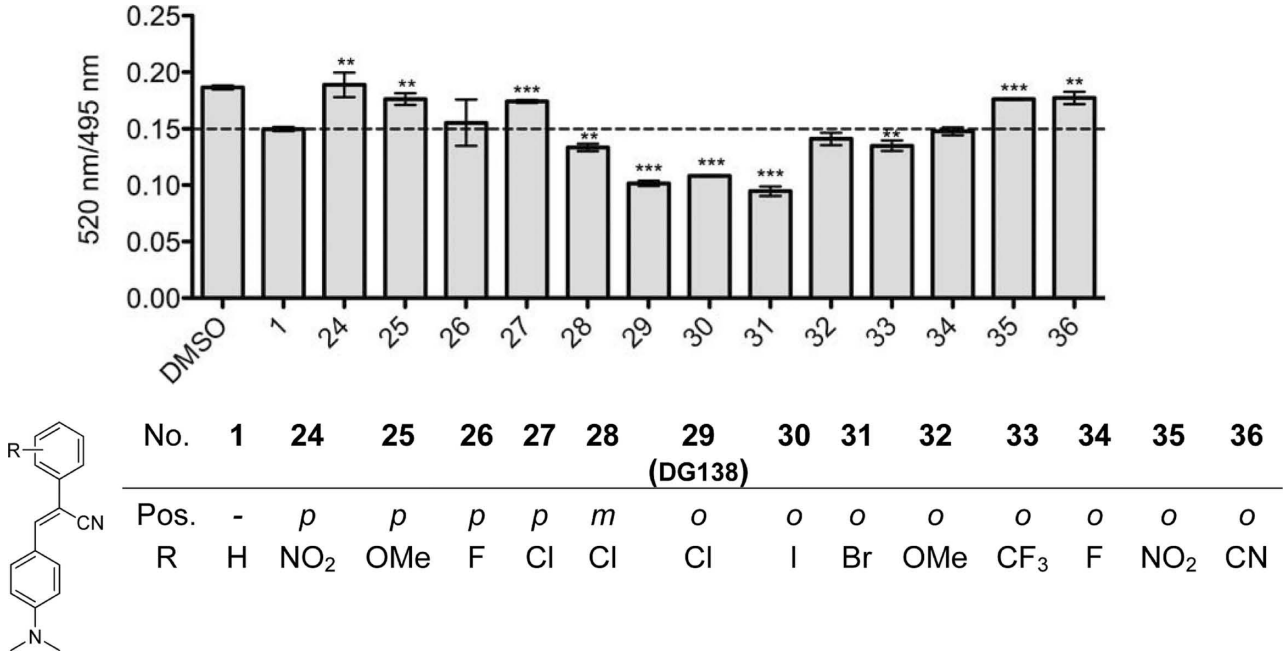

Figure 3. Activity of compound **1** and the indicated derivatives as PPARβ/δ ligands. All experimental details were as in Figure 2.

piperidine- (**16**), or azepane- (**17**) substituted structures present, we also tested two secondary amines (**18**, **19**).

Although the competitive TR-FRET assay showed only slight differences between these compounds, the piperidine analogue gave the best results in a cell-based luciferase reporter assay (data not shown). Hence, further compounds bearing six-membered heterocycles were synthesized. Introduction of a 4-methylpiperidino (**20**), a morpholino (**21**), and a piperazino (**22**) moiety, respectively, led to a significant gain in affinity. The best compound within this series was found to be **23**

dx.doi.org/10.1021/jm2017122 | J. Med. Chem. 2012, 55, 2858–2868

equipped with a 4-methylpiperazino substituent. The two secondary amines, the aniline- (**19**) as well as the cyclohexylamine-derivative (**18**), also possessed a higher binding affinity compared to **1** but could still not compete with **23**.

We then turned our attention to the second aromatic portion within this compound class (Figure 3). The initial screening hit **1** was likewise used as reference. However, any tested substituent introduced in *para*-position of this phenyl substituent led to a decrease in binding affinity, indicating that there might only be limited space available within the respective binding pocket (**24**–**27**). On the contrary, introducing a chlorine substituent in *meta*-position **28** gave a significant improvement in binding affinity. This effect was even more pronounced for this substituent in *ortho*-position as in compound **29** (DG138). Iodine as *ortho*-substituent **30** performed equally well while compound **31**, equipped with a bromine in this position, turned out to be the most potent ligand within this series. Introduction of other substituents with a stronger -I-effect such as **32**, **33**, and **34** only led to a slight increase in comparison to **1** or even resulted in a decrease in binding affinity when strong electron withdrawing groups (**35**, **36**) were introduced.

Combination of the substitution patterns of the most active compounds of both series, i.e., halogenation in the *ortho*-position and the introduction of a 4-methylpiperazine, finally led to derivative **37** (DG172) (see Scheme 1), analyzed in detail below.

Scheme 1. Synthesis of 37[a]

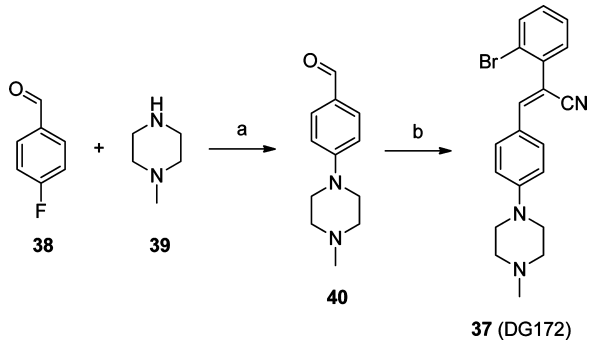

[a]Reagents and conditions: (a) K_2CO_3, DMSO, 100 °C, 78% (b) 2-bromophenylacetonitrile, pyrrolidine, MeOH, 60 °C, 79%.

The compounds described above are easily accessible via a Knoevenagel condensation, which exclusively yield the (*Z*)-isomers (for example, $^3J_{(H,C)}$ = 14.4 Hz for **1**), employing the corresponding aldehydes and phenylacetonitriles under basic conditions. For the preparation of several of the amino-derivatives, 4-bromophenylaldehyde was employed in the Knoevenagel reaction, followed by a Buchwald–Hartwig reaction[20–22] to introduce the respective amino substituent. In case of **37**, 4-fluorobenzaldehyde **38** was first reacted with 4-methylpiperazine **39** to **40**, followed by a knoevenagel condensation employing 2-bromophenylacetonitrile, as outlined in Scheme 1.

Binding Affinities and Inhibitory Properties of 29 and 37 in vitro. We next analyzed **37** in further detail with respect to its binding affinity, inhibitory properties, and specificity. First, **37** was compared to both **29** (harboring the *ortho*-halogenation but lacking the 4-methylpiperazine) and its parent molecule **1** in a competitive ligand binding assay. The data in Figure 4A shows that **29** possesses a significantly enhanced affinity compared to **1** and performed similarly as a published reference compound, GSK0660. As expected, **37** was the most potent compound with

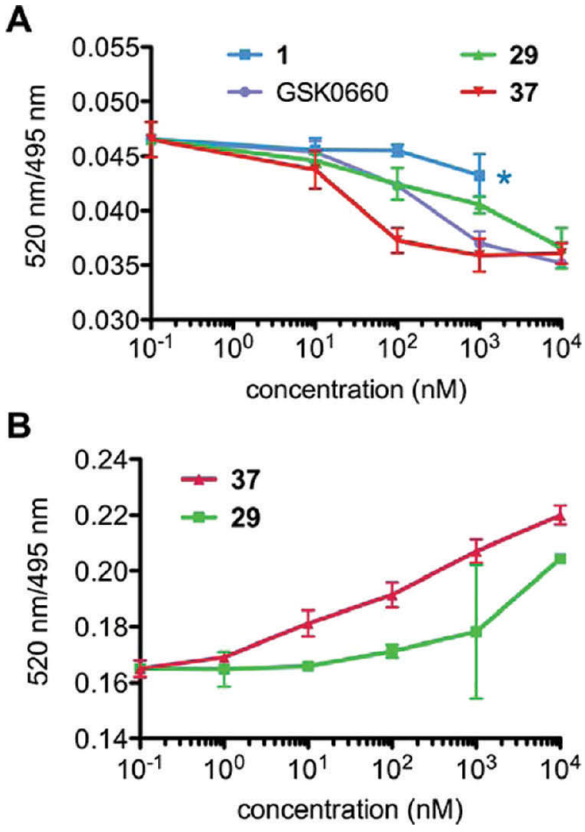

Figure 4. In vitro binding and interaction properties of compound **1** and its derivatives **29** and **37**. (A) FRET-based competitive ligand binding assay as in Figure 2. GSK0660 is included for comparison. *Measurement of **1** at 10 μM was not possible due to a lack of solubility. (B) Comparison of **29**- and **37**-induced binding of a corepressor-derived peptide to the PPARβ/δ LBD. Interaction of SMRT-ID2 peptide (fluorescein labeled) and recombinant GST-PPARβ/δ (labeled by a terbium-coupled anti-GST antibody) was measured by TR-FRET. In both panels, results are expressed as the ratio of fluorescence intensity at 520 nm (fluorescein emission excited by terbium emission) and 495 nm (terbium emission). All data points represent averages of triplicates (±SD). ***, **, and *: significant difference by *t* test compared to untreated sample ($P < 0.001$, $P < 0.01$, and $P < 0.05$, respectively).

an IC_{50} value of 26.9 nM, compared to ~180 nM for **29** and >300 nM for GSK0660 (values are averages from three independent experiments each analyzing five different concentrations as triplicates). The latter two values cannot be accurately determined due to a lack of solubility at high concentrations.

To evaluate the inhibitory properties of **29** and **37**, we investigated the effect of these compounds on the interaction of PPARβ/δ with the synthetic corepressor peptide SMRT-ID2 by TR-FRET. The data obtained by this assay (Figure 4B) show a clearly enhanced interaction for **37** compared to **29** and thus closely mirror the results obtained by the competitive binding assay (Figure 4A). The data also confirm both ligands as inverse agonists.

Specificity for PPARβ/δ. The PPAR subtype specificity of **29** and **37** was addressed by a competitive TR-FRET assay. The data in Figure 5 show that at 1 μM both compounds selectively competed for binding to PPARβ/δ. Competition for binding to PPARα or PPARγ was extremely low or undetectable. In contrast, the PPARα agonist GW7647, the PPARβ/δ agonist GW501516, and the PPARγ agonist GW1929 strongly interacted with the

dx.doi.org/10.1021/jm2017122 | J. Med. Chem. 2012, 55, 2858–2868

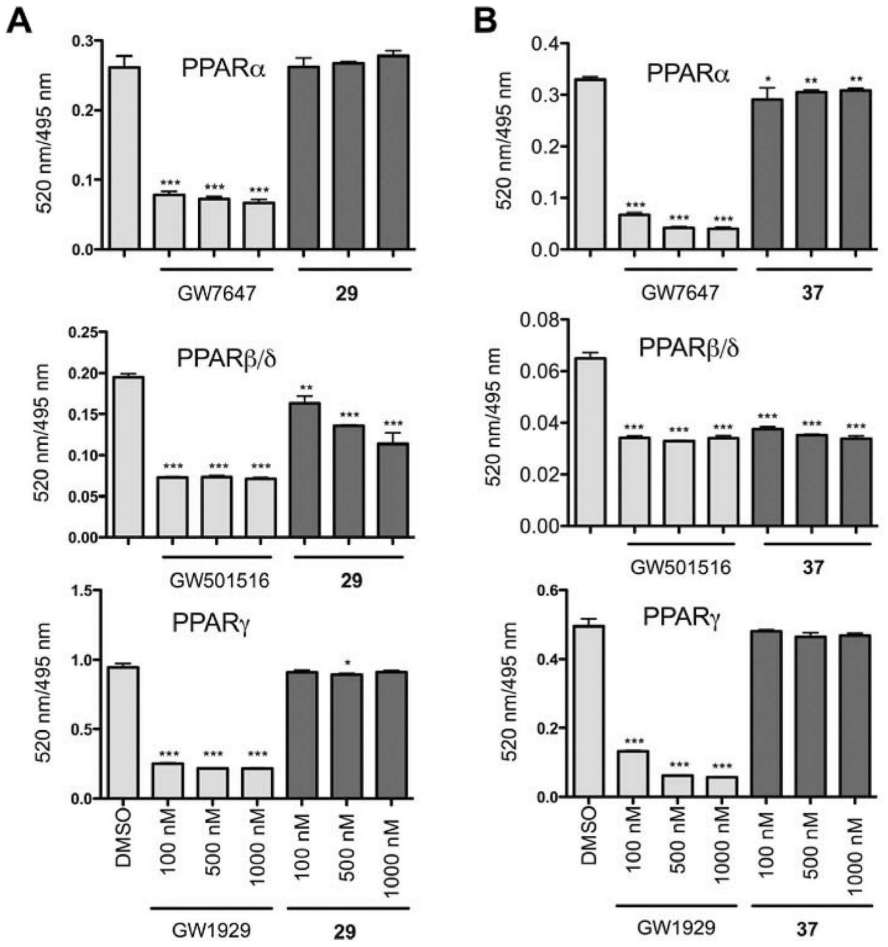

Figure 5. PPAR subtype binding specificity. Competition of **29** (A) or **37** (B) with Fluormone Pan-PPAR Green for binding to PPARα, PPARβ/δ, and PPARγ compared to the PPARα agonist GW7647 (top), the PPARβ/δ agonist L165,041 (middle), the PPARγ agonist GW1929 (bottom), or solvent (DMSO) only. Experimental details are described in Figure 4.

respective PPAR subtype (Figure 5), thus confirming the validity of the assay.

We next analyzed the effect of both compounds (and of GSK0660 for comparison) on the agonist-induced transcriptional activity of PPARα, PPARβ/δ, and PPARγ in a cell-based assay. As shown in Figure 6, treatment with subtype-selective agonists resulted in a 3−7.5-fold activation of the respective PPAR subtype in luciferase reporter assays. Whereas **29** and **37** had no significant effect on PPARα- or PPARγ-driven transcription, they both efficiently antagonized ligand activation of PPARβ/δ, which is consistent with the results of the in vitro ligand-binding assay described above.

Inhibition of Endogenous PPARβ/δ Target Gene Expression. The inverse agonistic properties of **29** and **37** were tested in an endogenous cellular context by investigating their effect on the established PPARβ/δ target gene *Angptl4*.[23,24] Toward this end, we performed titration experiments to determine the IC_{50} values for **29** and **37** in C2C12 mouse myoblasts (Figure 7A). The parent compound **1** and GSK0660 were included in this study for comparison. This analysis clearly revealed the superior effect of **37** (IC_{50} = 9.5 nM) compared to the other compounds, which showed IC_{50} values of 52 nM (**29**), >500 nM (**1**), and 48 nM (GSK0660), respectively (values are averages from three independent experiments each analyzing six different concentrations as triplicates). Because the tested compounds had no detectable effect on PPARα and PPARγ (Figures 5 and 6), it is very likely that the observed effect on *Angptl4* expression is mediated though PPARβ/δ. This is strongly supported by our observation that the inhibition of *Angptl4* expression by **37** was dependent on the presence of wild-type PPARβ/δ alleles (Figure 7B).

Effect on Corepressor Recruitment to Chromatin-Bound PPARβ/δ. To investigate the effect of **37** on the assembly of chromatin-associated corepressor complexes, we performed chromatin immune precipitation (ChIP) analyses of HDAC3 recruitment to the *ANGPTL4* gene in WPMY-1 human myofibroblasts. As can be seen in Figure 8A, **37** induced an enhanced recruitment of HDAC3 compared to solvent-treated cells (DMSO). The specificity of the ChIP assay was shown by the lack of antibody binding to an irrelevant region of the *PDK4* gene (Figure 8B) and by the lack of any detectable effect on HDAC3 binding (Figure 8A) of reference compound **41**, which is a pure PPARβ/δ antagonist and therefore unable to enhance corepressor recruitment.[17] The data in Figure 8A also show that GSK0660 and **37** have similar effects, which do not correlate with the higher potency of **37** to repress *ANGPTL4* transcription (Figure 7A). We attribute this to the possibility that other corepressors are instrumental in **37**-mediated repression, as suggested by the multitude of coregulators interacting with repressive PPAR complexes.

Pharmacokinetics in Mice. Finally, to determine the potential suitability of **29** and **37** for in vivo applications, pharmacokinetic studies were carried out in mice. **29** and **37** were administered intravenously (1 mg/kg) and orally (5 mg/kg),

dx.doi.org/10.1021/jm2017122 | J. Med. Chem. 2012, 55, 2858−2868

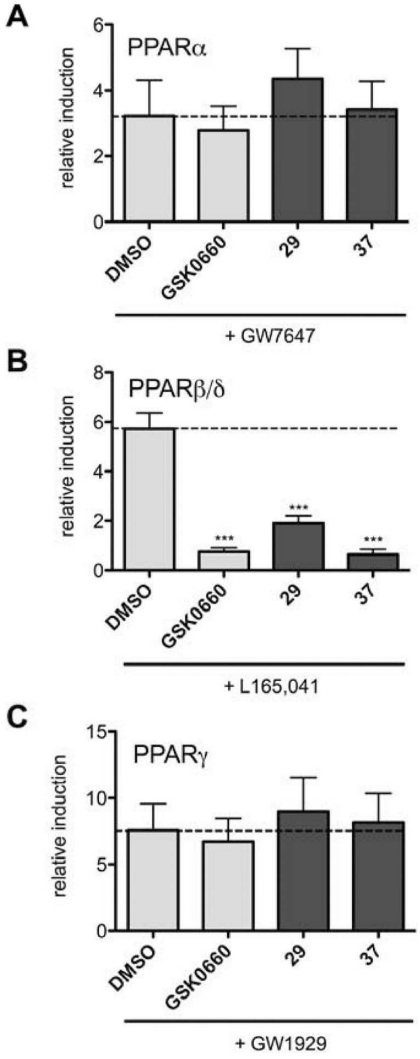

Figure 6. Effects on the agonist-induced transcriptional activity of LexA-PPARα (A), LexA-PPARβ/δ (B), and LexA-PPARγ (C). NIH3T3 cells were transiently transfected with a luciferase reporter plasmid containing multiple LexA binding sites. Four hours post-transfection, the cells were treated with the indicated inhibitory ligands (1 μM) for 48 h, followed by 300 nM of the PPARα agonist GW7647, 1 μM of the PPARβ/δ agonist L165,041, or 300 nM of the PPARγ agonist GW1929 or agonist solvent. GSK0660 (1 μM) is included for comparison. Induction values represent luciferase activities of agonist-treated cells relative to cells treated with agonist solvent. Statistical analysis was performed as in Figure 4.

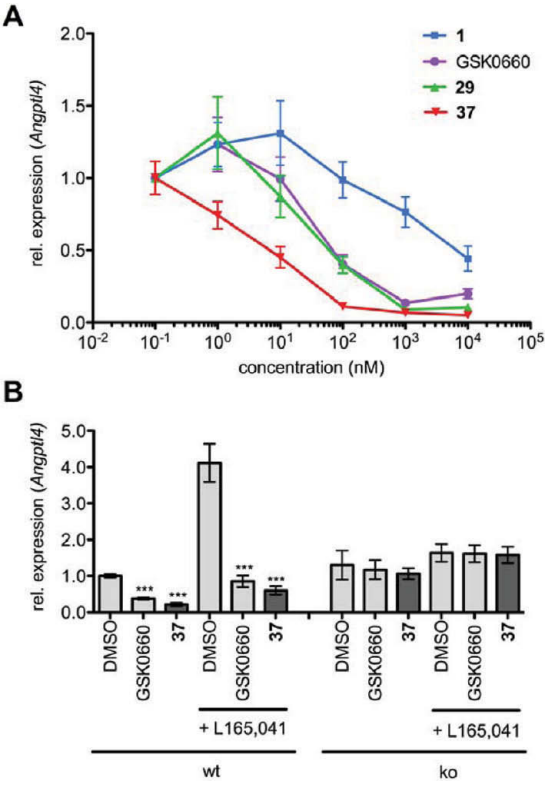

Figure 7. Impact on expression of the endogenous PPARβ/δ target gene *Angptl4*. (A) C2C12 mouse myoblasts were treated for 24 h with **1**, **29**, and **37** at the indicated concentration, and RNA was analyzed by RT-qPCR. GSK0660 is included for comparison. (B) Dependence on PPARβ/δ. Macrophages from *Ppard* wild-type (WT) and null (KO) mice were treated with the agonist L165,041 (500 nM), **37** (1 μM), GSK0660 (1 μM), or with solvent only (DMSO) for 6 h, and the expression of *Angptl4* was determined by RT-qPCR. Statistical analysis was performed as in Figure 4.

blood samples were analyzed 10 min to 12 h post-treatment by HPLC-MS (Figure 9), and basic pharmacokinetic parameters were determined. After intravenous administration of **37**, a plasma half-life of 76 min was measured, the mean clearance (CL) was 121 mL/min/kg, and the volume of distribution at steady state (Vss) 12.5 L/kg. Oral administration yielded a good exposure with an AUCinf of 8239 min·ng/mL and a peak plasma level (C_{max}) of 94 ng/mL (207 nM), which is clearly within the concentration range of maximal activity determined in vitro (IC_{50} = 23 nM; Figure 4A) or in cell culture (IC_{50} = 6.5 nM for C2C12 cells; Figure 7A). Furthermore, half-life (634 min) and bioavailability (72%) were in the desired range. This pharmacokinetic data set suggests that **37** is suitable for in vivo applications in mice, including its peroral administration. In contrast, despite an acceptable plasma half-life after intravenous injection of 76 min (CL = 176 mL/min/kg; Vss = 6.2 L/kg), **29** was detectable in the blood at very low levels (≤6 ng/mL) and for a short time following oral application (≤30 min), indicating a lack of bioavailability.

CONCLUSIONS

By screening a chemical compound library, we identified (*Z*)-3-[4-(dimethylamino)phenyl]-2-phenyloacrylnitrile (**1**) as an inhibitory PPARβ/δ ligand. A comprehensive SAR study revealed two modifications, *ortho*-halogenation and introduction of an *N*-4-methylpiperazine moiety, that greatly improved the binding affinity for PPARβ/δ and the efficiency of corepressors. The combination of these two critical modifications led to the discovery of (*Z*)-2-(2-bromophenyl)-3-{[4-(1-methyl-piperazine)-amino]phenyl}acrylonitrile (**37**), which is the most potent inverse agonist for PPARβ/δ known to date. **37** is PPAR-subtype selective and inhibits both agonist-induced and basal level PPRE-dependent transcription in cells. Most importantly, **37** has good oral pharmacokinetic properties, making it the first bioavailable PPARβ/δ-selective inverse agonist described to date. **37** therefore represents a useful novel tool to investigate the biological and pathophysiological functions of PPARβ/δ and to clarify its potential as a target for drug development.

EXPERIMENTAL SECTION

Ligands. {2-Methyl-4-[({4-methyl-2-[4-(trifluoromethyl)phenyl]-1,3-thiazol-5-yl}methyl)sulfanyl]phenoxy}acetic acid (GW501516) was

dx.doi.org/10.1021/jm2017122 | J. Med. Chem. 2012, 55, 2858–2868

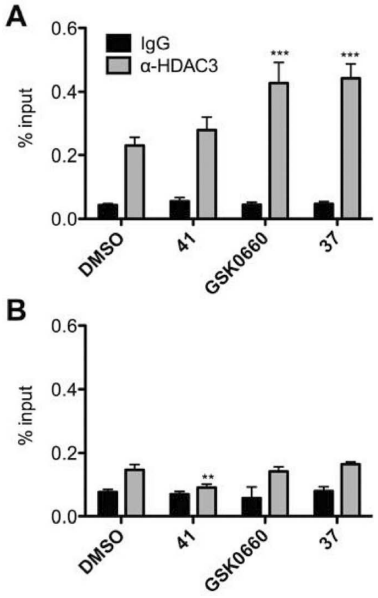

Figure 8. Corepressor binding to PPARβ/δ. The impact of **37** on recruitment of HDAC3 to the *ANGPTL4* promoter in WPMY-1 myofibroblasts was determined by ChIP. Compound **41** does not induce corepressor recruitment[17] and was used as a negative control. Cells were treated with the indicated compounds (1 μM) for 30 min. ChIP was carried out using antibodies against HDAC3 or a nonspecific rabbit IgG pool (negative control). DNA was amplified with primers encompassing the *ANGPTL4* PPREs (A) or a control region (B). Relative amounts of amplified DNA in immunoprecipitates were calculated by comparison with 1% of input DNA. Results are expressed as % input. Statistical analysis was performed as in Figure 4.

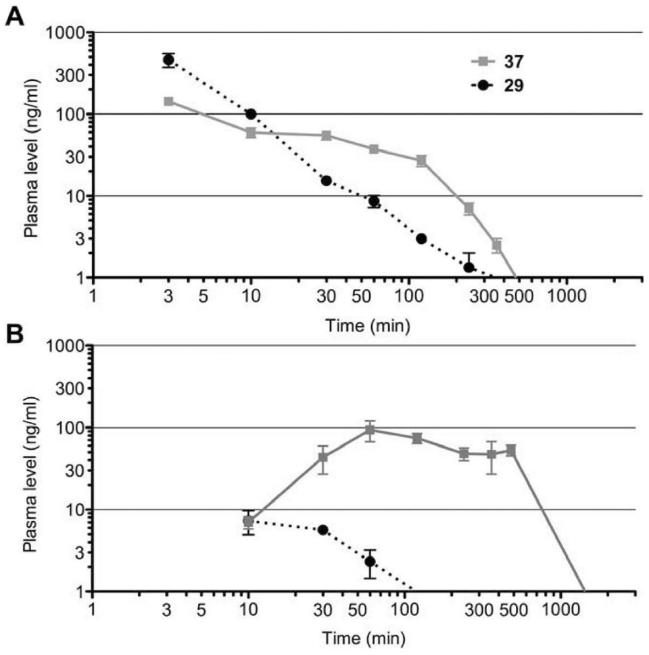

Figure 9. Pharmacokinetics in mice. **29** and **37** were administered either intravenously at a dose of 1 mg/kg (A) or orally at 5 mg/kg (B), and blood samples were analyzed by HPLC-MS/MS at the indicated time points post-treatment. Results represent averages of biological triplicates (±SD). Both compounds were undetectable at 24 h.

purchased from Axxora (Lörrach, Germany), *N*-(2-benzoylphenyl)-*O*-[2-(methyl-2-pyridinylamino)ethyl]-L-tyrosine hydrochloride (GW1929) and 4-[3-(2-propyl-3-hydroxy-4-acetyl)phenoxy]propyloxyphenoxy-acetic acid (L165,041) from Biozol (Eching, Germany), and 2-(4-{2-[4-cyclohexylbutyl(cyclohexylcarbamoyl)amino]ethyl}phenyl)sulfanyl-2-methylpropanoic acid (GW7647) from Sigma-Aldrich (Steinheim, Germany). Synthesis of GSK0660 and compound **41**, 3-{*N*-[4-(*tert*-butylamino)-2-methoxyphenyl]sulfamoyl}-thiophene-2-carboxylate (PT-S58), has been reported previously.[19]

Chemistry. Reagents and solvents that are commercially available were used without further purification. Thin layer chromatography was performed on precoated plates silica gel 60 F254, Merck. Flash column chromatography was performed on prepacked flash chromatography columns (PF 30-SIHP-JP/12G) purchased from Interchim and using a Büchi separation system. Cyclohexane was purchased in pa quality from Grüssing and distilled prior to use, and *iso*-hexane was purchased in technical quality and distilled prior to use.

^{1}H NMR and ^{13}C NMR spectra were recorded on a Jeol ECX-400 or on a Jeol ECA-500 spectrometer. Chemical shifts (δ) are given in ppm with the residual solvent signal used as reference ($CDCl_3$: s, 7.26 ppm [^{1}H] and t, 77.1 ppm [^{13}C]; DMSO-d_6: quint, 2.50 ppm [^{1}H] and septet, 40.1 ppm [^{13}C]). Unless otherwise noted, spectra with $CDCl_3$ as solvent were recorded at 20 °C while spectra with DMSO-d_6 as solvent were recorded at 30.0 °C. Peak patterns were described as folows: s (singlet), d (doublet), dd (double doublet), ddd (doublet of doublet of doublet), t (triplet), m (multiplet), sm (symmetric multiplet), bs (broad singlet), psd (pseudo doublet). Mass spectra were recorded on a double-focusing sector field spectrometer type 70-70H (Vacuum Generators) or on a double-focusing sector field spectrometer type AutoSpec (Micromass). Elemental combustion analyses were performed on a Vario MICRO cube (Elementar Analysensysteme GmbH, Hanau, Germany). Melting points were determined using a melting point meter KSP1N (A. Krüss Optronic GmbH, Hamburg, Germany) and are uncorrected.

All tested compounds were at least 95% pure as a single isomer, determined by NMR and combustion analysis.

Procedure A: To a solution of the respective phenylacetonitrile (1 equiv) and the corresponding benzaldehyde (1 equiv) in methanol (0.6 M) was added potassium hydroxide, and the reaction mixture was stirred at RT until TLC indicated full conversion of the starting material. The precipitate was collected, washed with water and hexane, and dried in vacuo.

Procedure B: To a solution of the respective phenylacetonitrile (1 equiv) and the corresponding benzaldehyde (1 equiv) in methanol (0.6 M) was added pyrrolidine, and the reaction mixture was stirred until TLC indicated full conversion of the starting material. The precipitate was collected, washed with water and hexane, and dried in vacuo.

Procedure C: (*Z*)-3-(4-Bromophenyl)-2-phenylacrylonitrile (1 equiv, prepared following procedure A) was dissolved in dry toluene (0.7 M) under argon atmosphere. (±)-BINAP (0.075 equiv), $Pd_2(dba)_3$ (0.05 equiv), sodium *tert*-butoxide (1.5 equiv), and the corresponding amine (2 equiv) were added, and the suspension was stirred at 80 °C until thin layer chromatography indicated full conversion of the starting material. The reaction mixture was diluted with DCM, filtered through a pad of Celite, absorbed on silica gel, and purified by flash chromatography.

*(Z)-3-{4-[(Dimethylamino)methyl]phenyl}-2-phenylacrylonitrile Hydrochloride (**14**).* To a solution of 4-[(dimethylamino)methyl]-benzaldehyde (105 mg, 0.90 mmol) and phenylacetonitrile (105 mg, 0.90 mmol) in methanol (2 mL) was added potassium hydroxide (50 mg, 0.90 mmol), and the reaction mixture was stirred for 24 h at RT. The reaction mixture was diluted with EtOAc, and the organic phase was washed with water, saturated potassium hydrogencarbonate solution and brine, dried over $MgSO_4$, filtered, and concentrated in vacuo. The free base was obtained by flash chromatography (hexane/EtOAc, gradient from 0 to 50% in 15 min) and was afterward converted to the hydrochloride salt **14** (120 mg, 0.40 mmol, 45%) by precipitation from EtOAc with HCl (5−6 M in *i*-PrOH); mp above decomposition temperature. ^{1}H NMR (DMSO-d_6) δ 11.04 (bs, 1H), 8.07 (s, 1H), 7.97 (psd, J = 8.2 Hz, 2H), 7.78−7.71 (m, 4H), 7.54−7.48 (m, 2H), 7.47−7.42 (sm, 1H), 4.31 (s, 2H), 2.68 (s, 6H). ^{13}C NMR (DMSO-d_6) δ 142.6, 135.2, 134.1, 133.3, 132.1, 130.1, 129.9, 129.8, 126.4, 118.3, 111.9, 59.4, 42.1. HRMS (EI) calcd for $C_{18}H_{18}N_2$

dx.doi.org/10.1021/jm2017122 | J. Med. Chem. 2012, 55, 2858−2868

$[M]^+$ 262.146999; found 262.145737. Anal. Calcd for $C_{18}H_{19}ClN_2$: C, 72.35; H, 6.41; N, 9.37. Found: C, 71.83; H, 6.52; N, 9.21.

*(Z)-2-Phenyl-3-[4-(piperidin-1-yl)phenyl]acrylonitrile (**16**).* According to procedure B, employment of 4-(piperidin-1-yl)benzaldehyde (492 mg, 2.60 mmol), benzyl cyanide (305 mg, 2.60 mmol), and pyrrolidine (185 mg, 2.60 mmol) gave rise to **16** as a yellow solid (150 mg, 0.52 mmol, 20%); mp 128 °C. ^{1}H NMR ($CDCl_3$) δ 7.84 (psd, J = 8.9 Hz, 2H), 7.66−7.61 (m, 2H), 7.44−7.38 (m, 3H), 7.35−7.30 (m, 1H), 6.92 (psd, J = 7.8 Hz, 2H), 3.37−3.31 (m, 4H), 1.76−1.60 (m, 6H). ^{13}C NMR ($CDCl_3$) δ 152.8, 142.4, 135.5, 131.4, 129.0, 128.3, 125.6, 123.2, 119.4, 114.5, 105.6, 48.9, 25.5, 24.5. HRMS (EI) calcd for $C_{20}H_{20}N_2$ $[M]^+$ 288.162649; found 288.164001. Anal. Calcd for $C_{20}H_{20}N_2$: C, 83.30; H, 6.99; N, 9.71. Found: C, 83.23; H, 7.14; N, 9.81.

*(Z)-3-[4-(Cyclohexylamino)phenyl]-2-phenylacrylonitrile (**18**).* According to procedure C, utilization of (*Z*)-3-(4-bromophenyl)-2-phenylacrylonitrile (200 mg, 0.70 mmol), (±)-BINAP (32.9 mg, 0.053 mmol), $Pd_2(dba)_3$ (32.2 mg, 0.035 mmol), sodium *tert*-butoxide (102 mg, 1.06 mmol), and cyclohexylamine (140 mg, 1.41 mmol) yielded, after purification by flash chromatography (*iso*-hexane/EtOAc, gradient from 0 to 25% in 12 min), **18** as a yellow solid (94 mg, 0.31 mmol, 44%); mp 122 °C. ^{1}H NMR (DMSO-d_6) δ 7.74 (psd, J = 8.7 Hz, 2H), 7.69 (s, 1H), 7.64−7.60 (m, 2H), 7.45−7.39 (m, 2H), 7.33−7.28 (sm, 1H), 6.64 (psd, J = 8.7 Hz, 2H), 6.40 (d, J = 7.8 Hz, 1H), 3.33−3.23 (sm, 1H), 1.93−1.86 (sm, 2H), 1.74−1.65 (sm, 2H), 1.61−1.53 (sm, 1H), 1.39−1.27 (sm, 2H), 1.21−1.10 (m, 3H). ^{13}C NMR ($CDCl_3$) δ 149.5, 142.8, 135.7, 131.7, 129.0, 128.1, 125.6, 122.3, 119.6, 112.6, 104.5, 51.4, 33.3, 25.8, 25.0. HRMS (EI) calcd for $C_{21}H_{22}N_2$ $[M]^+$ 302.178299; found 302.178004. Anal. Calcd for $C_{21}H_{22}N_2$: C, 83.40; H, 7.33; N, 9.26. Found: C, 83.27; H, 7.26; N, 9.10.

*(Z)-2-Phenyl-3-[4-(phenylamino)phenyl]acrylonitrile (**19**).* Following procedure C, usage of (*Z*)-3-(4-bromophenyl)-2-phenylacrylonitrile (200 mg, 0.70 mmol), (±)-BINAP (32.9 mg, 0.053 mmol), $Pd_2(dba)_3$ (32.2 mg, 0.035 mmol), sodium *tert*-butoxide (102 mg, 1.06 mmol), and aniline (131 mg, 1.41 mmol) yielded, after purification by flash chromatography (*iso*-hexane/EtOAc, gradient from 0 to 25% in 12 min), **19** as a yellow solid (110 mg, 0.37 mmol, 53%); mp 162 °C. ^{1}H NMR ($CDCl_3$) δ 7.85 (psd, J = 8.7 Hz, 2H), 7.67−7.63 (m, 2H), 7.45−7.44 (m, 3H), 7.38−7.32 (m, 3H), 7.21−7.17 (m, 2H), 7.11−7.04 (m, 3H). ^{13}C NMR ($CDCl_3$) δ 146.1, 142.1, 141.0, 135.2, 131.4, 129.6, 129.2, 128.6, 125.8, 125.5, 123.0, 120.2, 119.1, 115.7, 107.0. HRMS (EI) calcd for $C_{21}H_{16}N_2$ $[M]^+$ 296.131349; found 296.129489. Anal. Calcd for $C_{21}H_{16}N_2$: C, 85.11; H, 5.44; N, 9.45. Found: C, 84.78; H, 5.66; N, 9.19.

*(Z)-3-[4-(4-Methylpiperidin-1-yl)phenyl]-2-phenylacrylonitrile (**20**).* According to procedure C, utilization of (*Z*)-3-(4-bromophenyl)-2-phenylacrylonitrile (200 mg, 0.70 mmol), (±)-BINAP (32.9 mg, 0.053 mmol), $Pd_2(dba)_3$ (32.2 mg, 0.035 mmol), sodium *tert*-butoxide (102 mg, 1.06 mmol), and 4-methylpiperidine (140 mg, 1.41 mmol) rendered, after purification by flash chromatography (*iso*-hexane/DCM, 5:2), **20** as a yellow solid (194 mg, 0.64 mmol, 91%); mp 120 °C. ^{1}H NMR (DMSO-d_6) δ 7.83 (psd, J = 8.9 Hz, 2H), 7.78 (s, 1H), 7.68−7.63 (m, 2H), 7.46−7.41 (m, 2H), 7.36−7.31 (sm, 1H), 6.99 (psd, J = 9.2 Hz, 2H), 3.92−3.85 (sm, 2H), 2.84−2.76 (sm, 2H), 1.69−1.62 (sm, 2H), 1.63−1.50 (sm, 1H), 1.21−1.08 (sm, 2H), 0.90 (d, J = 6.4 Hz, 3H). ^{13}C NMR ($CDCl_3$) δ 152.6, 142.4, 135.5, 131.3, 129.0, 128.3, 125.6, 123.2, 119.4, 114.5, 105.6, 48.2, 33.7, 31.0, 22.0. HRMS (EI) calcd for $C_{21}H_{22}N_2$ $[M]^+$ 302.178299; found 302.178744. Anal. Calcd for $C_{21}H_{22}N_2$: C, 83.40; H, 7.33; N, 9.26. Found: C, 83.20; H, 7.30; N, 8.81.

*(Z)-2-Phenyl-3-[4-(piperazin-1-yl)phenyl]acrylonitrile (**22**).* (*Z*)-3-(4-Bromophenyl)-2-phenylacrylonitrile (100 mg, 0.35 mmol) was dissolved in dry toluene (2 mL) under an argon atmosphere. Tri-*tert*-butylphosphine (14.2 mg, 0.070 mmol), $Pd_2(dba)_3$ (16.1 mg, 0.018 mmol), sodium *tert*-butoxide (101 mg, 1.06 mmol), and piperazine (182 mg, 2.11 mmol) were added, and the suspension was stirred at 120 °C for 15 h. The reaction mixture was diluted with DCM, filtered through a pad of Celite, absorbed on silica gel, and purified by flash chromatography (DCM/methanol, 50:1), giving rise to **22** as a yellow wax (53.1 mg, 0.18 mmol, 52%). ^{1}H NMR (DMSO-d_6) δ 7.84 (psd, J = 9.2 Hz, 2H), 7.80 (s, 1H), 7.68−7.64 (m, 2H), 7.47−7.41 (m, 2H), 7.37−7.31 (sm, 1H), 6.99 (psd, J = 9.2 Hz, 2H), 3.23−3.19 (sm, 4H), 2.81−2.77 (sm, 4H). ^{13}C NMR ($CDCl_3$) δ 152.8, 142.2, 135.3, 131.2, 129.0, 128.4, 125.7, 124.1, 119.1, 114.5, 106.5, 48.8, 45.9. HRMS (EI) calcd for $C_{19}H_{19}N_3$ $[M]^+$ 289.157898; found 289.155945.

*(Z)-3-[4-(4-Methylpiperazin-1-yl)phenyl]-2-phenylacrylonitrile (**23**).* According to procedure B, employment of 4-(4-methylpiperazin-1-yl)benzaldehyde (265 mg, 1.30 mmol), benzyl cyanide (152 mg, 1.30 mmol), and pyrrolidine (92 mg, 1.30 mmol) furnished **23** as a yellow solid (268 mg, 0.88 mmol, 68%); mp 143 °C. ^{1}H NMR (DMSO-d_6) δ 7.84 (psd, J = 8.9 Hz, 2H), 7.81 (s, 1H), 7.69−7.64 (m, 2H), 7.47−7.41 (m, 2H), 7.37−7.32 (sm, 1H), 7.02 (psd, J = 9.2 Hz, 2H), 3.30 (t, J = 5.0 Hz, 4H), 2.41 (t, J = 5.0 Hz, 4H), 2.19 (s, 3H). ^{13}C NMR (DMSO-d_6) δ 152.7, 143.2, 135.2, 131.5, 129.6, 128.8, 125.7, 123.5, 119.5, 114.5, 104.7, 54.9, 47.2, 46.3. HRMS (EI) calcd for $C_{20}H_{21}N_3$ $[M]^+$ 303.173548; found 303.171852. Anal. Calcd for $C_{20}H_{21}N_3$: C, 79.17; H, 6.98; N, 13.85. Found: C, 78.95; H, 7.01; N, 13.86.

*(Z)-2-(4-Chlorophenyl)-3-[4-(dimethylamino)phenyl]acrylonitrile (**27**).* According to procedure A, usage of 4-(dimethylamino)benzaldehyde (351 mg, 2.35 mmol), 2-(4-chlorophenyl)acetonitrile (357 mg, 2.35 mmol), and potassium hydroxide (132 mg, 2.35 mmol) furnished **27** as a yellow solid (326 mg, 1.15 mmol, 49%); mp 193 °C. ^{1}H NMR ($CDCl_3$) δ 7.85 (psd, J = 8.9 Hz, 2H), 7.55 (psd, J = 8.9 Hz, 2H), 7.38−7.35 (m, 3H), 6.74 (psd, J = 8.9 Hz, 2H), 3.06 (s, 6H). ^{13}C NMR ($CDCl_3$) δ 152.0, 142.9, 134.2, 133.8, 131.5, 129.1, 126.7, 121.4, 119.3, 111.7, 103.2, 40.2. HRMS (EI) calcd for $C_{17}H_{15}ClN_2$ $[M]^+$ 282.092376; found 282.093166. Anal. Calcd for $C_{17}H_{15}ClN_2$: C, 72.21; H, 5.35; N, 9.91. Found: C, 72.06; H, 5.37; N, 9.85.

*(Z)-2-(3-Chlorophenyl)-3-[4-(dimethylamino)phenyl]acrylonitrile (**28**).* According to procedure A, employment of 4-(dimethylamino)-benzaldehyde (585 mg, 3.92 mmol), 2-(3-chlorophenyl)acetonitrile (595 mg, 3.92 mmol), and potassium hydroxide (220 mg, 3.92 mmol) gave rise to **28** as a yellow solid (710 mg, 2.51 mmol, 49%); mp 132 °C. ^{1}H NMR ($CDCl_3$) δ 7.85 (psd, J = 8.9 Hz, 2H), 7.60 (t, J = 1.9 Hz, 1H), 7.50 (sm, 1H), 7.38 (s, 1H), 7.33 (t, J = 7.8 Hz, 1H), 7.26 (sm, 1H), 6.71 (psd, J = 9.1 Hz, 2H), 3.06 (s, 6H). ^{13}C NMR ($CDCl_3$) δ 152.0, 143.6, 137.6, 135.0, 131.7, 130.2, 127.9, 125.4, 123.7, 121.2, 119.2, 111.7, 102.8, 40.1. MS (EI) m/z (%) 282.1 (100) $[M]^+$. Anal. Calcd for $C_{17}H_{15}ClN_2$: C, 72.21; H, 5.35; N, 9.91. Found: C, 72.35; H, 5.51; N, 9.82.

*(Z)-2-(2-Chlorophenyl)-3-[4-(dimethylamino)phenyl]acrylonitrile (**29**).* Following procedure B, usage of 4-(dimethylamino)benzaldehyde (351 mg, 2.35 mmol), 2-(2-chlorophenyl)acetonitrile (357 mg, 2.35 mmol), and pyrrolidine (167 mg, 2.35 mmol) at 60 °C furnished **29** as a yellow solid (326 mg, 1.15 mmol, 49%); mp 99 °C. ^{1}H NMR ($CDCl_3$) δ 7.85 (psd, J = 8.9 Hz, 2H), 7.46−7.40 (m, 2H), 7.33−7.26 (m, 2H), 7.12 (s, 1H), 6.73 (psd, J = 8.9 Hz, 2H), 3.06 (s, 6H). ^{13}C NMR ($CDCl_3$) δ 152.0, 148.4, 135.6, 133.2, 131.5, 131.0, 130.4, 129.7, 127.4, 121.2, 119.0, 111.7, 101.8, 40.2. HRMS (EI) calcd for $C_{17}H_{15}ClN_2$ $[M]^+$ 282.092376; found 282.094431. Anal. Calcd for $C_{17}H_{15}ClN_2$: C, 72.21; H, 5.35; N, 9.91. Found: C, 72.43; H, 5.53; N, 10.00.

*(Z)-3-[4-(Dimethylamino)phenyl]-2-(2-iodophenyl)acrylonitrile (**30**).* To a solution of 4-dimethylaminobenzaldehyde (161 mg, 1.08 mmol) and 2-(2-iodophenyl)acetonitrile (263 mg, 1.08 mmol) in methanol (2 mL) was added pyrrolidine (145 mg, 1.08 mmol), and the reaction mixture was stirred for 18 h at 60 °C. The reaction mixture was diluted with EtOAc, and the organic phase was washed with water, saturated potassium hydrogencarbonate solution, and brine, dried over $MgSO_4$, filtered, and concentrated in vacuo. Flash chromatography (cyclohexane/EtOAc, gradient from 0 to 30% in 12 min) furnished **30** as a yellow solid (185 mg, 0.49 mmol, 46%); mp 134 °C. ^{1}H NMR ($CDCl_3$) δ 7.94−7.91 (m, 1H), 7.85 (psd, J = 8.9 Hz, 2H), 7.42−7.36 (m, 2H), 7.04 (ddd, J = 7.7, 6.6, 2.5 Hz, 1H), 6.99 (s, 1H), 6.73 (psd, J = 9.2 Hz, 2H), 3.06 (s, 6H). ^{13}C NMR ($CDCl_3$) δ 152.1, 148.5, 141.1, 140.1, 131.4, 130.5, 129.9, 128.7, 121.0, 118.8, 111.7, 106.6, 98.7, 40.2. HRMS (EI) calcd for $C_{17}H_{15}IN_2$ $[M]^+$ 374.028001; found 374.024834. Anal. Calcd for $C_{17}H_{15}IN_2$: C, 54.56; H, 4.04; N, 7.49. Found: C, 54.82; H, 4.16; N, 7.45.

*(Z)-2-(2-Bromophenyl)-3-[4-(dimethylamino)phenyl]acrylonitrile (**31**).* A solution of 2-bromophenylacetonitrile (376 mg, 1.93 mmol)

dx.doi.org/10.1021/jm2017122 | J. Med. Chem. 2012, 55, 2858−2868

and 4-dimethylaminobenzaldehyde (288 mg, 1.93 mmol) in morpholine (2 mL) was stirred for 12 h at 120 °C. The reaction mixture was absorbed onto silica, and flash chromatography (*iso*-hexane/EtOAc/DCM, 18:1:1) gave rise to **31** as yellow solid (184 mg, 0.56 mmol, 29%); mp 140 °C. ^{1}H NMR ($CDCl_3$) δ 7.85 (psd, J = 8.9 Hz, 2H), 7.64 (dd, J = 8.0, 1.1 Hz, 1H), 7.41 (dd, J = 7.6, 1.8 Hz, 1H), 7.35 (td, J = 7.6, 1.4 Hz, 1H), 7.21 (ddd, J = 7.6, 1.8, 0.5 Hz, 1H), 7.07 (s, 1H), 6.72 (psd, J = 9.2 Hz, 2H), 3.06 (s, 6H). ^{13}C NMR ($CDCl_3$) δ 152.1, 148.4, 137.5, 133.6, 131.4, 131.2, 129.8, 127.9, 123.2, 121.1, 118.9, 111.7, 103.5, 40.2. HRMS (EI) calcd for $C_{17}H_{15}BrN_2$ $[M]^+$ 326.041860; found 326.042488. Anal. Calcd for $C_{17}H_{15}BrN_2$: C, 62.40; H, 4.62; N, 8.56. Found: C, 62.34; H, 4.79; N, 8.44.

*(Z)-3-[4-(Dimethylamino)phenyl]-2-(2-methoxyphenyl)-acrylonitrile (**32**).* To a solution of 4-dimethylaminobenzaldehyd (304 mg, 2.04 mmol) and 2-(2-methoxyphenyl)acetonitrile (300 mg, 2.04 mmol) in methanol (4 mL) was added pyrrolidine (145 mg, 2.04 mmol), and the reaction mixture was stirred for 48 h at 60 °C. The reaction mixture was diluted with EtOAc, and the organic phase was washed with water, saturated potassium hydrogencarbonate solution, and brine, dried over $MgSO_4$, filtered, and concentrated in vacuo. **32** was obtained after flash chromatography (cyclohexane/EtOAc/DCM, 8:1:1) as a yellow solid (111 mg, 0.40 mmol, 20%); mp 97 °C. ^{1}H NMR ($CDCl_3$) δ 7.84 (psd, J = 8.7 Hz, 2H), 7.38 (dd, J = 7.6, 1.6 Hz, 1H), 7.32 (ddd, J = 8.2, 7.4, 1.6 Hz, 1H), 7.28 (s, 1H), 6.99 (td, J = 7.6, 1.1 Hz, 1H), 6.94 (dd, J = 8.2, 0.7 Hz, 1H), 6.76 (psd, J = 7.1 Hz, 2H), 3.91 (s, 3H), 3.05 (s, 6H). ^{13}C NMR ($CDCl_3$) δ 157.0, 151.6, 146.5, 131.2, 129.9, 129.7, 125.9, 122.1, 121.0, 119.6, 111.6, 111.5, 102.0, 55.9, 40.2. HRMS (EI) calcd for $C_{18}H_{18}N_2O$ $[M]^+$ 278.141913; found 278.140550. Anal. Calcd for $C_{18}H_{18}N_2O$: C, 77.67; H, 6.52; N, 10.06. Found: C, 77.25; H, 6.61; N, 9.74.

*(Z)-3-[4-(Dimethylamino)phenyl]-2-(2-(trifluoromethyl)phenyl)-acrylonitrile (**33**).* A solution of 2-(2-trifluoromethylphenyl)acetonitrile (200 mg, 1.08 mmol) and 4-dimethylaminobenzaldehyde (161 mg, 1.08 mmol) in morpholine (2 mL) was stirred for 24 h at 120 °C and subsequently absorbed onto silica gel. Flash chromatography (*iso*-hexane/EtOAc, 5:1) gave rise to **33** as a yellow solid (67 mg, 0.21 mmol, 20%); mp 110 °C. ^{1}H NMR ($CDCl_3$) δ 7.82 (psd, J = 8.9 Hz, 2H), 7.76–7.72 (m, 1H), 7.61–7.56 (m, 1H), 7.52–7.46 (m, 2H), 6.98 (s, 1H), 6.80 (psd, J = 8.2 Hz, 2H), 3.07 (s, 6H). ^{13}C NMR ($CDCl_3$) δ 152.1, 148.3, 147.1, 135.7, 132.2, 132.0, 131.3, 129.3, 128.7, 124.0 (d, $J_{C,F}$ = 274.0 Hz), 121.0, 119.2, 111.6, 100.7, 40.0. HRMS (EI) calcd for $C_{18}H_{15}F_3N_2$ $[M]^+$ 316.118733; found 316.117731. Anal. Calcd for $C_{18}H_{15}F_3N_2$: C, 68.35; H, 4.78; N, 8.86. Found: C, 68.58; H, 5.18; N, 8.75.

*(Z)-3-[4-(Dimethylamino)phenyl]-2-(2-fluorophenyl)acrylonitrile (**34**).* Following procedure B, usage of 4-(dimethylamino)benzaldehyde (442 mg, 2.96 mmol), 2-(2-fluorophenyl)acetonitrile (400 mg, 2.96 mmol), and pyrrolidine (463 mg, 6.51 mmol) gave rise to **34** as a yellow solid (583 mg, 2.19 mmol, 74%); mp 106 °C. ^{1}H NMR ($CDCl_3$) δ 7.86 (psd, J = 8.9 Hz, 2H), 7.54 (td, J = 7.8, 1.8 Hz, 1H), 7.42 (s, 1H), 7.32–7.26 (sm, 1H), 7.19 (td, J = 7.6, 1.1 Hz, 1H), 7.12 (ddd, J = 11.2, 8.2, 1.1 Hz, 1H), 6.71 (psd, J = 9.2 Hz, 2H), 3.06 (s, 6H). ^{13}C NMR ($CDCl_3$) δ 159.8 (d, $J_{C,F}$ = 250.4 Hz), 152.0, 147.4 (d, $J_{C,F}$ = 7.8 Hz), 131.6, 129.7 (d, $J_{C,F}$ = 3.0 Hz), 129.6 (d, $J_{C,F}$ = 8.7 Hz), 124.6 (d, $J_{C,F}$ = 3.0 Hz), 124.2 (d, $J_{C,F}$ = 11.6 Hz), 121.5, 119.3, 116.5 (d, $J_{C,F}$ = 23.1 Hz), 111.6, 98.7 (d, $J_{C,F}$ = 1.9 Hz), 40.1. HRMS (EI) calcd for $C_{17}H_{15}FN_2$ $[M]^+$ 266.121927; found 266.123324. Anal. Calcd for $C_{17}H_{15}FN_2$: C, 76.67; H, 5.68; N, 10.52. Found: C, 76.57; H, 5.73; N, 10.50.

*(Z)-2-(2-Bromophenyl)-3-[4-(4-methylpiperazin-1-yl)phenyl]-acrylonitrile Dihydrochloride (**37**).* To a solution of 2-(2-bromophenyl)-acetonitrile (480 mg, 2.45 mmol) and 4-(4-methylpiperazino)benzaldehyde (500 mg, 2.45 mmol) in methanol (4 mL) was added pyrrolidine (174 mg, 2.45 mmol). The reaction mixture was stirred for 48 h at 60 °C and subsequently absorbed onto silica gel. The free base was obtained by flash chromatography (DCM/MeOH, 49:1) and was afterward converted to the dihydrochloride salt **37** (806 mg, 1.93 mmol, 79% yield) by precipitation from EtOAc with HCl (5–6 M in *i*PrOH); mp above decomposition temperature. ^{1}H NMR (DMSO-d_6, 80 °C, 500 MHz) δ 11.46 (bs, 1H), 9.96 (bs, 1H), 7.85 (psd, J = 8.9 Hz, 2H), 7.71 (d, J = 8.0 Hz, 1H), 7.51 (dd, J = 7.7, 1.7 Hz, 1H), 7.48–7.45 (sm, 1H), 7.37–7.33 (sm, 1H), 7.32 (s, 1H), 7.10 (psd, J = 8.9 Hz, 2H), 4.05–3.95 (m, 2H), 3.49–3.29 (m, 4H), 3.18–3.05 (m, 2H), 2.77 (s, 3H). ^{13}C NMR (DMSO-d_6) δ 151.7, 148.6, 136.9, 133.7, 132.1, 131.4, 131.3, 129.1, 124.2, 122.8, 118.5, 115.3, 105.3, 52.1, 44.6, 42.4. HRMS (EI) calcd for $C_{20}H_{20}BrN_3$ $[M]^+$ 381.084059; found 381.087401. Anal. Calcd for $C_{20}H_{22}BrCl_2N_3$: C, 52.77; H, 4.87; N, 9.23. Found: C, 52.68; H, 4.97; N, 9.18.

Time-Resolved Fluorescence Resonance Energy Transfer (TR-FRET) Assays in Vitro. Ligand binding was determined by TR-FRET in vitro[25] using the Lanthascreen TR-FRET PPARβ/δ competitive binding assay as described.[26,27] The interaction of the PPARβ/δ LBD with a fluorescein-labeled corepressor peptide derived from the silencing mediator for retinoid and thyroid hormone receptors interaction domain 2 (SMRT-ID2) was determined using the Lanthascreen TR-FRET PPARβ/δ coregulator assay.[27] Assays were carried out and evaluated as described.

Chemical Compound Library Screening. The Open Chemical Repository of the NCI/NIH Developmental Therapeutics Program consisting of the Approved Oncology Drugs Set III (97 compounds), the Diversity Set III (1597 compounds), the Mechanistic Set (879 compounds), and the Natural Product Set II (120 compounds) was initially screened for compounds binding to the PPARβ/δ LBD using the competitive TR-FRET assay described above. Compounds showing significant competition (n = 129) were subsequently validated in triplicates using TR-FRET-based coactivator and corepressor peptide recruitment assays (see above).[27]

Cell Culture. WPMY-1 human myofibroblasts[28] (ATCC, CRL-2854), C2C12 murine myoblasts[29] (kindly provided by Dr. Thomas Braun, Bad Nauheim, Germany), and NIH3T3 cells were maintained in DMEM supplemented with 10% fetal bovine serum, 100 U/mL penicillin, and 100 μg/mL streptomycin in a humidified incubator at 37 °C and 5% CO_2.

Transcription, Gene Expression, and Chromatin Analyses. Luciferase reporter assays were performed and evaluated as reported previously. LexA-PPAR expression plasmids and the 7 L-TATAi luciferase reporter construct have been described elsewhere.[30,31] RT-qPCR analyses of endogenous *Angptl4* expression and statistical analyses were carried out as described,[17] using *L27* as the normalizer. ChIP analysis was performed as reported elsewhere.[24,32]

Pharmacokinetics in Mice. In vivo pharmacokinetic studies were performed by Cerep, Redmond, WA. Briefly, compounds were formulated in DMSO/Solutol HS 15/PBS, pH 7.4 (5/5/90, v/v/v) and administered iv (1 mg/kg) and po (5 mg/kg) to male CD-1 mice by tail vein injection and gastric gavage, respectively. Blood samples were taken at eight time points post injection by parallel sampling (three mice each; see Figure 9 for details). Plasma samples were processed by acetonitrile precipitation and analyzed by HPLS-MS/MS following standard procedures.

■ ASSOCIATED CONTENT

Ⓢ Supporting Information

Properties of compounds identified by library screening as PPARβ/δ ligands, Analysis of stilbene derivatives as potential PPARβ/δ ligands, Analysis of compound **1** (NSC636948) and derivatives by competitive in vitro ligand binding assay, and experimental procedures for further compounds. This material is available free of charge via the Internet at http://pubs.acs.org.

■ AUTHOR INFORMATION

Corresponding Author

*For W.D.: phone, +49 6421 2825810; E-mail, wibke.diederich@staff.uni-marburg.de. For R.M.: phone, +49 6421 2866236; E-mail, rmueller@imt.uni-marburg.de.

Author Contributions

§The first two authors contributed equally to this work.

Notes

The authors declare no competing financial interest.

■ ACKNOWLEDGMENTS

We thank Klaus Weber, Margitta Alt, and Julia Dick for expert technical assistance. This work is supported by grants to R.M. from the Deutsche Forschungsgemeinschaft (SFB-TR17/A3) and the LOEWE-Schwerpunkt "Tumor and Inflammation" of the state of Hesse.

■ ABBREVIATIONS USED

ANGPTL4, angiopoietin-like 4 protein; *ANGPTL4*, angiopoietin-like 4 gene (human); *Angptl4*, angiopoietin-like 4 gene (mouse); BCL-6, B-cell chronic lymphatic leukemia/lymphoma 6 protein; ChIP, chromatin immune precipitation; CL, mean clearance; DBD, DNA binding domain; FRET, fluorescence resonance energy transfer; GST, gluthatione *S*-transferase; HAT, acetyl transferase; HDAC, histone deacetylase; LBD, ligand binding domain; NCoR, nuclear receptor corepressor; *PDK4*, pyruvate dehydrogenase kinase 4 gene; PPAR, peroxisome proliferator-activated receptor; PPRE, peroxisome proliferator responsive element; RT-qPCR, real-time quantitative polymerase chain reaction; RXR, retinoid X receptor; SAR, structure−activity relationship; SMRT, silencing mediator for retinoid and thyroid hormone receptors; SMRT-ID2, SMRT interaction domain 2; SHARP, SMRT and HDAC-associated repressor protein; TR-FRET, time-resolved fluorescence resonance energy transfer; Vss, volume of distribution at steady state

■ REFERENCES

(1) Lonard, D. M.; O'Malley, B. W. Nuclear receptor coregulators: judges, juries, and executioners of cellular regulation. *Mol. Cell* **2007**, *27*, 691−700.

(2) Desvergne, B.; Michalik, L.; Wahli, W. Transcriptional regulation of metabolism. *Physiol. Rev.* **2006**, *86*, 465−514.

(3) Zoete, V.; Grosdidier, A.; Michielin, O. Peroxisome proliferator-activated receptor structures: ligand specificity, molecular switch and interactions with regulators. *Biochim. Biophys. Acta* **2007**, *1771*, 915−925.

(4) Peraza, M. A.; Burdick, A. D.; Marin, H. E.; Gonzalez, F. J.; Peters, J. M. The toxicology of ligands for peroxisome proliferator-activated receptors (PPAR). *Toxicol. Sci.* **2006**, *90*, 269−295.

(5) Glass, C. K.; Saijo, K. Nuclear receptor transrepression pathways that regulate inflammation in macrophages and T cells. *Nature Rev. Immunol.* **2010**, *10*, 365−376.

(6) Michalik, L.; Wahli, W. Peroxisome proliferator-activated receptors (PPARs) in skin health, repair and disease. *Biochim. Biophys. Acta* **2007**, *1771*, 991−998.

(7) Peters, J. M.; Gonzalez, F. J. Sorting out the functional role(s) of peroxisome proliferator-activated receptor-beta/delta (PPARbeta/delta) in cell proliferation and cancer. *Biochim. Biophys. Acta* **2009**, *1796*, 230−241.

(8) Montagner, A.; Rando, G.; Degueurce, G.; Leuenberger, N.; Michalik, L.; Wahli, W. New insights into the role of PPARs. *Prostaglandins, Leukotrienes Essent. Fatty Acids* **2011**, *85*, 235−243.

(9) Yu, S.; Reddy, J. K. Transcription coactivators for peroxisome proliferator-activated receptors. *Biochim. Biophys. Acta* **2007**, *1771*, 936−951.

(10) Shi, Y.; Hon, M.; Evans, R. M. The peroxisome proliferator-activated receptor delta, an integrator of transcriptional repression and nuclear receptor signaling. *Proc. Natl. Acad. Sci. U.S.A.* **2002**, *99*, 2613−2618.

(11) Adhikary, T.; Kaddatz, K.; Finkernagel, F.; Schönbauer, A.; Meissner, W.; Scharfe, M.; Jarek, M.; Blöcker, H.; Müller-Brüsselbach, S.; Müller, R. Genomewide analyses define different modes of transcriptional regulation by peroxisome proliferator-activated receptor-beta/delta (PPARbeta/delta). *PLoS One* **2011**, *6*, e16344.

(12) Lee, C. H.; Chawla, A.; Urbiztondo, N.; Liao, D.; Boisvert, W. A.; Evans, R. M.; Curtiss, L. K. Transcriptional repression of atherogenic inflammation: modulation by PPARdelta. *Science* **2003**, *302*, 453−457.

(13) Zaveri, N. T.; Sato, B. G.; Jiang, F.; Calaoagan, J.; Laderoute, K. R.; Murphy, B. J. A novel peroxisome proliferator-activated receptor delta antagonist, SR13904, has anti-proliferative activity in human cancer cells. *Cancer Biol. Ther.* **2009**, *8*, 1252−1261.

(14) Shearer, B. G.; Wiethe, R. W.; Ashe, A.; Billin, A. N.; Way, J. M.; Stanley, T. B.; Wagner, C. D.; Xu, R. X.; Leesnitzer, L. M.; Merrihew, R. V.; Shearer, T. W.; Jeune, M. R.; Ulrich, J. C.; Willson, T. M. Identification and characterization of 4-chloro-*N*-(2-{[5-trifluoromethyl)-2-pyridyl]sulfonyl}ethyl)benzamide (GSK3787), a selective and irreversible peroxisome proliferator-activated receptor delta (PPARdelta) antagonist. *J. Med. Chem.* **2010**, *53*, 1857−1861.

(15) Palkar, P. S.; Borland, M. G.; Naruhn, S.; Ferry, C. H.; Lee, C.; Sk, U. H.; Sharma, A. K.; Amin, S.; Murray, I. A.; Anderson, C. R.; Perdew, G. H.; Gonzalez, F. J.; Müller, R.; Peters, J. M. Cellular and pharmacological selectivity of the peroxisome proliferator-activated receptor-beta/delta antagonist GSK3787. *Mol. Pharmacol.* **2010**, *78*, 419−430.

(16) Shearer, B. G.; Steger, D. J.; Way, J. M.; Stanley, T. B.; Lobe, D. C.; Grillot, D. A.; Iannone, M. A.; Lazar, M. A.; Willson, T. M.; Billin, A. N. Identification and characterization of a selective peroxisome proliferator-activated receptor beta/delta (NR1C2) antagonist. *Mol. Endocrinol.* **2008**, *22*, 523−529.

(17) Naruhn, S.; Toth, P. M.; Adhikary, T.; Kaddatz, K.; Pape, V.; Dörr, S.; Klebe, G.; Müller-Brüsselbach, S.; Diederich, W. E.; Müller, R. High-affinity peroxisome proliferator-activated receptor beta/delta-specific ligands with pure antagonistic or inverse agonistic properties. *Mol. Pharmacol.* **2011**, *80*, 828−838.

(18) Toth, P. M.; Naruhn, S.; Pape, V. F.; Dörr, S. M.; Klebe, G.; Müller, R.; Diederich, W. E. Development of Improved PPARbeta/delta Inhibitors. *ChemMedChem* **2012**, *7*, 159−170.

(19) Kasuga, J.; Ishida, S.; Yamasaki, D.; Makishima, M.; Doi, T.; Hashimoto, Y.; Miyachi, H. Novel biphenylcarboxylic acid peroxisome proliferator-activated receptor (PPAR) delta selective antagonists. *Bioorg. Med. Chem. Lett.* **2009**, *19*, 6595−6599.

(20) Guram, A. S.; Rennels, R. A.; Buchwald, S. L. A Simple Catalytic Method for the Conversion of Aryl Bromides to Arylamines. *Angew. Chem., Int. Ed.* **1995**, *34*, 1348−1350.

(21) Jiang, L.; Buchwald, S. L. *Palladium-Catalyzed Aromatic Carbon−Nitrogen Bond Formation*; WILEY-VCH Verlag GmbH & Co: Weinheim, Germany, 2004; Vol. 2, pp 699−760.

(22) Louie, J.; Hartwig, J. F. Palladium-catalyzed synthesis of arylamines from aryl halides. Mechanistic studies lead to coupling in the absence of tin reagents. *Tetrahedron Lett.* **1995**, *36*, 3609−3612.

(23) Mandard, S.; Zandbergen, F.; Tan, N. S.; Escher, P.; Patsouris, D.; Koenig, W.; Kleemann, R.; Bakker, A.; Veenman, F.; Wahli, W.; Muller, M.; Kersten, S. The direct peroxisome proliferator-activated receptor target fasting-induced adipose factor (FIAF/PGAR/ANGPTL4) is present in blood plasma as a truncated protein that is increased by fenofibrate treatment. *J. Biol. Chem.* **2004**, *279*, 34411−34420.

(24) Kaddatz, K.; Adhikary, T.; Finkernagel, F.; Meissner, W.; Müller-Brüsselbach, S.; Müller, R. Transcriptional profiling identifies functional interactions of TGFβ and PPARβ/δ signaling: synergistic induction of ANGPTL4 transcription. *J. Biol. Chem.* **2010**, *285*, 29469−29479.

(25) Stafslien, D. K.; Vedvik, K. L.; De Rosier, T.; Ozers, M. S. Analysis of ligand-dependent recruitment of coactivator peptides to RXRbeta in a time-resolved fluorescence resonance energy transfer assay. *Mol. Cell. Endocrinol.* **2007**, *264*, 82−89.

(26) Rieck, M.; Meissner, W.; Ries, S.; Müller-Brüsselbach, S.; Müller, R. Ligand-mediated regulation of peroxisome proliferator-activated receptor (PPAR) beta/delta: a comparative analysis of PPAR-selective agonists and all-trans retinoic acid. *Mol. Pharmacol.* **2008**, *74*, 1269−1277.

(27) Naruhn, S.; Meissner, W.; Adhikary, T.; Kaddatz, K.; Klein, T.; Watzer, B.; Müller-Brüsselbach, S.; Müller, R. 15-Hydroxyeicosatetraenoic

acid is a preferential peroxisome proliferator-activated receptor β/δ agonist. *Mol. Pharmacol.* **2010**, *77*, 171−184.
(28) Webber, M. M.; Trakul, N.; Thraves, P. S.; Bello-DeOcampo, D.; Chu, W. W.; Storto, P. D.; Huard, T. K.; Rhim, J. S.; Williams, D. E. A human prostatic stromal myofibroblast cell line WPMY-1: a model for stromal−epithelial interactions in prostatic neoplasia. *Carcinogenesis* **1999**, *20*, 1185−1192.
(29) Yaffe, D.; Saxel, O. Serial passaging and differentiation of myogenic cells isolated from dystrophic mouse muscle. *Nature* **1977**, *270*, 725−727.
(30) Fauti, T.; Müller-Brüsselbach, S.; Kreutzer, M.; Rieck, M.; Meissner, W.; Rapp, U.; Schweer, H.; Kömhoff, M.; Müller, R. Induction of PPARbeta and prostacyclin (PGI2) synthesis by Raf signaling: failure of PGI2 to activate PPARbeta. *FEBS J.* **2006**, *273*, 170−179.
(31) Jérôme, V.; Müller, R. Tissue-specific, cell cycle-regulated chimeric transcription factors for the targeting of gene expression to tumor cells. *Hum. Gene Ther.* **1998**, *9*, 2653−2659.
(32) Stockert, J.; Adhikary, T.; Kaddatz, K.; Finkernagel, F.; Meissner, W.; Müller-Brüsselbach, S.; Müller, R. Reverse crosstalk of TGFβ and PPARβ/δ signaling identified by transcriptional profiling. *Nucleic Acids Res.* **2011**, *39*, 119−131.

The inverse agonist DG172 triggers a PPARβ/δ-independent myeloid lineage shift and promotes GM-CSF/IL-4-induced dendritic cell differentiation

Sonja Lieber, Frithjof Scheer, Florian Finkernagel, Wolfgang Meissner, Gavin Giehl, Cornelia Brendel, Wibke E. Diederich, Sabine Müller-Brüsselbach and Rolf Müller

Institute of Molecular Biology and Tumor Research (IMT), Center for Tumor Biology and Immunology (ZTI), Philipps University, Marburg, Germany (S.L., F.F., W.M., S.M.-B., R.M.); Institute of Pharmaceutical Chemistry, Center for Tumor Biology and Immunology (ZTI), Philipps University, Marburg, Germany (F.S., W.E.D.); and Clinic for Hematology, Oncology and Immunology, Center for Tumor Biology and Immunology (ZTI), Philipps University, Marburg, Germany (G.G., C.B.).

RUNNING TITLE: DG172 promotes the differentiation of dendritic cells

CORRESPONDING AUTHOR: Dr. Rolf Müller, Institute of Molecular Biology and Tumor Research (IMT), Center for Tumor and Immunobiology (ZTI), Philipps University, Hans-Meerwein-Straße 3, 35043 Marburg, Germany. Email: rmueller@imt.uni-marburg.de

ABSTRACT

The stilbene derivative DG172 was developed as a highly selective inhibitory PPARβ/δ ligand. Here, we describe a novel PPARβ/δ-independent, yet highly specific effect of DG172 on the differentiation of bone marrow cells (BMCs). DG172 strongly augmented GM-CSF-induced differentiation of primary BMCs from *Ppard* null mice into two specific populations, characterized as mature ($CD11c^{hi}MHCII^{hi}$) and immature ($CD11c^{hi}MHCII^{lo}$) dendritic cells. IL-4 synergized with DG172 to shift the differentiation from $MHCII^{lo}$ cells to mature dendritic cells in vitro. The promotion of DC differentiation occurred at the expense of differentiation to granulocytic $Gr1^{+}Ly6B^{+}$ cells. In agreement with these findings, transcriptome analyses showed a strong DG172-mediated repression of genes encoding neutrophilic markers in both differentiating wildtype and *Ppard* null cells, while macrophage/DC marker genes were upregulated. DG172 also inhibited the expression of transcription factors driving granulocytic differentiation (*Cebpe, Gfi1, Klf5*), and increased the levels of transcription factors promoting macrophage/DC differentiation (*Irf4, Irf8, Spib, Spic*). DG172 exerted these effects only at an early stage of BMC differentiation induced by GM-CSF, did not affect M-CSF triggered differentiation to macrophages and had no detectable PPARβ/δ-independent effect on other cell types tested. Structure-function analyses demonstrated that the 4-methylpiperazine moiety in DG172 is required for its effect on DC differentiation, but is dispensable for PPARβ/δ binding. Based on this data we developed a new compound, DG228, which enhances DC differentiation in the absence of significant PPARβ/δ binding.

ABBREVIATIONS: Angptl4, angiopoietin-like 4; DG172, (Z)-2-(2-bromophenyl)-3-((4-(1-methyl-piperazine)amino)phenyl)acrylnitrile; BMC, bone marrow cell; DC, dendritic cell; DMEM, Dulbecco's minimal essential medium; DMSO, dimethylsulfoxide; FACS, fluorescence-activated cell sorting; GM-CSF, granulocyte-macrophage-colony-stimulating factor; GW501516, [2-methyl-4-[[[4-methyl-2-[4-(trifluoromethyl)phenyl]-5-thiazolyl]methyl]thio]phenoxy]-acetic acid; M-CSF, macrophage-colony-stimulating factor; MFI, mean fluorescence intensity; PBS, phosphate-buffered saline; Pdk4, pyruvate dehydrogenase kinase 4; PPAR, peroxisome proliferator-activated receptor; RT-qPCR, real-time quantitative polymerase chain reaction; ChIP, chromatin immunoprecipitation; TR-FRET, time-resolved fluorescence resonance energy transfer; ST247, methyl 3-(*N*-(4-(hexylamino)-2-methoxyphenyl)sulfamoyl)thiophene-2-carboxylate.

Introduction

Peroxisome proliferator-activated receptors (PPARs) are nuclear receptors that function as ligand-inducible transcription factors in lipid metabolism and immune regulation (Kostadinova et al., 2005; Wahli and Michalik, 2012; Yang et al., 2010). Consistent with their physiological functions PPARs are associated with major human diseases, including hyperlipidemia, diabetes, arteriosclerosis, inflammatory disorders and cancer (Desvergne et al., 2006; Peters et al., 2012; Wahli and Michalik, 2012). Consequently, their potential as therapeutic targets has led to the development of subtype-selective, high affinity ligands (Peraza et al., 2006).

PPARβ/δ serves as a receptor for a broad range of natural agonistic ligands with function in inflammatory processes, including unsaturated fatty acids (Xu et al., 1999), prostaglandin I_2 (prostacyclin) (Lim et al., 1999) and 15-hydroxyeicosatetraenoic acid (15-HETE) (Naruhn et al., 2010). Different laboratories and companies have developed a number of PPARβ/δ-specific agonistic ligands (Peraza et al., 2006), several of which are well characterized and have been used in numerous experimental studies. Synthetic antagonistic ligands for PPARβ/δ have explored to a much lesser extent, but several inhibitory compounds have been described over the past years. These include the irreversible inhibitor and partial PPARγ agonist GSK3787 (Palkar et al., 2010; Shearer et al., 2010), the PPARβ/δ-specific GSK0660 (Shearer et al., 2008) and its improved derivative ST247 (Naruhn et al., 2011; Toth et al., 2012), and the stilbene DG172 (Lieber et al., 2012). These ligands act as inverse agonists, as indicated by their inhibitory effect on the basal expression of PPARβ/δ target genes and an increased recruitment of transcriptional corepressors (Naruhn et al., 2011). DG172 is a PPARβ/δ-selective compound characterized by a high affinity and potent repressive effects on PPARβ/δ target genes (Lieber et al., 2012).

There is a large body of evidence implicating PPARβ/δ in inflammation-associated processes (Kostadinova et al., 2005; Wahli and Michalik, 2012; Yang et al., 2010), including T-helper cell function (Kanakasabai et al., 2010) and macrophage polarization (Kang et al., 2008; Odegaard et al., 2008). Nevertheless, the precise role of PPARβ/δ in immune cell differentiation and regulation is still poorly understood. We therefore sought to analyze the effect of PPARβ/δ ligands on differentiating bone marrow cells from wild type and *Ppard* null mice. At an early stage of this study it became evident that DG172 strongly influenced bone marrow cell (BMC) differentiation induced by granulocyte-macrophage-colony-stimulating factor (GM-CSF), whereas the genetic disruption of *Ppard*, the agonist GW501516 and the inverse agonist ST247 affected differentiation only to a marginal extent, indicating a PPARβ/δ-independent mechanism.

Exposure of mouse bone marrow cells to GM-CSF as the only growth factor or cytokine results in a mixed population of adherent and non-adherent cells consisting of macrophages, dendritic cells and neutrophils (Inaba et al., 1992). While the numbers of non-adherent granulocytic cells decrease in these cultures within a few days, loosely adhering immature dendritic cells and strongly adherent macrophages increase. Inclusion of IL-4 strongly shifts the balance towards the differentiation to immature dendritic cells (Schuler et al., 1999), while the addition of macrophage-colony-stimulating factor (M-CSF; CSF-1) instead of GM-CSF produces a basically pure population of macrophages (Weischenfeldt and Porse, 2008). The different myeloid cell types can be identified by selectively expressed surface markers, such as Gr1 (Ly6G) on neutrophils and MHCII, CD11c and F4/80 on dendritic cells and macrophages (Inaba et al., 1992; Lee et al., 2013; Leon et al., 2004; Schuler et al., 1999; Weischenfeldt and Porse, 2008). Lineage specification is determined by key transcription factors that drive differentiation along a specific path, such as C/EBPε and Gfi1 for neutrophils or Spi1 (PU.1) and Irf8 for monocytic cells (Rosenbauer and Tenen, 2007). We used this experimental system in the present study to investigate in detail the DG172-induced lineage shift in BMC differentiation.

Materials and Methods

Cell culture

Bone marrow cells were isolated from mice as described (Resnitzky et al., 1986) and cultured in RPMI 1640 supplemented with 10% fetal calf serum, 25 mM HEPES, 100U/ml penicillin, 100µg/ml streptomycin, 1mM sodium pyruvate and recombinant GM-CSF (20 ng/ml) (PeproTech, Hamburg, Germany) for 6 days, if not indicated otherwise. In some experiments IL-4 (5 or 200 ng/ml, as indicated) (PeproTech, Hamburg, Germany) and/or lipopolysaccharide (LPS; 100 ng/ml) (Sigma-Aldrich, Taufkirchen, Germany) were added, or M-CSF (Biomol, Hamburg, Germany; 20 ng/ml) was used instead of GM-CSF. Thioglycollate-elicited macrophages were obtained as described (Naruhn et al., 2011). NIH3T3 cells were cultured in Dulbecco's modified Eagle's medium (DMEM), complemented with 10% fetal calf serum, 2mM L-glutamine, 100U/ml penicillin, 100µg/ml streptomycin. Cells were maintained in a humidified incubator at 37 °C and 5% CO_2.

Ligands

DG172, its derivatives as well as ST247 were synthesized as previously described (Toth et al., 2012; Lieber et al., 2012). GW501516 was purchased from Axxora (Lörrach, Germany). Experimental details for DG195 and DG228 are described in the Supplemental Methods.

Mice

C57Bl6 mice were purchased from Jackson Laboratory (Bar Harbor, Maine). *Ppard* null (epiblast-specific disruption of *Ppard*) and wt mice were generated by crossing floxed *Ppard* mice (Barak et al., 2002) and Sox2-Cre mice (Hayashi et al., 2002) as described (Scholtysek et al., 2013). The floxed *Ppard* mice were kindly provided by Dr. R. Evans (Salk Institute, La Jolla, CA). Sox2-Cre mice were obtained from Jackson Laboratory (Bar Harbor, Maine). Genotyping was performed with the following primers: *Ppard* intron 3 (forward: GGC TGG GTC ACA AGA GCT ATT GTC TC), *Ppard* exon 4 (forward: GGC GTG GGG ATT TGC CTG CTT CA); *Ppard* intron 4 (reverse: GAG CCG CCT CTC GCC ATC CTT TCA G; fragment sizes: *Ppard* wt: 360 bp; *Ppard* floxed: 400 bp; *Ppard* ko: 240 bp; *Cre* (forward: CCT GGA AAA TGC TTC TGT CCG; reverse: CAG GGT GTT ATA AGC AAT CCC); fragment size: 390 bp.

FACS analyses

Cells were washed with PBS incubated with 10 µg/ml TruStain fcX (BioLegend, San Diego, CA) for 10 min at 4° C to block unspecific Fc-binding, and subsequently stained with the following antibodies for 30 min at 4°C: FITC-labeled anti-mouse CD14 (Sa14-2), APC/Cy7-labeled anti-mouse F4/80 (BM8), APC-labeled anti-mouse MHCII (I-A/I-E) (M5/114.15.2), Pe-Cy7-labeled anti-mouse CD11c (N418), Pacific blue-labeled anti-mouse Ly-6G (1A8), PerCP-Cy5.5-labeled anti-mouse CD14 (Sa2-8), PE-labeled anti-mouse F4/80 (BM8) (BioLegend, San Diego, CA) and FITC-labeled anti-mouse Ly-6B.2 (7/4) (Biozol, Eching, Germany). Isotype control antibodies were as follows: FITC-labeled rat IgG2α,κ, APC/Cy7-labeled rat IgG2β,κ, APC-labeled rat IgG2β,κ, PeCy7-labeled Hamster IgG, Pacific blue-labeled rat IgG2α,κ, PerCP-Cy5.5-labeled rat IgGα,κ, PE-labeled rat IgG2β,κ and FITC-labeled rat IgG2α (BioLegend, San Diego, CA). Cells were analyzed using a FACSCanto flow cytometer and FlowJo 9.5.1 software (BD Biosciences). Data were plotted using biexponential transformation.

Immunoblotting of S100A8

Cells were lysed in (60mM TrisHCl, pH 7.5, 30mM NaCl, 0,1mM EGTA, 1% Triton X-100, and a Roche protease inhibitor mix). Cell lysates were subjected to SDS-PAGE on 20% gels and immunoblotting was performed with the Trans-Blot Turbo Transfer System (BioRad, München, Germany) using the optimized protocol for low MW proteins, a rat anti-mouse monoclonal antibody against S100a8/Mrp8 (Biozol, Eching, Germany) and a HRP-labeled second antibody (Cell Signaling Technology, Leiden, Netherlands). Bands were visualized by ChemiDoc MP Imaging System and quantified using Image Lab 5.0 software (BioRad, München, Germany).

Quantitative RT-PCR

cDNA was synthesized from 0.1-1 µg of RNA using oligo(dT) and random primers and the iScript kit (Biorad, Germany). qPCR was performed in a Mx3000P Real-Time PCR system (Stratagene, La Jolla, CA) for 40 cycles at an annealing temperature of 60 °C. PCR reactions were carried out using the Absolute QPCR SYBR Green Mix (Abgene, Hamburg, Germany) and a primer concentration of 0.2 µM following the manufacturer's instructions. *L27* was used as normalizer. Comparative expression analyses were statistically analyzed by Student's *t*-test (two-tailed, equal variance) and corrected for multiple hypothesis testing via the Bonferroni method. RT-qPCR primer sequences are listed in Table S1.

Microarrays

Mouse Agilent 4-plex Array 44K, design id 028005, were used for the analysis of the gene expression of the different samples in a reference-design assay as previously published (Kaddatz et al., 2010). Raw microarray data were normalized using the 'loess' method implemented within the limma package of R/Bioconductor (Smyth, 2005). Probes were assigned to genes as described (Adhikary et al., 2011) using Ensembl release 70. Probes were considered regulated if they had a minimum intensity value of 5 and a comparison specific change as specified in the Results. Raw and normalized microarray data from this publication have been submitted to the EBI ArrayExpress and assigned the identifier [accession: E-MTAB-2628vi]. All data is MIAME compliant.

Time-Resolved Fluorescence Resonance Energy Transfer TR-FRET assay

Ligand binding was determined by TR-FRET in vitro using the Lanthascreen TR-FRET PPARβ/δ competitive binding assay (Life Technologies, Darmstadt, Germany) as described (Naruhn et al., 2011).

Results

DG172 promotes the differentiation of DCs from GM-CSF-induced mouse BMCs and reduces Ly6b$^+$/Gr1$^+$ granulocytic cells

After differentiation of BMCs for 9 days in the presence of GM-CSF, IL-4 and/or DG172 the loosely attached and floating cells were collected and cultured for another 3 days under the same conditions. Compared to cells with GM-CSF only (Fig. 1A), cells showed morphological alterations upon co-treatment with DG172 (more spindle-shaped cells; panel B) or IL-4 (larger, rounded cells; panel C). Addition of LPS to the latter triggered a mature dendritic cells morphology (Fig. 1D), as described (Dearman et al., 2009). A very similar effect was observed when DG172 was used instead of LPS (Fig. 1E), while no further morphological

changes were seen when both DG172 and IL-4 were added (Fig. 1F). These observations suggested that DG172 synergizes with IL-4 to promote the differentiation into mature DC.

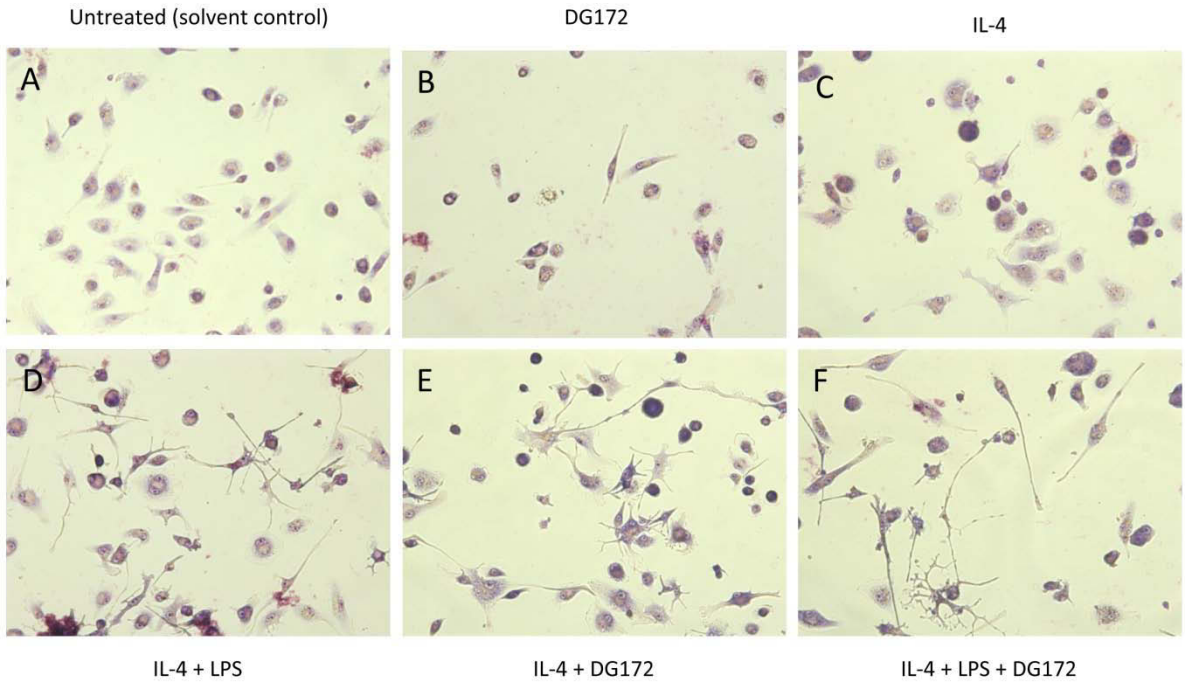

Fig. 1. Effect of DG172 on the morphology of BMCs differentiated in vitro. BMCs were differentiated for 9 days in the presence of GM-CSF. IL-4 (200 ng/ml) and/or DG172 (1 µM) were added as indicated. Loosely attached and floating cells were collected, cultured for another 3 days under the same conditions. In panels E and F, LPS (100 ng/ml) was added for the last 2 days of culture.

FACS analysis of DC surface markers CD11c and MHCII confirmed the morphological observations. Fig. 2 shows three distinct populations: MHCII^{-}, CD11c^{hi}/MHCII^{lo} and CD11c^{hi}/MHCII^{hi}, subsequently referred to as P1, P2 and P3, respectively (Fig. 2A). DG172 increased both P2 and P3. This effect was observed in both wt (Fig. 2A, B) and *Ppard* null cultures (Fig. 2C, D) and was therefore independent of PPARβ/δ. IL-4 at a low concentration of 1 ng/ml synergized with DG172 by further increasing P3 (Fig. 2-D).

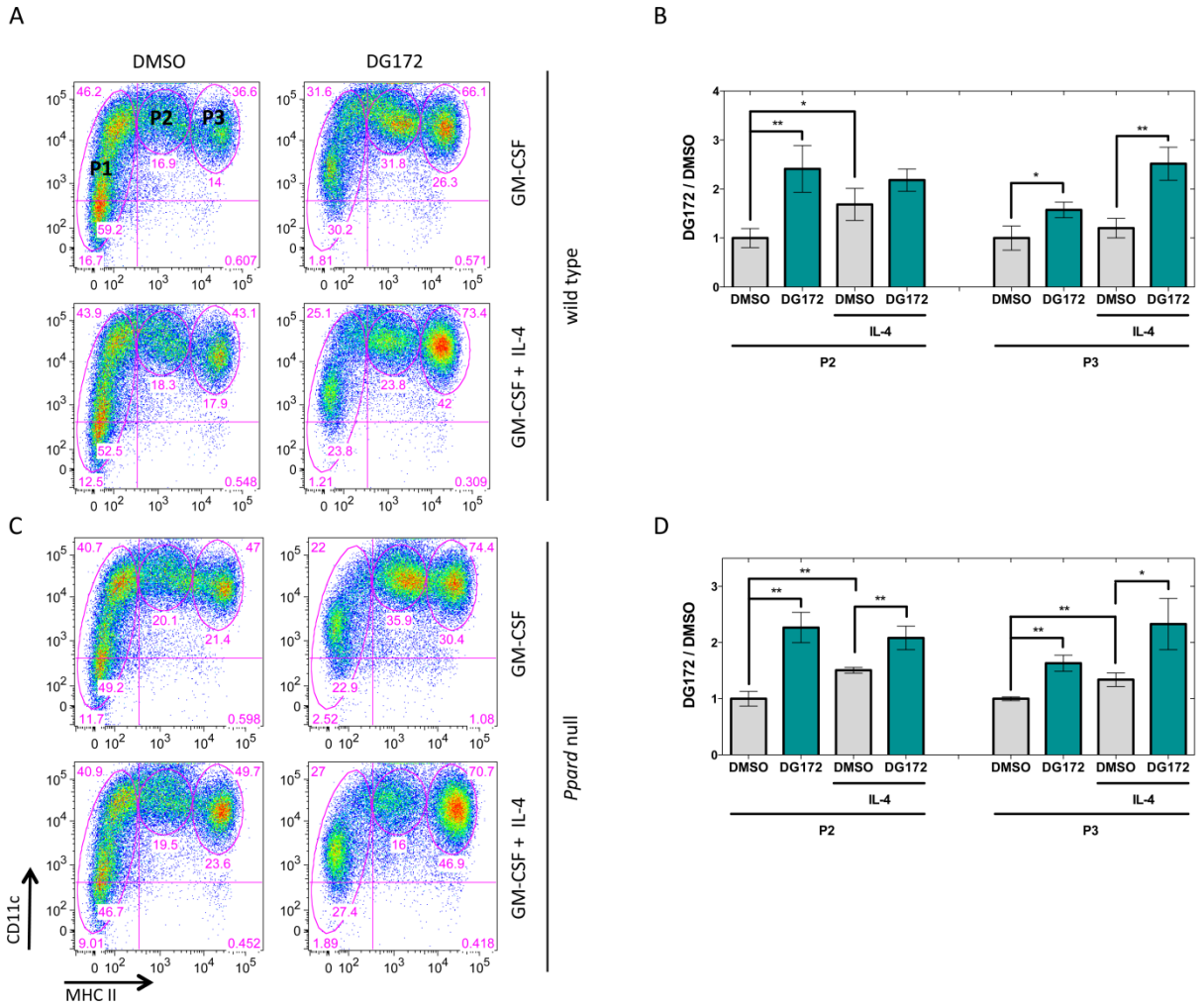

Fig. 2. Effect of DG172 on the dendritic cell surface markers CD11c and MHCII by differentiating BMCs. BMCs from wt (A, B) and *Ppard* null (C, D) mice were differentiated with GM-CSF ± IL-4 (1 ng/ml) in the absence or presence of DG172 for 6 days. Surface expression of CD11c and MHCII was determined by FACS in non-adherent cells. Three cell population showing distinct expression patterns were identified (P1, P2, P3) and the fractions of these cells relative to the total population are indicated (%). Panels A and C show representative experiments and panels B and D the data from three independent experiments (average ± SD). *: $p<0.05$; **: $p<0.01$ by t-test.

This data supports the view that DG172 promotes DC differentiation, which was further investigated by additional FACS phenotyping using the myeloid surface markers CD14 and F4/80. As shown in Fig. 3A and B, P3 cells exhibited a lower mean fluorescence intensity (MFI) for CD14 than P1 and P2 cells. In P2 cells the CD14 MFI level decreased further upon DG172 treatment, consistent with the promotion of their differentiation to DCs (Mahnke et al., 1997). In contrast, the MFI measured for F4/80 was higher on P2 and P3 compared to P1 cells, but was reduced by DG172 in both P2 and P3 (Fig. 3C, D). Decreasing F4/80 surface expression has previously been reported for differentiating DCs (Leon et al., 2004). The P2 and P3 populations thus likely comprise $CD11c^{hi}/MHCII^{lo}$ immature and $CD11c^{hi}/MHCII^{hi}$ mature DCs, respectively. These are clearly distinguished from the P1 population, which is composed of $MHCII^{-}$ cells and presumably represent cells at an early stage of differentiation.

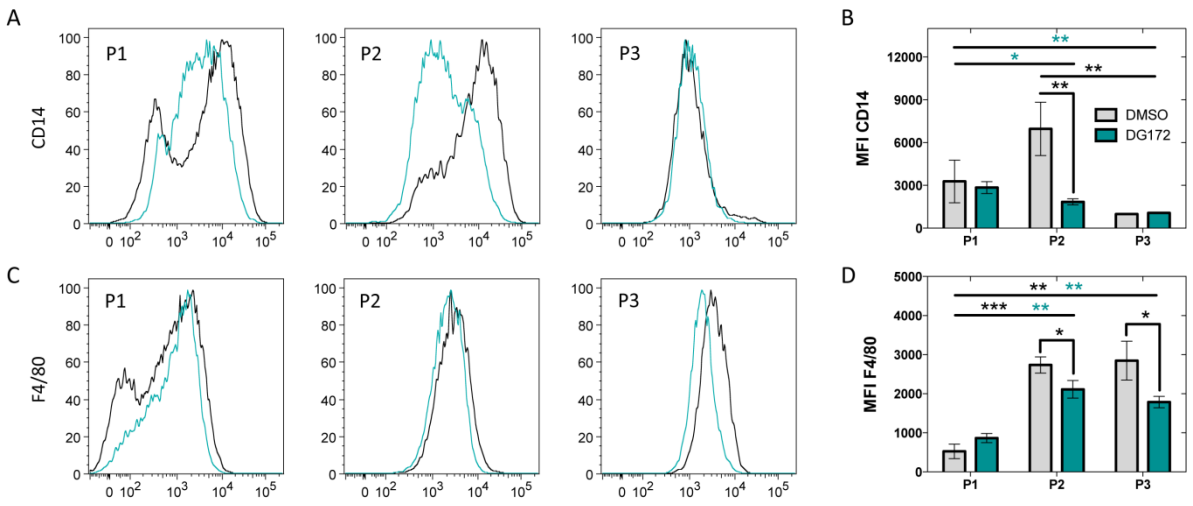

Fig. 3. CD14 and F4/80 levels on subpopulations of differentiating BMCs differing in dendritic surface marker expression. Surface expression of CD14 (A, B) and F4/80 (C, D) on differentiating non-adherent BMCs (GM-CSF) from *Ppard* null mice was determined by FACS and gated to the P1, P2 and P3 populations defined in Figure 2. The data are presented as histograms of CD14 and F4/80 surface expression levels. Numbers represent MFI values. Panels A and C show representative experiments and panels B and D the data from three independent experiments (average ± SD). *: p<0.05; **: p<0.01; ***: p<0.001 by t-test.

The described effects were specific for GM-CSF induced dendritic cell differentiation, since no DG172 effects were observed on differentiation to macrophages triggered by M-CSF (Fig. S1).

To analyze the fate of granulocytic cells we determined the surface markers Ly6B and Gr1 (LY6C) in the same samples. FACS analysis identified 3 distinct subpopulations in cells treated with DG172 (day 1-6): $Ly6B^{-}Gr1^{-}$, $Ly6B^{+}Gr1^{-}$ and $Ly6B^{+}Gr1^{+}$, defined as populations PA, PB and PC in Fig. 4A, with PC cells representing differentiated neutrophils. Gating for these subpopulations showed that only the double-negative PA cells were positive for CD11c and MHCII expression, which is in agreement with the conclusion that the P3 cells defined in Fig. 2 represent mature DCs.

Granulocytic cells decreased in GM-CSF-induced BMC cultures after 48 h, as shown by the shrinking number of $Ly6b^{+}/Gr1^{+}$ cells (Fig. 4B, top) (Lee et al., 2013), an effect that was clearly enhanced by DG172 (Fig. 4B, bottom). These observations are consistent with the conclusion that DG172 promotes DC differentiation at the expense of granulocytes.

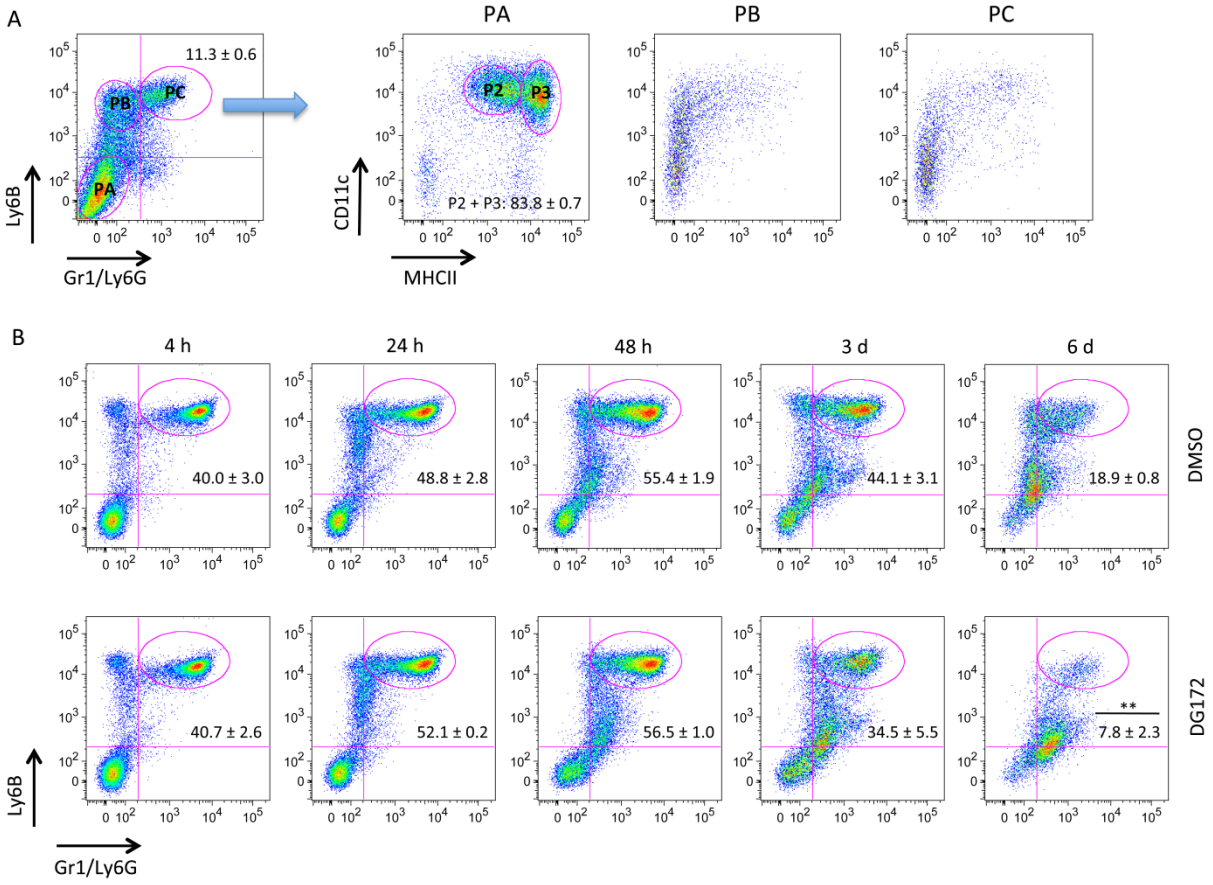

Fig. 4. Effect of DG172 on the granulocytic surface markers Ly6B and Gr1 (Ly6G) on differentiating BMCs. (A) CD11c and MHCII levels in relation to Ly6B and Gr1 surface expression. BMCs treated with GM-CSF and DG172 (day 1-6; combined adherent and floating cells) were gated for the PA, PB and PC subpopulations defined in the left panel and analyzed for surface expression of CD11c and MHCII. (B) BMCs were exposed to in GM-CSF for 1 day, followed by cultivation in GM-CSF ± DG172 for the indicated times. Surface expression of Ly6B and Gr1 on non-adherent cells was determined by FACS. Dot plots show the results of a representative experiment; numbers next to the PC area are the average of three independent experiments (± SD). **: $p<0.01$ by t-test between DMSO and DG172-treated cells.

DG172-induced transcriptome changes in GM-CSF-induced mouse BMCs

To gain further insight into the DG172-triggered alterations to BMC differentiation we performed microarray analyses of cells exposed to GM-CSF in the presence or absence of the ligand (5 days incubation; sample subsequently referred to as d 1-6). To be able to identify PPARβ/δ-independent effects of DG172 in this system we included in this study the inverse PPARβ/δ agonist ST247 and the PPARβ/δ agonist GW501516. As shown by the Venn diagram in Fig. 5A, only a small fraction (n=66; threshold 2-fold) of all DG172-repressed genes (n=598) was also repressed by ST247, and an even smaller number (n=19) was activated by GW501516. In addition, we compared the effect of DG172 on BMCs from both wild type and *Ppard* null mice and found a substantial number of genes to be repressed by DG172 irrespective of the *Ppard* status (n=227). An analogous situation was found with DG172-activated genes (n=702; Fig. 5B). Of these genes, only a small fraction was also activated by ST247 (n=40) or repressed by GW501516 (n=31). Furthermore, a large fraction

of genes (n=162) was induced by DG172 in a PPARβ/δ-independent fashion. Datasets S1A and 1B list all genes repressed or activated by DG-172 in cells from *Ppard* null mice.

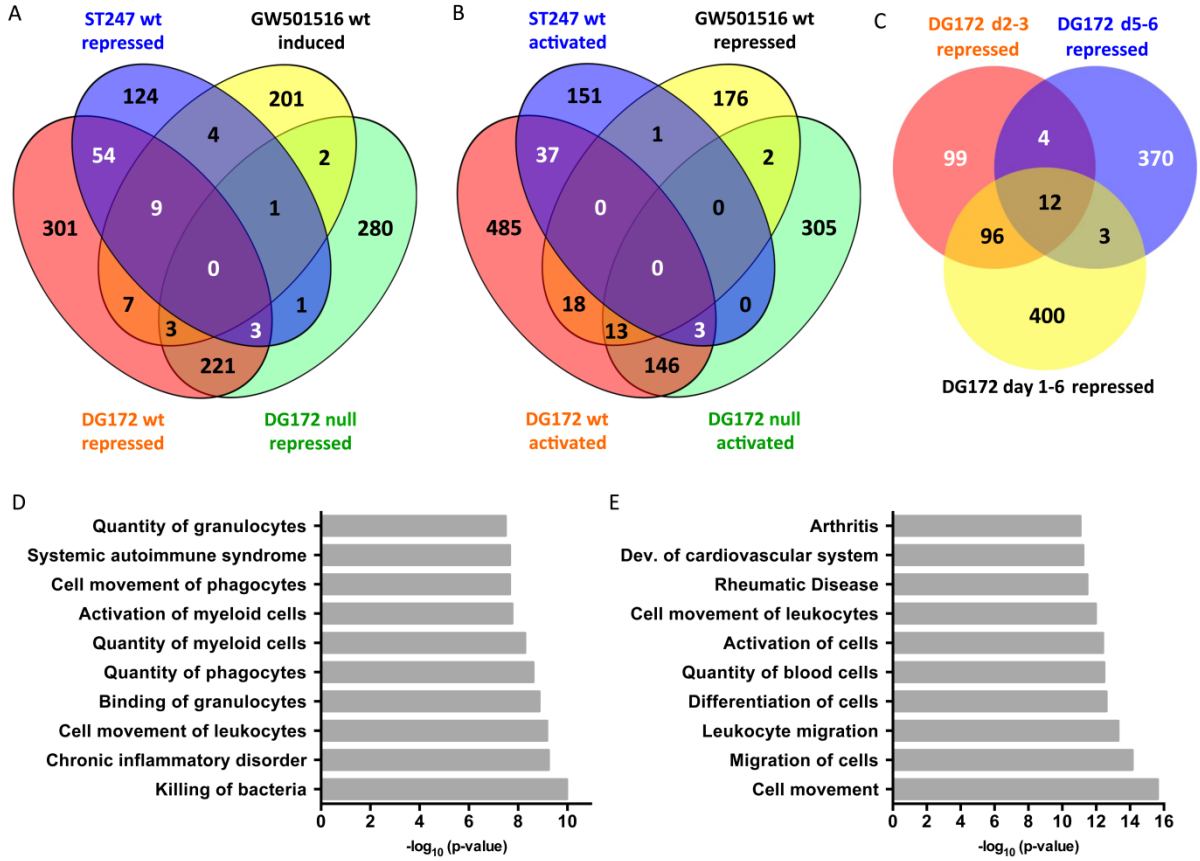

Fig. 5. Effect of PPARβ/δ ligands on the transcriptome of GM-CSF differentiated BMCs from wt and *Ppard* null mice.
A, BMCs from wt and *Ppard* null mice were differentiated with GM-CSF for 6 days in the presence of the agonist GW501516 or the inverse agonists DG172 or ST247. The Venn diagram shows the overlap of genes induced by GW501516 and repressed by DG172 or ST247. **B,** Venn diagram as in panel a, except that the directions of regulation are opposite. **C,** Venn diagram showing the stage-specific effect of DG172. BMCs from *Ppard* null mice were differentiated with GM-CSF for 3 (top left) or 6 days (top right, bottom) in the presence of DG172 from day 2-3, day 5-6 or during the entire culture period (day 1-6). **D,** Annotation of DG172-repressed genes (day 2-3; ≥2-fold) according to "functions and diseases" using Ingenuity Pathway Analysis. **E,** Annotation of DG172-acivated genes (day 2-3; ≥1.5-fold).

To gain further insights into the effect of DG172 on differentiation, we performed microarray analyses on BMC cultures that were exposed to DG172 for only 1 day, either from day 2 to 3 (2-3d) or from day 5 to 6 (5-6d), and then harvested for microarray analysis. The data in Fig. 5C and Datasets S2 and S3 clearly suggest a stage-specific effect of DG172: while more than 20% (n=108) of all genes (n= 511 in total in the d1-6 sample) were repressed in the d2-3 sample, only a marginal number of genes (n=15) in the d5-6 sample coincided with those in the d1-6 sample (n=389 in total).

Both the DG172-repressed and DG172-activated genes (d2-3 *Ppard* null BMCs) were functionally annotated according to "functions and diseases" using Ingenuity Pathway Analysis (Fig. 5D, E). Top categories according to p-values were "Inflammatory Response",

"Cellular Movement", "Hematological System Development and Function" and "Immune Cell Trafficking", associated with the functions listed in Figure 5D and E. This data clearly connect the DG172-regulated genes to the observed effect on GM-CSF-induced BMC differentiation.

This conclusion is clearly supported when the regulated genes are analyzed according to their functions in cells of the two major myeloid lineages. The summary of microarray data in Fig. 6A shows a strong down-regulation of genes selectively expressed by neutrophils, such as *S100A8, S100A9, Ltf* (lactoferrin), *Mpo* (myeloperoxidase) and *Hp* (haptoglobin). In contrast, genes characteristic of the antigen-presenting cells were upregulated, including five different H2 MHC genes, *CD80* (B7-1), *CD86* (B7-2) and *CD209* (DC-SIGN). These results were confirmed by RT-qPCR in all instances tested (Fig. 6B). We also detected a strong PPARβ/δ-independent DG172-mediated repression of S100A8 protein expression by immunoblot analysis (≥10-fold; Fig. 6C).

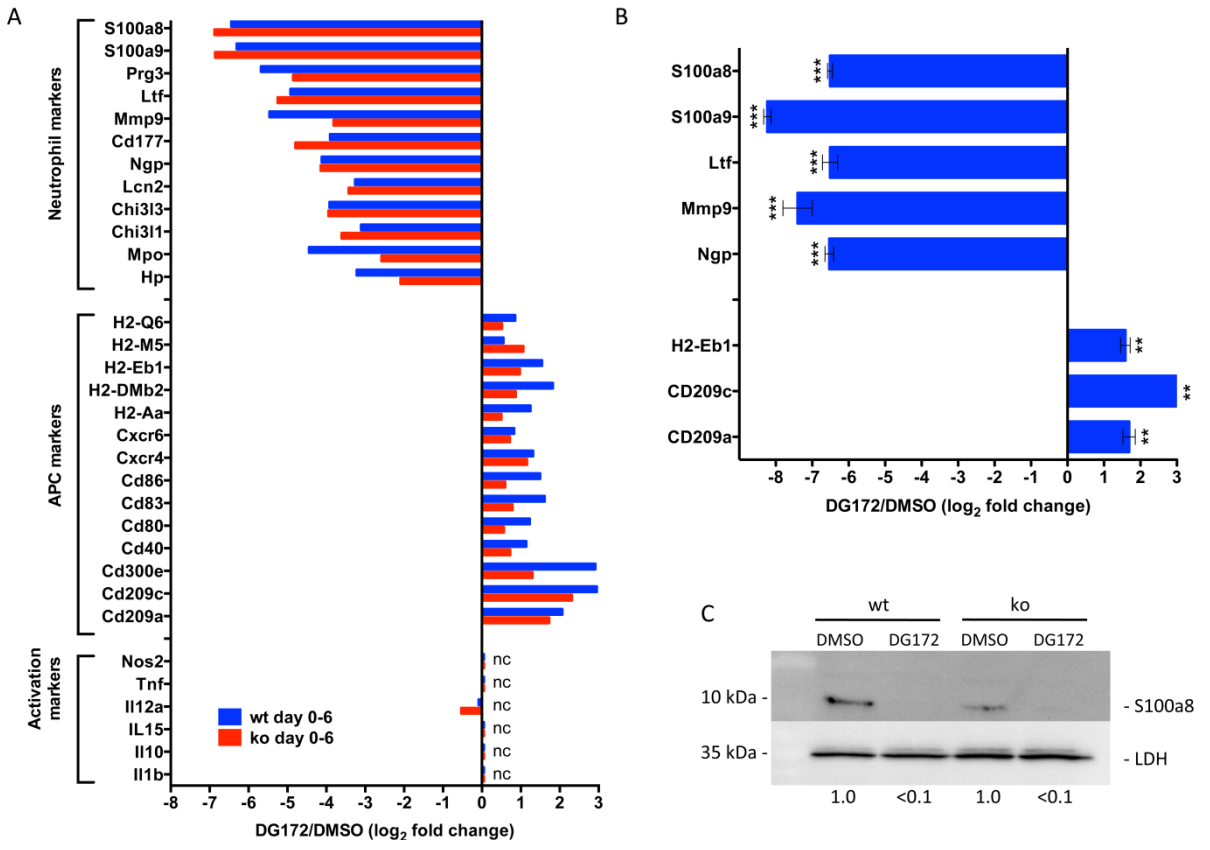

Fig. 6. Effect of DG172 on specific target genes in GM-CSF treated BMCs.
A, Summary bar plot of microarray data for neutrophil markers, APC markers and activation markers. nc, no change. **B,** RT-qPCR validation for individual genes. Values are the average of triplicates; error bars represent the standard deviation. *: $p<0.05$ by t-test relative to solvent control; **: $p<0.01$; ***: $p<0.001$. **C,** Validation of S100A8 protein down-regulation by DG172. Aquantitation of the data is shown below the immunoblot (normalized to 1.0 for untreated wt or null cells).

Myeloid differentiation is governed by several key transcription factors (Rosenbauer and Tenen, 2007). We therefore analyzed the regulation of the corresponding genes by DG172 in our experimental system. While *Klf5, Gfi 1* and *Cebpe*, which are selective for the granulocytic lineage, were down-regulated in both d0-6 and d2-3 DG172-exposed BMC cultures, the macrophage/DC-associated genes *Spib, Spic, Irf4* and *Irf8* were up-regulated (Fig. 7A). The fact that these genes were not regulated in d5-6 cells indicates that this DG172 effect is restricted to an early stage of differentiation. Several of these transcription factors indeed represent master switches for lineage determination (see Fig. 7B). The microarray data could also be confirmed by RT-qPCR (Fig. 7C). These results thus strongly confirm the conclusion that DG172 switches the GM-CSF-induced differentiation of BMCs in favor of APCs.

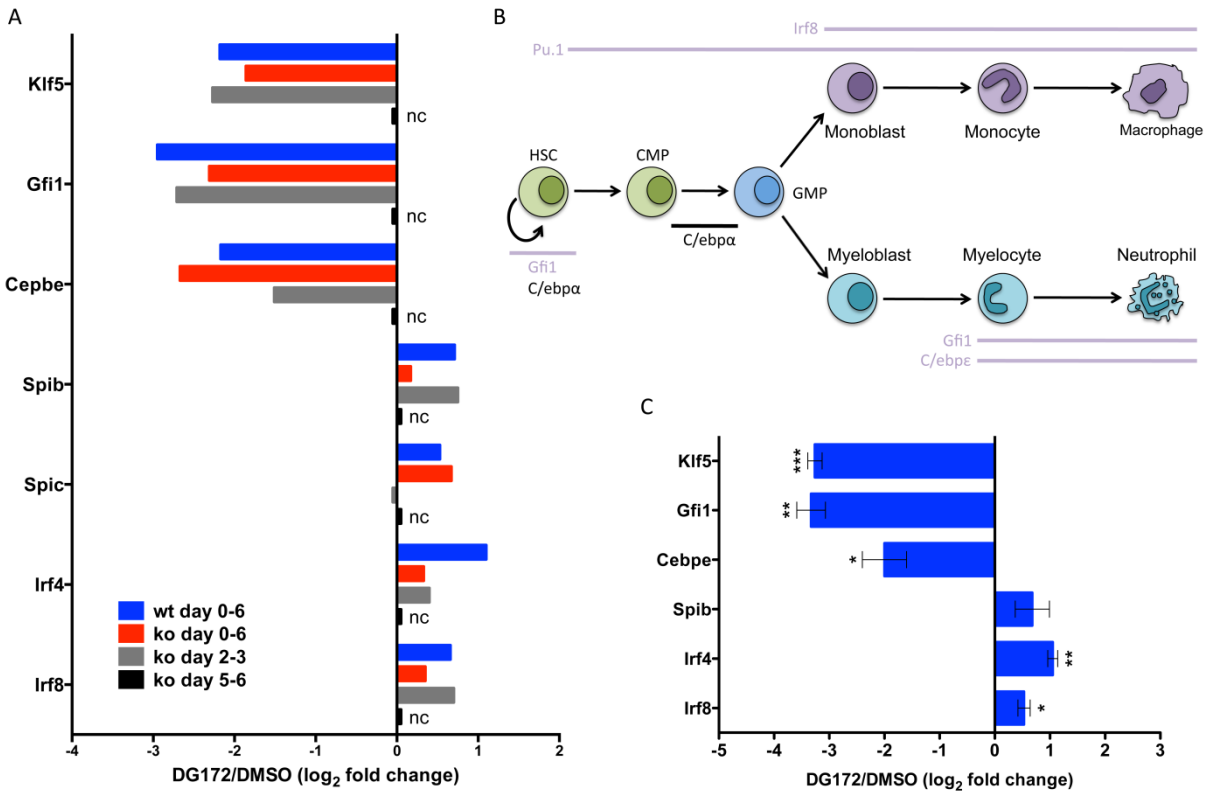

Fig. 7. Effect of DG172 on genes encoding myeloid transcription factors in GM-CSF treated BMCs.
A, Summary bar plot of microarray data. nc, no change. **B,** Schematic representation of the role of transcription factors in myeloid differentiation pathways. **C,** RT-qPCR validation for individual genes in d2-3 cells. Values are the average of triplicates; error bars represent the standard deviation. *: $p<0.05$ by t-test relative to solvent control; **: $p<0.01$; ***: $p<0.001$.

DG172 acts at a specific stage of GM-CSF-induced differentiation

We next sought to identify the critical stage of differentiation affected by DG172. The expression data in Figs. 5 and 7 strongly suggested that the effect of DG172 on BMC differentiation is restricted to an early stage around day 2. FACS analyses of CD11c and

MHCII on day 6 BMCs exposed to DG172 at different times after initiating GM-CSF-induced differentiation confirmed this conclusion. As shown in Fig. 8, the DG172-induced increase in CD11c^{hi}MHCII^{hi} cells was observed only, when DG was added prior to day 4.

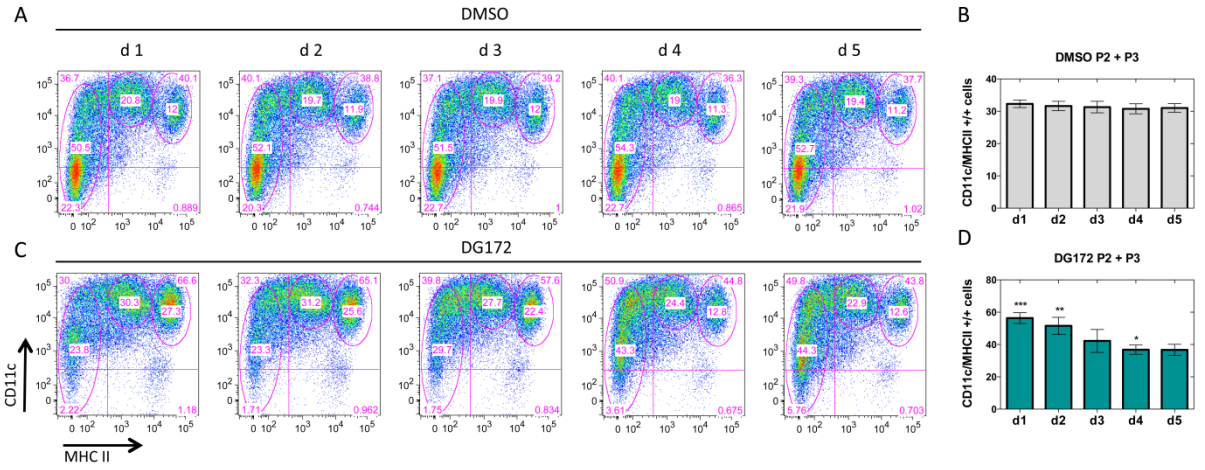

Fig. 8. Stage-dependent effect of DG172 on dendritic cell surface markers on differentiating BMCs. BMCs from wt mice were differentiated with GM-CSF for 6 days and solvent (DMSO; panel A and B) or DG172 (panel C and D) was added at the indicated times after initiating GM-CSF treatment. Surface expression of CD11c and MHCII on non-adherent cells was determined by FACS. Subpopulations were defined as in Fig. 2. Panels A and C show representative experiments and panels B and D the data from three independent experiments (average ± SD). *: p<0.05; **: p<0.01; ***: p<0.001 by t-test between DMSO and DG172 treated cells.

In the same experimental setting, a clearly stage-dependent effect was also seen on the repression of granulocytic marker genes *S100a8, S100a9* and *Mmp9* (Fig. 9A, top).

Differentiation of BMCs with M-CSF to macrophages had no significant effect on *S100a8*, although the canonical PPARβ/δ target gene *Adrp* was strongly repressed (Fig. 9B). Consistent with this result, no DG172 effect on *S100a8* was observed with primary macrophages obtained from either wild type of *Ppard* null mice (Fig. 9C, left panel) in the presence of a strong repression of the PPARβ/δ target gene *Angptl4* (Fig. 9C, right panel). Likewise, *Angptl4*, but not *S100a8* was repressed by DG172 in NIH3T3 fibroblasts (Fig. 9C, rightmost bars). Taken together these results clearly demonstrate that the PPARβ/δ independent effect of DG172 is both cell type and differentiation stage specific.

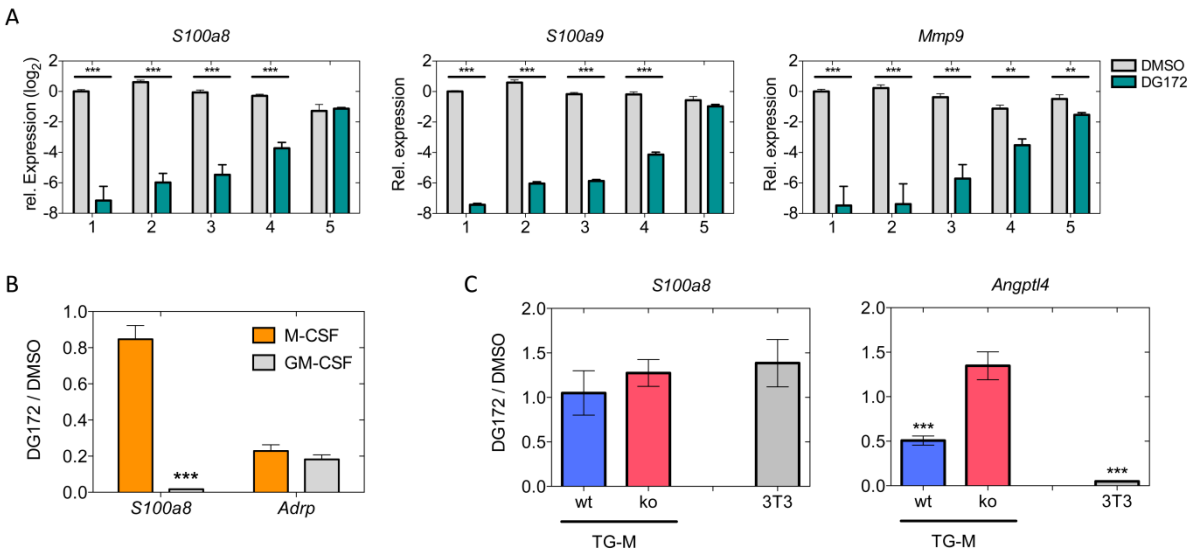

Fig. 9. Stage- and cell type-specific effects of DG172 on transcription of myeloid marker genes but not on PPARβ/δ target genes.
A, BMCs from wt mice were differentiated with GM-CSF for 6 days and DG172 was added at the indicated times after initiating GM-CSF treatment. Expression of the granulocytic marker genes *S100a8, S100a9* and *Mmp9* was determined by RT-qPCR and normalized to *L27* (relative expression = 1.0 for DMSO on day 1). **B,** Repression of *S100a8* expression in BMCs differentiated with GM-CSF, but not after M-CSF-induced differentiation to macrophages, while the direct PPARβ/δ target gene *Adrp* is repressed in both conditions. **C,** Repression of *Angptl4*, but not *S100a8*, in thioglycollate-elicited peritoneal macrophages from wt or *Ppard* null mice and in NIH3T3 fibroblasts. Data in B and C are represented as the ratio of expression in DG172 and DMSO treated cells (average of triplicate). Error bars indicate the standard deviation. **: p<0.01; ***: p<0.001 by t-test.

Differential effects of structural derivatives of DG172 on DC differentiation and PPARβ/δ binding

Finally, we investigated whether the PPARβ/δ dependent and independent effects of DG172 could be associated with specific structurally features, and might thus be potentially separable. To address this issue we synthesized 6 derivatives of DG172 (highlighted in blue in Fig. 10) and analyzed the potential of these compounds (i) to promote GM-CSF-induced BMC differentiation (FACS analysis of CD11c and MHCII expression) and (ii) to interact with the PPARβ/δ ligand binding domain *in vitro* (competitive TR-FRET). The data in Fig. 10 indicate that the *N*-methylpiperazine residue is required for the enhanced differentiation into P2 and P3 cells, since a significant effect was observed only with those 3 compounds carrying this moiety (DG132, DG172, DG195). In contrast, PPARβ/δ binding was affected to a considerably lesser extent, as long as a halogen atom was introduced in the ortho (DG138, DG195) or meta (DG208) position of the opposing phenyl substituent. Consequently, DG139, bearing a para chloro and a *N*-dimethylamino substituent, not only lacked the effect on BMC differentiation, but also failed to interact with PPARβ/δ. These results suggested that a separation of the two activities exerted by DG172 is possible. We therefore replaced the *N*-diemthylamino moiety in DG139 with a *N*-methylpiperazine residue yielding DG228 (red in Fig. 10). In agreement with our prediction, DG228 had a strong effect on BMC differentiation,

but only weakly bound to PPARβ/δ (IC50 >10 µM compared to the parent compound 27 nM for DG172). Collectively, these data indicate that the *N*-methylpiperazine residue is essential for the PPARβ/δ-independent effect of DG172 on BMC differentiation, while the position of the halogen atom in the phenyl substituent is crucial for PPARβ/δ binding.

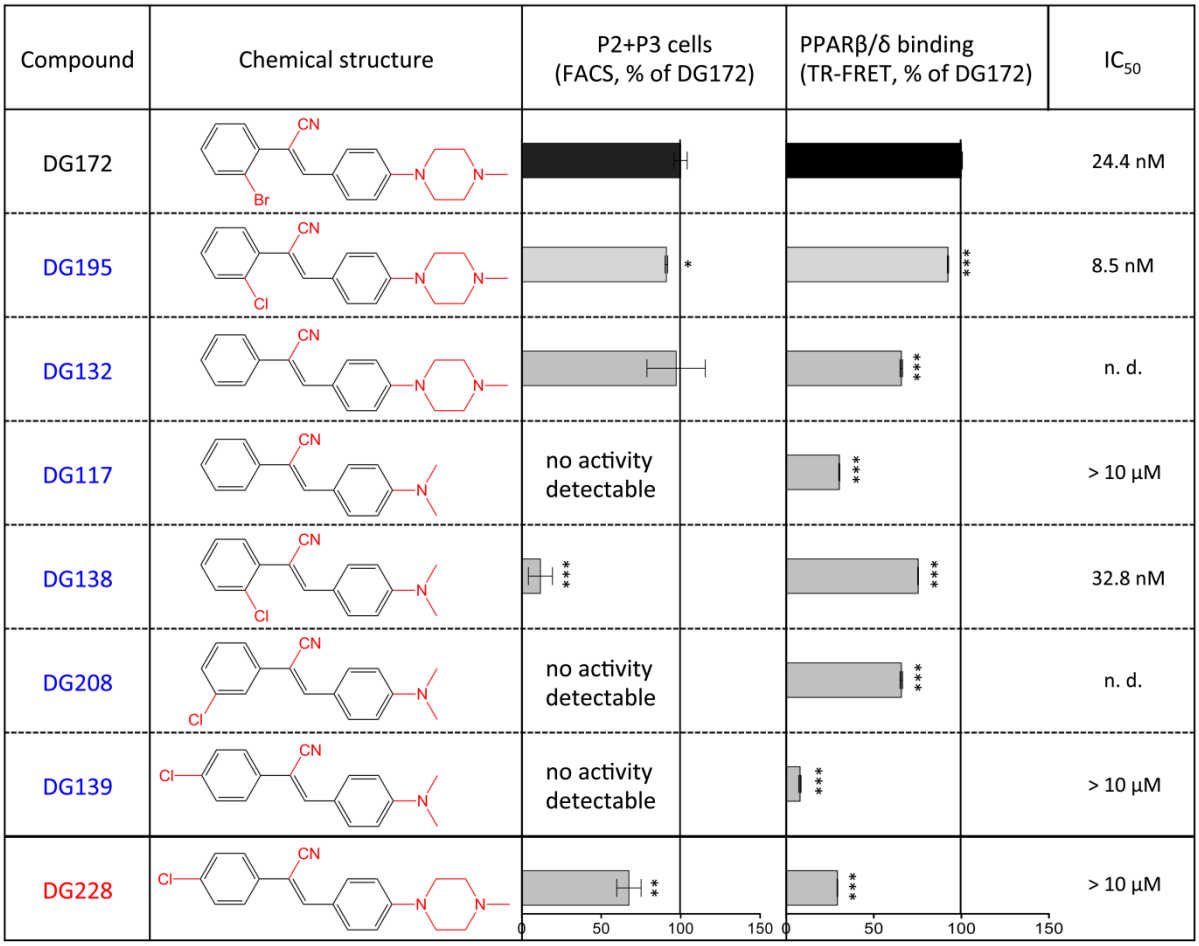

Fig. 10. Differential effects of structural alterations to DG172 on GM-CSF-induced BMC differentiation and PPARβ/δ binding.
The DG172 derivatives indicated on the left were tested for their effects to promote BMC differentiation to P2 and P3 cells (CD11c^{hi}MHCII^{lo} and CD11c^{hi}MHCII^{hi} cells) and interaction with the PPARβ/δ ligand binding domain in vitro (competitive TR-FRET). All values represented by bars were calculated relative to the effect of DG172 (DG172 value – DMSO value normalized to 100%) at a concentration of 1 µM for all compounds. IC_{50} values were determined by titration over a range of 0.1 nM – 10 µM (competitive TR-FRET) as previously described (Lieber et al., 2012). n.d., not determined. Data represent the average of triplicates. Error bars indicate the standard deviation. *: p<0.05 by t-test; **: p<0.01; ***: p<0.001 relative to DG172.

Discussion

Our FACS data show that DG172 strongly augments CD11c^{hi}MHCII^{hi} cells in GM-CSF-induced BMC cultures, in particular in the presence of IL-4 (population P3; Fig. 2). Furthermore, exposure of GM-CSF/IL-4-treated cultures to DG172 induced tightly adherent cells displaying the typical morphology of mature DCs (Fig. 1). DG172 also induced a second population in GM-CSF-induced BMC cultures, which we characterized as CD11c^{hi}MHCII^{lo} cells (population P2; Figs. 2 and 3). MHCII^{lo} cells have previously been described in early

GM-CSF-induced bone marrow cultures (Masurier et al., 1999). It is likely that this population comprises immature DCs, as suggested by their apparent conversion to P3 cells by IL-4 (Fig. 2). This may also explain the synergistic action of the two mediators: DG172 promotes the differentiation from P1 to P2 cells, and from P2 to P3 cells, with the latter further promoted by IL-4. However, adherent cells represent a substantial fraction of the P2 population (not shown), suggesting that these are macrophages rather than undifferentiated DCs. It is therefore likely that P2 cells present a mixed population of committed monocytic cells with the potential to differentiate to DCs, as previously suggested by others (Masurier et al., 1999).

DG172 treatment also led to a reduction of granulocytic cells in GM-CSF-induced BMC cultures (Figs. 4B and 6), indicating that DG172 induces a lineage switch by favoring the DC lineage at the expense of granulocytic differentiation. In contrast to macrophages and DCs, neutrophils are present in freshly isolated BMCs (see early time points in Fig. 4B) and are partly replaced by BMCs differentiating along the granulocytic lineage after a few days of culture (Inaba et al., 1992). This replenishment by new granulocytes is apparently prevented by DG172, which can be explained by at least two different models. DG172 either pushes cells around the stage of the granulocyte macrophage progenitor (GMP) into the monocytic lineage, thereby depleting the progenitor pool for granulocytic differentiation, or alternatively, DG172 actively blocks differentiation to granulocytes, thus favoring monocytic/DC differentiation. As DC differentiation is promoted by pro-inflammatory stimuli (Dearman et al., 2009), it is important to note that we did not observe any effect on the expression of genes encoding pro-inflammatory cytokines, including *Tnf* and *Il1b* (Fig. 6A).

DG172 acts at a relatively early stage of differentiation, i.e. during the first 2 days of exposing BMCs to GM-CSF, as shown by its effect on the expression of genes coding for myeloid transcriptional regulators (Fig. 7) and the DC surface markers CD11c and MHCII (Fig. 8). While the granulocytic transcription factor genes *Cepbe, Gfi1* and *Klf5* were down-regulated by DG172 on day 2, factors associated with the macrophage/DC lineage, such as *Spib, Spic, Irf4* and *Irf8*, were up-regulated (Diakiw et al., 2012; Halene et al., 2010; Rosenbauer and Tenen, 2007; Schotte et al., 2004; Tamura et al., 2005; Yamanaka et al., 1997). Several of these transcriptional regulators have lineage determining functions. Gfi1, for instance, is not only indispensible for granulocyte differentiation (Hock et al., 2003), but also inhibits macrophage differentiation by repressing the activity of Spi1 (Pu.1) (Dahl et al., 2007). Vice versa, high levels of Spi1 inhibit the transcription of *Gfi1* by inducing the repressors Egr2 and Nab2, thereby blocking neutrophil differentiation (Laslo et al., 2006). RT-qPCR showed only a weak DG172 effect on *Spi1* (data not shown; *Spi1* is not represented in the microarray). However, the partial redundancy of Spi subtypes suggest that SpiB and SpiC have similarly crucial functions in myeloid differentiation (Garrett-Sinha et al., 2001).

Other examples are C/EBPε, whose different isoforms are endowed with the ability to specifically reprogram myeoid lineage commitment (Bedi et al., 2009; Halene et al., 2010) and Irf8, which extinguishes neutrophil production and promotes dendritic cell lineage commitment (Becker et al., 2012). These and other studies have clearly shown that hematopoietic cell fate is dependent on several key transcription factors, and that the dosage of each of these factors and their expression relative to each other plays a pivotal role (Mak et al., 2011). The fact that DG172 influences the expression of these transcription factors is consistent with its presumed action at an early stage of GM-CSF-induced differentiation, perhaps around the stage of the GMP, which would also provide a likely explanation for its profound effect on myeloid lineage determination. Ingenuity Upstream Regulator Analysis (Fig. S 2) identified the SRF and its co activators MKL1 and MKL2 and the transcription factors C/EBPα and C/EBPε as the most significantly affected pathways in DG172-treated cells (d2-3). Although the latter finding is consistent with our data showing a strong repression of the *Cebpe* gene by DG172, a potential involvement of SRF is difficult to judge at present, since this transcription factor has previously not been associated with myeloid differentiation.

An important issue is the open question which protein is targeted by DG172 to achieve its effect on BMC differentiation. Since DG172 is a stilbene and thus bears some structural resemblance to tamoxifen, we tested its binding to the estrogen receptor in vitro using a competitive TR-FRET assay, but were unable to detect any interaction (data not shown). Likewise, no binding was measurable to PPARα, PPARγ and RARα in analogous assays. We also asked, whether DG172 might be a ligand for aryl hydrocarbon receptor (AhR) because the structurally similar stilbene 4-hydroxytamoxifen can induce AhR target genes (DuSell et al., 2010), and AhR is required for DC differentiation in mice (Nguyen et al., 2010; Vogel et al., 2013). However, we did not see any agonistic or antagonistic effect of DG172 on *Cyp1a1*, one of the major AhR target genes, in cells with functional AhR signaling (data not shown). Furthermore, AhR ligands are known to regulate AhR target genes in differentiated macrophages (Bessede et al., 2014), which does not apply to DG172 (Fig. 9).

The nuclear receptor Nur77 (Nr4a1) plays an essential role in myeloid differentiation in mice (Hanna et al., 2011), and its target genes overlap with those identified in our microarray analyses (Fig. 5-7). However, DG172 had no detectable effect on Nur77 target genes in cell types other than GM-CSF-induced BMCs, although these genes responded to the Nur77 ligand DIM-C-pPhOCH(3) (Cho et al., 2008) (data not shown). We also tested the possibility that DG172 is an antagonist of Nur77 by applying DG172 together with DIM-C-pPhOCH(3), but could not detect any effect. It is therefore unlikely that Nur77 is a target of DG172.

It is also possible that the PPARβ/δ-independent function of DG172 is not mediated by a

nuclear receptor, as has been reported for the regulation of AMPK by PPAR ligands (Lee and Kim, 2010). A systematic approach to identify the relevant DG172 target(s) will require a cellular system that is amenable to genome-wide RNA interference experiments or the biochemical purification of drug-protein complexes, which, due to the highly selective nature of DG172's effect on myeloid differentiation, is currently not available.

Since DG172 is orally bioavailable we also tested its potential effect in mice, but were unable to detect any alterations to the composition of the bone marrow by FACS analysis using the same markers as in Figs. 2-4 (data not shown). It is therefore possible that the effects seen in BMC cultures occur in vivo only in specific conditions, e.g. certain disease-associated processes. The use of DG172 in mouse models of inflammation, infection or cancer may shed some light on this question in the future. Notwithstanding these open questions pertaining to its effects in vivo, DG172 (or its novel more selective derivative DG228; Fig. 10) may also prove useful to improve the generation of DCs from human BMCs or monocytes, for instance for therapeutic applications.

Acknowledgements

We are grateful to Stefan Bauer (Marburg) for advice and useful discussions, to Ronald Evans (Salk Institute) for providing floxed *Ppard* mice, to Dr. Michael Krause for help with microarrays and to Julia Dick for expert technical assistance with animal experiments.

Authorship Contributions

Participated in research design: Diederich, Brendel, Müller-Brüsselbach, Müller.
Conducted experiments: Lieber, Scheer, Meissner, Giehl.
Contributed new reagents or analytic tools: Diederich, Brendel.
Performed data analysis: Finkernagel, Müller-Brüsselbach, Müller.
Wrote or contributed to the writing of the manuscript: Lieber, Müller-Brüsselbach, Müller.

References

Adhikary T, Kaddatz K, Finkernagel F, Schönbauer A, Meissner W, Scharfe M, Jarek M, Blöcker H, Müller-Brüsselbach S and Müller R (2011) Genomewide analyses define different modes of transcriptional regulation by peroxisome proliferator-activated receptor-beta/delta (PPARbeta/delta). *PLoS One* **6**: e16344.

Barak Y, Liao D, He W, Ong ES, Nelson MC, Olefsky JM, Boland R and Evans RM (2002) Effects of peroxisome proliferator-activated receptor delta on placentation, adiposity, and colorectal cancer. *Proc Natl Acad Sci U S A* **99**: 303-308.

Becker AM, Michael DG, Satpathy AT, Sciammas R, Singh H and Bhattacharya D (2012) IRF-8 extinguishes neutrophil production and promotes dendritic cell lineage commitment in both myeloid and lymphoid mouse progenitors. *Blood* **119**: 2003-2012.

Bedi R, Du J, Sharma AK, Gomes I and Ackerman SJ (2009) Human C/EBP-epsilon activator and repressor isoforms differentially reprogram myeloid lineage commitment and differentiation. *Blood* **113**: 317-327.

Bessede A, Gargaro M, Pallotta MT, Matino D, Servillo G, Brunacci C, Bicciato S, Mazza EM, Macchiarulo A, Vacca C, Iannitti R, Tissi L, Volpi C, Belladonna ML, Orabona C, Bianchi R, Lanz TV, Platten M, Della Fazia MA, Piobbico D, Zelante T, Funakoshi H, Nakamura T, Gilot D, Denison MS, Guillemin GJ, DuHadaway JB, Prendergast GC, Metz R, Geffard M, Boon L, Pirro M, Iorio A, Veyret B, Romani L, Grohmann U, Fallarino F and Puccetti P (2014) Aryl hydrocarbon receptor control of a disease tolerance defence pathway. *Nature*.

Cho SD, Lei P, Abdelrahim M, Yoon K, Liu S, Guo J, Papineni S, Chintharlapalli S and Safe S (2008) 1,1-bis(3'-indolyl)-1-(p-methoxyphenyl)methane activates Nur77-independent proapoptotic responses in colon cancer cells. *Mol Carcinog* **47**: 252-263.

Dahl R, Iyer SR, Owens KS, Cuylear DD and Simon MC (2007) The transcriptional repressor GFI-1 antagonizes PU.1 activity through protein-protein interaction. *J Biol Chem* **282**: 6473-6483.

Dearman RJ, Cumberbatch M, Maxwell G, Basketter DA and Kimber I (2009) Toll-like receptor ligand activation of murine bone marrow-derived dendritic cells. *Immunology* **126**: 475-484.

Desvergne B, Michalik L and Wahli W (2006) Transcriptional regulation of metabolism. *Physiol Rev* **86**: 465-514.

Diakiw SM, Kok CH, To LB, Lewis ID, Brown AL and D'Andrea RJ (2012) The granulocyte-associated transcription factor Kruppel-like factor 5 is silenced by hypermethylation in acute myeloid leukemia. *Leuk Res* **36**: 110-116.

DuSell C D, N elson E R, Wittmann B M, F retz J A, Kazmin D , Thomas RS, P ike JW and McDonnell DP (2010) Regulation of aryl hydrocarbon receptor function by selective estrogen receptor modulators. *Mol Endocrinol* **24**: 33-46.

Garrett-Sinha LA, Dahl R, Rao S , B arton K P and Simon MC (2001) PU.1 exhibits partial functional redundancy with Spi-B, but not with Ets-1 or Elf-1. *Blood* **97**: 2908-2912.

Halene S, Gaines P, Sun H, Zibello T, Lin S, Khanna-Gupta A, Williams SC, Perkins A, Krause D and B erliner N (2010) C /EBPepsilon directs granulocytic-vs-monocytic lineage determination and confers chemotactic function via Hlx. *Exp Hematol* **38**: 90-103.

Hanna RN, Carlin LM, Hubbeling HG, Nackiewicz D, Green AM, Punt JA, Geissmann F and Hedrick CC (2011) The t ranscription factor N R4A1 (Nur77) co ntrols bone marrow differentiation and the survival of Ly6C- monocytes. *Nat Immunol* **12**: 778-785.

Hayashi S , Lewis P, Pevny L and McMahon AP (2002) Efficient gene modulation in mouse epiblast using a Sox2Cre transgenic mouse strain. *Mech Dev* **119 Suppl 1**: S97-S101.

Hock H, Hamblen MJ, Rooke HM, Traver D, Bronson RT, Cameron S and Orkin SH (2003) Intrinsic requirement for zinc finger transcription factor Gfi-1 in neutrophil differentiation. *Immunity* **18**: 109-120.

Inaba K, Inaba M, Romani N, Aya H, Deguchi M, Ikehara S, Muramatsu S and Steinman RM (1992) Generation o f l arge num bers of dendr itic cells from m ouse bon e m arrow cu ltures supplemented with granulocyte/macrophage colony-stimulating factor. *J Exp Med* **176**: 1693-1702.

Kaddatz K , A dhikary T, Fi nkernagel F , M eissner W, M üller-Brüsselbach S and M üller R (2010) Transcriptional profiling identifies functional interactions of TGFβ and PPARβ/δ signaling: synergistic induction of ANGPTL4 transcription. *J Biol Chem* **285**: 29469-29479.

Kanakasabai S , C hearwae W, Walline C C, Iams W, A dams S M an d B right JJ (2010) Peroxisome pr oliferator-activated r eceptor del ta agonists inhibit T hel per t ype 1 (Th1) and Th17 responses in experimental allergic encephalomyelitis. *Immunology* **130**: 572-588.

Kang K , R eilly S M, K arabacak V, Gangl M R, F itzgerald K , H atano B a nd Lee C H (2008) Adipocyte-derived Th2 cytokines and myeloid PPARdelta regulate macrophage polarization and insulin sensitivity. *Cell Metab* **7**: 485-495.

Kostadinova R, Wahli W and Michalik L (2005) PPARs in diseases: control mechanisms of inflammation. *Curr Med Chem* **12**: 2995-3009.

Laslo P, Spooner CJ, Warmflash A, Lancki DW, Lee HJ, Sciammas R, Gantner BN, Dinner AR and S ingh H (2006) M ultilineage t ranscriptional pr iming and det ermination o f alternate hematopoietic cell fates. *Cell* **126**: 755-766.

Lee P Y, Wang J X, P arisini E , D ascher C C and N igrovic PA (2013) Ly6 family pr oteins i n neutrophil biology. *J Leukoc Biol* **94**: 585-594.

Lee WH and Kim SG (2010) AMPK-Dependent Metabolic Regulation by PPAR Agonists. *PPAR Res* **2010**.

Leon B, Martinez del Hoyo G, Parrillas V, Vargas HH, Sanchez-Mateos P, Longo N, Lopez-Bravo M and Ardavin C (2004) Dendritic cell differentiation potential of mouse monocytes: monocytes represent immediate precursors of CD8- and CD8+ splenic dendritic cells. *Blood* **103**: 2668-2676.

Lieber S, Scheer F, Meissner W, Naruhn S, Adhikary T, Müller-Brüsselbach S, Diederich WE and Müller R (2012) (Z)-2-(2-bromophenyl)-3-{[4-(1-methyl-piperazine)amino]phenyl}acrylonitrile (DG172): an orally bioavailable PPARbeta/delta-selective ligand with inverse agonistic properties. *J Med Chem* **55**: 2858−2868.

Lim H, Gupta RA, Ma WG, Paria BC, Moller DE, Morrow JD, DuBois RN, Trzaskos JM and Dey SK (1999) Cyclo-oxygenase-2-derived prostacyclin mediates embryo implantation in the mouse via PPARdelta. *Genes Dev* **13**: 1561-1574.

Mahnke K, Becher E, Ricciardi-Castagnoli P, Luger TA, Schwarz T and Grabbe S (1997) CD14 is expressed by subsets of murine dendritic cells and upregulated by lipopolysaccharide. *Adv Exp Med Biol* **417**: 145-159.

Mak KS, Funnell AP, Pearson RC and Crossley M (2011) PU.1 and Haematopoietic Cell Fate: Dosage Matters. *Int J Cell Biol* **2011**: 808524.

Masurier C, Pioche-Durieu C, Colombo BM, Lacave R, Lemoine FM, Klatzmann D and Guigon M (1999) Immunophenotypical and functional heterogeneity of dendritic cells generated from murine bone marrow cultured with different cytokine combinations: implications for anti-tumoral cell therapy. *Immunology* **96**: 569-577.

Naruhn S, Meissner W, Adhikary T, Kaddatz K, Klein T, Watzer B, Müller-Brüsselbach S and Müller R (2010) 15-hydroxyeicosatetraenoic acid is a preferential peroxisome proliferator-activated receptor β/δ agonist. *Mol Pharmacol* **77**: 171-184.

Naruhn S, Toth PM, Adhikary T, Kaddatz K, Pape V, Dörr S, Klebe G, Müller-Brüsselbach S, Diederich WE and Müller R (2011) High-affinity peroxisome proliferator-activated receptor beta/delta-specific ligands with pure antagonistic or inverse agonistic properties. *Mol Pharmacol* **80**: 828-838.

Nguyen NT, Kimura A, Nakahama T, Chinen I, Masuda K, Nohara K, Fujii-Kuriyama Y and Kishimoto T (2010) Aryl hydrocarbon receptor negatively regulates dendritic cell immunogenicity via a kynurenine-dependent mechanism. *Proc Natl Acad Sci U S A* **107**: 19961-19966.

Odegaard JI, Ricardo-Gonzalez RR, Red Eagle A, Vats D, Morel CR, Goforth MH, Subramanian V, Mukundan L, Ferrante AW and Chawla A (2008) Alternative M2 activation of

Kupffer cells by PPARdelta ameliorates obesity-induced insulin resistance. *Cell Metab* **7**: 496-507.

Palkar PS, Borland MG, Naruhn S, Ferry CH, Lee C, Sk UH, Sharma AK, Amin S, Murray IA, Anderson CR, Perdew GH, Gonzalez FJ, Müller R and Peters JM (2010) Cellular and pharmacological selectivity of the peroxisome proliferator-activated receptor-beta/delta antagonist GSK3787. *Mol Pharmacol* **78**: 419-430.

Peraza MA, Burdick AD, Marin HE, Gonzalez FJ and Peters JM (2006) The toxicology of ligands for peroxisome proliferator-activated receptors (PPAR). *Toxicol Sci* **90**: 269-295.

Peters JM, Shah YM and Gonzalez FJ (2012) The role of peroxisome proliferator-activated receptors in carcinogenesis and chemoprevention. *Nat Rev Cancer* **12**: 181-195.

Resnitzky D, Yarden A, Zipori D and Kimchi A (1986) Autocrine beta-related interferon controls c-myc suppression and growth arrest during hematopoietic cell differentiation. *Cell* **46**: 31-40.

Rosenbauer F and Tenen DG (2007) Transcription factors in myeloid development: balancing differentiation with transformation. *Nat Rev Immunol* **7**: 105-117.

Scholtysek C, Katzenbeisser J, Fu H, Uderhardt S, Ipseiz N, Stoll C, Zaiss MM, Stock M, Donhauser L, Bohm C, Kleyer A, Hess A, Engelke K, David JP, Djouad F, Tuckermann JP, Desvergne B, Schett G and Kronke G (2013) PPARbeta/delta governs Wnt signaling and bone turnover. *Nat Med*: 19.

Schotte R, Nagasawa M, Weijer K, Spits H and Blom B (2004) The ETS transcription factor Spi-B is required for human plasmacytoid dendritic cell development. *J Exp Med* **200**: 1503-1509.

Schuler G, Lutz MB, Bender A, Thurner B, Röder C, Young J and Romani N (1999) A guide to the isolation and propagation of dendritic cells, in Dendritic Cells: Biology and Clinical Applications (Lotze MT and Thomson AW eds) pp 515-533, Academic San Diego, CA, USA.

Shearer BG, Steger DJ, Way JM, Stanley TB, Lobe DC, Grillot DA, Iannone MA, Lazar MA, Willson TM and Billin AN (2008) Identification and characterization of a selective peroxisome proliferator-activated receptor beta/delta (NR1C2) antagonist. *Mol Endocrinol* **22**: 523-529.

Shearer BG, Wiethe RW, Ashe A, Billin AN, Way JM, Stanley TB, Wagner CD, Xu RX, Leesnitzer LM, Merrihew RV, Shearer TW, Jeune MR, Ulrich JC and Willson TM (2010) Identification and characterization of 4-chloro-N-(2-{[5-trifluoromethyl)-2-pyridyl]sulfonyl}ethyl)benzamide (GSK3787), a selective and irreversible peroxisome proliferator-activated receptor delta (PPARdelta) antagonist. *J Med Chem* **53**: 1857-1861.

Smyth GK (2005) Limma: linear models for microarray data, in Bioinformatics and Computational Biology Solutions using R and Bioconductor

(Gentleman R, Carey V, Dudoit S, Irizarry R and Huber W eds) pp 397-420, Springer, New York.

Tamura T, Tailor P, Yamaoka K, Kong HJ, Tsujimura H, O'Shea JJ, Singh H and Ozato K (2005) IFN regulatory factor-4 and -8 govern dendritic cell subset development and their functional diversity. *J Immunol* **174**: 2573-2581.

Toth PM, Naruhn S, Pape VF, Dörr SM, Klebe G, Müller R and Diederich WE (2012) Development of Improved PPARbeta/delta Inhibitors. *ChemMedChem* **7**: 159-170.

Vogel CF, Wu D, Goth SR, Baek J, Lollies A, Domhardt R, Grindel A and Pessah IN (2013) Aryl hydrocarbon receptor signaling regulates NF-kappaB RelB activation during dendritic-cell differentiation. *Immunol Cell Biol* **91**: 568-575.

Wahli W and Michalik L (2012) PPARs at the crossroads of lipid signaling and inflammation. *Trends Endocrinol Metab* **23**: 351-363.

Weischenfeldt J and Porse B (2008) Bone Marrow-Derived Macrophages (BMM): Isolation and Applications. *CSH Protoc* **2008**: pdb prot5080.

Xu HE, Lambert MH, Montana VG, Parks DJ, Blanchard SG, Brown PJ, Sternbach DD, Lehmann JM, Wisely GB, Willson TM, Kliewer SA and Milburn MV (1999) Molecular recognition of fatty acids by peroxisome proliferator-activated receptors. *Mol Cell* **3**: 397-403.

Yamanaka R, Kim GD, Radomska HS, Lekstrom-Himes J, Smith LT, Antonson P, Tenen DG and Xanthopoulos KG (1997) CCAAT/enhancer binding protein epsilon is preferentially up-regulated during granulocytic differentiation and its functional versatility is determined by alternative use of promoters and differential splicing. *Proc Natl Acad Sci U S A* **94**: 6462-6467.

Yang Y, Lovett-Racke AE and Racke MK (2010) Regulation of Immune Responses and Autoimmune Encephalomyelitis by PPARs. *PPAR Res* **2010**: 104705.

FOOTNOTES

This work was supported by grants from the Deutsche Forschungsgemeinschaft to R. Müller [Mu601/13] and W. Diederich [DI 827/4-1] and from the Wilhelm-Sander-Stiftung to S. Müller-Brüsselbach.

Reprint requests should be addressed to Dr. Rolf Müller, Institute of Molecular Biology and Tumor Research (IMT), Center for Tumor and Immunobiology (ZTI), Philipps University, Hans-Meerwein-Straße 3, 35043 Marburg, Germany. Email: rmueller@imt.uni-marburg.de